Investigating the Co-Evolution of Tumor Antigens and the Anti-Tumor Immune Response

By

Nicole S Little

B.Sc., University of Victoria, 2013

A Thesis Submitted in Partial Fulfillment

Of the Requirements of the Degree of

MASTER OF SCIENCE

In the Department of Biochemistry and Microbiology

Investigating the Co-Evolution of Tumor Antigens and
the Anti-Tumor Immune Response

By

Nicole S Little
B.Sc., University of Victoria, 2013

Supervisory Committee

Dr. Brad H Nelson (Department of Biochemistry and Microbiology)
Supervisor

Dr. Robert Burke (Department of Biochemistry and Microbiology)
Department Member

Dr. Perry Howard (Department of Biology)
Outside Member, University of Victoria

Dr. Megan Levings (Faculty of Medicine, Department of Surgery)
Outside Member, University of British Columbia

Abstract

Supervisory Committee

Dr. Brad H Nelson (Department of Biochemistry and Microbiology)

Supervisor

Dr. Robert Burke (Department of Biochemistry and Microbiology)

Department Member

Dr. Perry Howard (Department of Biology)

Outside Member

Dr. Megan Levings (Faculty of Medicine, Department of Surgery, University of British Columbia)

Outside Member

Background: High-grade serous carcinoma (HGSC) can exhibit high intratumoral heterogeneity (ITH). Despite a strong association between tumor-infiltrating lymphocytes (TIL) and survival in HGSC, ITH may have profound impacts on the anti-tumor T cell response. Yet, it is unknown how anti-tumor T cell responses contend with ITH over time in HGSC. Previous studies in melanoma and HGSC both showed tumor-reactive T cell clones emerge over time with their cognate tumor-antigens. Therefore, I hypothesized patients would share a common mechanism of T cell evolution to respond to ITH in HGSC. If so, I expect to see similar patterns of tumor recognition between primary and recurrent disease.
Methods: Tumor-associated lymphocytes (TAL) were expanded from primary and recurrent ascites samples using high-dose IL-2 and a rapid-expansion protocol (REP). Following expansion, TAL were assessed for recognition of autologous tumor by IFN-γ ELISPOT and flow cytometry for CD137. $CD137^+$ tumor-reactive TAL were FACS-purified and the tumor-reactive T cell repertoire was profiled by deep sequencing of TCRβ chains (TCRseq). Tumor-reactive TCR clonotypes were compared between primary and recurrent disease to elucidate differences in tumor-reactive populations over time in HGSC.
Results: Patient TAL recognized tumor in two out of three cases. In patient IROC 060, the tumor became more immunogenic between primary and recurrent disease, which may reflect expression of new antigens and/or loss of an immunosuppressive phenotype. In patient IROC 106, the tumor remained immunogenic between primary and recurrent disease, which may reflect maintenance of stable antigen expression and an immune-sensitive phenotype. Patient IROC 034 did not exhibit any tumor-reactivity, suggesting tumor-reactivity is not ubiquitous in HGSC. FACS-purification of $CD137^+$ T cells followed by

TCRseq was successfully performed on T cell populations of both high- and low-abundance, suggesting TCRseq can be performed on populations containing very few T cells. TCRseq results that profiled the clonal repertoire of tumor-reactive TAL from primary and recurrent disease in two patients, IROC 060 and IROC 106, showed both patients had evidence of T cell loss and T cell emergence between primary and recurrent disease. Further, IROC 106 had evidence of T cell clones that were maintained between primary and recurrent disease.

Conclusions: Anti-tumor T cell responses from ascites are both diverse between patients and dynamic within a patient, suggesting various mechanisms of T cell evolution to contend with ITH in HGSC. I developed a pipeline for the identification of tumor-reactive TCR sequences without the need for *a priori* knowledge of specific antigens. Additionally, this pipeline is feasible for very low-abundance samples, such as tumor-reactive T cells.

Significance: This study provides early insights into how TAL contend with ITH in HGSC. Ultimately, these results will inform the design of adoptive T cell therapy for recurrent HGSC.

Table of Contents

Abbreviations

ACT – adoptive cell therapy

ALL – acute lymphoblastic leukemia

APC – antigen presenting cell

CA-125 – cancer antigen – 125

CAF – cancer associated fibroblasts

CAIX – carboxy-anhydrase-IX

CAR – chimeric antigen receptor

CD – cluster of differentiation

CEF – CMV, EBV, and Influenza

CLL – chronic leukocytic leukemia

CMV – Cytomegalovirus

CT – cancer testis

CTL – cytotoxic T lymphocyte

CTLA-4 – cytotoxic T lymphocyte-associated antigen – 4

D – diversity (region of the TCR)

DC – dendritic cell

DMSO – dimethyl sulfoxide

EBV – Epstein-Barr Virus

ELISPOT – enzyme-linked immunoSPOT

EMT – epithelial to mesenchymal transition

EpCAM – epithelial cell adhesion molecule

FACS – fluorescence-activated cell sorting

FBS – fetal bovine serum

FFPE – formalin-fixed paraffin-embedded

GSC – Michael Smith Genome Sciences Centre

HGSC – high-grade serous carcinoma

HPV – Human Papilloma Virus

HSDL-1 – hydroxysteroid dehydrogenase like – 1

IDO – indolamine 2,3-dioxygenase

IFN-γ – interferon-γ

IHC – immunohistochemistry

IL – interleukin

IRF – immune response factor

IROC – Immune Response to Ovarian Cancer

ITH – intratumoral heterogeneity

J – joining (region of the TCR)

JAK – Janus kinase

MAGE – melanoma antigen gene

MART-1 – melanoma antigen recognized by T cells – 1

MDSC – myeloid-derived suppressor cell

MHC – Major Histocompatibility Complex

MSC – mesenchymal stem cells

PBMC – peripheral blood mononuclear cell

PD-1 – programmed death – 1

pDC – plasmacytoid dendritic cell

PD-L1 – PD-ligand 1

PD-L2 – PD-ligand 2

PHA – phytohemagglutinin

PMA/IM – Phorbol 12-myristate 13-acetate and ionomycin

PRR – Pattern Recognition Receptor

REP – rapid expansion protocol

RETM – Renaissance Essential Tumor Media

scFv – single chain variable fragment

TAL – tumor-associated lymphocyte

TAM – tumor associated macrophage

TCR – T cell receptor

TCRseq – TCR sequencing

TdT – terminal dideoxytransferase

TGF-β – transforming growth factor - β

T_H – helper T lymphocyte

TIL – tumor-infiltrating lymphocyte

TIM-3 – T cell immunoglobulin mucin – 3

TME – tumor microenvironment

TNF – tumor necrosis factor

TNFRSF – tumor necrosis factor receptor super family

TTR – Tumour Tissue Repository

Treg – regulatory T lymphocyte

V – variable (region of the TCR)

List of Tables

List of Figures

Acknowledgements

First, I want to thank Dr. Brad Nelson, who graciously accepted me, a naïve, curious, science-loving, "pre-med" kid, into his lab three years ago. His guidance, support, and enthusiasm throughout my degree has been unwavering. Together I feel we've created a cool project has the potential to make a great impact on ACT of recurrent tumors, and for that I feel nothing but immense gratitude and pride. I also want to thank my supervisory committee, Dr. Robert Burke, Dr. Perry Howard, and Dr. Megan Levings, for being an incredible source of intellect, advice, and support throughout my degree.

None of this work would have started without the help of every single member of the Nelson lab, past and present. They not only gave me scientific guidance, they enriched every day of my experience in graduate school and helped to make these past three years some of the best in my life. In particular, I need to thank Dr. Spencer Martin, Dr. David Kroeger, Dr. Maartje Wouters, Dr. Julie Nielsen, Dr. Kwame Twumasi-Boateng, and Darin Wick for their invaluable guidance in experimental design and teaching me to think about interpretation of results while designing experiments, rather than quizzically staring at data afterwards wishing I had done things differently. They also provided (lots of) constructive criticism for every aspect of this project from start to finish. Their feedback helped to ensure even if there were no positive results, I'd still be confident in them. Also, to Dr. Maartje Wouters and Dr. Stephen Redpath, my words in this thesis cannot repay you for the help you gave me while writing this thesis. So, I hope the beer and tea does.

Next, I want to thank Dr. John Webb. John was an invaluable mentor in helping me learn the ins and outs of human T cell culture as well as the nuances of flow cytometry and FACS. Together, John, Spence, and Dave taught how to do FACS. Without them, I would have never learned the nuances of the Influx and would still be sitting with a hopeless look sprawled across my face, staring into the depths of the sorter, not knowing why the side stream won't appear (are the plates turned on, Nicole?), or why dots aren't appearing on the screen (is the Sortware acquiring, Nicole?). Without these guys, I wouldn't have even close to the same appreciation of FACS-sorting and flow cytometry, nor the knowledge and skill I have today. Additionally, I could not have done this project without Victoria Hodgson, who so kindly ensured my T cells were taken care of if I had to leave town and helped develop a few ELISPOTs for me while I scrambled to get 70+ FACS samples washed, filtered, and ready to run on the Influx cell sorter so I could leave the lab before 11:00pm on sort days.

I'd also like to thank all the members of the TTR: Dr. Peter Watson, Jodi LeBlanc, Sindy Babinsky, Tania Castillo-Pelayo, and Victoria Hartman. The TTR was responsible for consenting patients and

collecting samples for IROC, without which none of us would be able to do the work that we do every day.

I would also like to extend immense gratitude to the staff at the Michael Smith Genome Sciences Centre, particularly Dr. Robert Holt, Dr. Roger Moore, Thomas Zheng, and Leslie Alfaro, for their patience and hard work required to optimize the TCRseq pipeline for my samples. They were also a source of very thoughtful and helpful advice for this part of the project, which was wonderful.

Further, I would also like to sincerely thank all members of the Holt lab, and David Ko from the Terry Fox Laboratories flow core at the BC Cancer Research Centre in Vancouver, for allowing me to come to their centre for a week for the small price of good beer and good donuts. Without their generosity and hospitality, I would not have been able to complete the necessary experiments prior to my thumb surgery.

To all my friends and family members, thank you for caring for me and supporting me through this degree. First, to my Mom and Dad, for making sure I ate vegetables while I wrote my thesis, making sure I had dinner when I spent late nights in the lab, and providing love and support while I pursued my goal. Second, to Braden, who managed to make sure that I took time away to do fun stuff like go to Las Vegas, spend time with the dogs, and go fishing, but also unconditionally supported and encouraged me when I had to get down to work. Third, to my sister, Kate, who let me stay with her when I need to stay late for work (or a good lab party) and who also gave me the kind of sympathy, love, and kindness that can only come from another person who is equally stressed out about school and life. Thank you to Sarah MacPherson, my desk neighbour and co-graduate student, who ensured every week was enjoyable with “Taste Tuesdays,” “Good Data Mondays,” and “Fancy Fridays.” Also, to members of the “robust” squad, Victoria Hodgson, Eunice Kwok, Tania Castillo-Pelayo, Victoria Hartman, and Heather Derocher, thank you for your steadfast support and encouragement as well as the care package that helped me get through the stressful few months of thesis writing.

I also can’t leave out fetal bovine serum. Although I hate the stuff, FBS taught me a lesson in the value of perseverance despite immense disappointment and frustration.

Last, but most importantly, I must thank the incredible donations from each of the IROC patients. They selflessly donated their tissue, ascites, and blood with the altruistic hope that their samples would go towards making ovarian cancer easier to bear for patients in the future. I only hope I would be so generous if faced with the prospects of going through the treatment process and living the rest of my life with ovarian cancer. I hope that my work honours their memory.

Preface

The research in this thesis was conducted with approval from both the University of Victoria Human Research Ethics Board, protocol number 17-126, and the University of British Columbia Research Ethics Board, certificate number H07-00463. Funding was provided by the Canadian Cancer Society Research Institute (CCSRI) and the Canadian Institutes of Health Research (CIHR). Particularly, I would like to acknowledge the Canada Graduate Scholarships – Master's Program award I received when I began this research three years ago.

This thesis aims to identify predominant mechanisms in immune-mediated control of highly heterogeneous ovarian tumors. Chapter 1, the introduction, provides relevant background and context for the data presented in chapters 2 and 3.

The work in this thesis was conducted by Nicole Shannon Little. I designed and conducted the experiments in both chapters 2 and 3 using patient specimens collected by the Tumour Tissue Repository of the BC Cancer Agency through a prospective study titled "The Immune Response to Ovarian Cancer" (IROC). Building on the development of robust assays such as ELISPOT, flow cytometry, and FACS, I adapted each technique and optimized their use in my experimental pipeline. Immunohistochemistry was performed by Katy Milne, Research Assistant III at the Deeley Research Centre.

For chapter 3, I determined which analyses should be performed on the next-generation TCR sequencing (TCRseq) data. However, bioinformatic analysis of the raw TCRseq data was conducted by Phineas Hamilton, post-doctoral fellow at the Deeley Research Centre. All subsequent interpretation of TCRseq data was done by me.

Chapter 1 - Introduction

1.1 T Cell-Mediated Immune Responses

T lymphocytes (T cells) mediate exquisitely specific destruction of intracellular pathogens such as viruses. They survey cells throughout the body searching for specific targets on infected cells that trigger a full-blown assault against a pathogen, while leaving surrounding healthy normal cells intact. In this way, T cells can mediate clearance of intracellular pathogens while leaving the host relatively unharmed.

To elicit a T cell response, members of the two arms of the immune system, innate and adaptive, must communicate. While the innate immune system is poised to rapidly respond to conserved molecular patterns common to pathogens, the adaptive immune system has evolved the capacity to specifically recognize any potential pathogen. To initiate a cell-mediated immune response, cells from the innate immune system recognize pathogens through pattern recognition receptors (PRR), phagocytose these pathogens, and traffic to lymph nodes. Pathogenic proteins are then processed into peptide fragments by professional antigen presenting cells (APC) such as dendritic cells (DC), macrophages, and B cells. Pathogenic peptides are presented on the surface of APCs in molecular complexes called Major Histocompatibility Complex (MHC). MHC class I is expressed on all nucleated cells in the body, while MHC class II is typically restricted to APCs. In a process called T cell priming, APCs present these pathogenic proteins in the context of MHC to naïve cells of the adaptive immune response: $CD8^+$ cytotoxic T lymphocytes (CTL) and $CD4^+$ helper T lymphocytes (T_H). Following priming, T cells become activated, divide, and traffic out of the lymph node to the site of infection, where they mediate infection clearance.[1]

$CD4^+$ T_H cells orchestrate the adaptive immune response. They provide the appropriate signals to direct the right type of adaptive immune response to a specific pathogenic insult. Through their T cell receptor (TCR), $CD4^+$ T cells recognize peptide antigens, displayed in the context of MHC class II. Once the $CD4^+$ TCR recognizes its cognate antigen in MHC class II, it will secrete cytokines that help stimulate an appropriate and robust immune response.[2] $CD4^+$ responses promote cell-mediated immune responses through secretion of cytokines such as interferon-γ (IFN-γ) and tumor necrosis factor-α (TNF-α) which ultimately help APCs induce $CD8^+$ T cell priming and differentiation into effector CTLs.[2,3]

$CD8^+$ CTL are the direct effectors of the cell-mediated immune response. They act by specifically targeting infected cells and inducing cell-mediated apoptosis. In contrast to $CD4^+$ T cells, $CD8^+$ T cells recognize peptide antigen in the context of MHC class I. Upon TCR engagement, an immunological synapse forms between the T cell and its target, while a series of signaling events are initiated within the T cell that ultimately lead to release of effector molecules such as IFN-γ, granzymes, and perforin. Perforin molecules form polymers that bind to the target cell membrane at the immunological synapse. This creates pores for granzymes to enter the target cell cytoplasm and initiate a cascade of events that results in lysis of the target cell and elimination of the pathogen. Further, IFN-γ acts to increase target cell expression of MHC class I and II molecules to promote further immune-mediated killing.[2–4]

Direct comparisons can be made between the immune response to intracellular pathogens and to tumors. In the same way that anti-viral T cells recognize viral antigens, T cells recognize tumor antigens and can mediate anti-tumor responses.[5] Due to the exquisite specificity of antigen recognition through the TCR, T cells can distinguish minute differences between tumor cells and healthy cells, ultimately leading to tumor cell killing while leaving healthy, normal cells intact.[6] Indeed, tumor-infiltrating T cells (TIL) confer improved prognosis,[7–9] and have been shown to directly recognize and kill tumor cells in a number of cancer settings.[10,11]

1.1.1 The T Cell Receptor

The specificity of T cells for their cognate antigen is defined by the TCR. The αβ TCR is a membrane-spanning polypeptide complex composed of one α- (TCRα) and one β-chain (TCRβ) linked by a disulfide bond.[14] The intracellular domain of the TCR complex associates with numerous signaling domains that activate signaling cascades that result in T cell activation, effector function, survival, and proliferation.[14,15] More specifically, the hypervariable region of the TCR confers antigen specificity and is created when the variable (V), diversity (D), and joining (J) regions of the TCR genomic loci are rearranged during T cell development. To further increase TCR variability, terminal deoxynucleotidyl transferase (TdT) adds nucleotides to V(D)J junctions. The resultant region, where the D and J segments join, is known as the CDR3 region. The CDR3 region forms the centre of the antigen-binding site on the TCR and directly binds cognate peptide in the context of MHC.[16–18] The human genome encodes 52 V_β segments, ~70 V_α segments, 2 D segments at the TCRβ locus only, 13 J_β segments, and 62 J_α segments. Therefore, with all the combinatorial possibilities of V(D)J recombination at each TCR locus and the pairing of one recombined TCRα and TCRβ chain to form the full TCR, there are 10^{18} unique TCRs

possible that each recognize unique antigens and confer immunity against an enormously broad range of targets.[19]

1.1.2 Markers of T Cell Activation

Following activation, T cells up-regulate many cell surface molecules, such as programmed death-1 (PD-1), CD69, and several members of the tumor necrosis factor receptor super family (TNFRSF) including CD137, OX-40, and CD40 ligand (CD40L). These surface molecules perform important functions *in vivo*, and they can be used to detect activated T cells *in vivo* and *in vitro*. PD-1 and CD69 are expressed on activated T cells, but they function to suppress T cell activity. CD69 is a C-type lectin domain family member and is the earliest T cell activation marker expressed following stimulation (≤4 hours), making it an appealing target for identifying recently activated T cells.[20,21] Upon binding its ligand, CD69L, CD69 stimulates secretion of TGFβ, and suppresses the expression of pro-inflammatory cytokines such as IL-17 and IFN-γ. Therefore, CD69 functions to suppress T cell responses.[20,22–24] In contrast to CD69, PD-1 expression peaks at 48-hours post-stimulation.[25] PD-1 inhibits T cell activity by recruiting SHP-2 and dephosphorylating CD28.[26–28] This inhibition is dependent on PD-1 binding to its ligands PD-L1 and PD-L2.[29–31] Mechanisms of PD-1-mediated T cell inhibition are discussed further in section 1.3.4.2.1.

In contrast to CD69 and PD-1, which inhibit T cell function, CD137, OX-40, and CD40L promote T cell effector function, proliferation, and survival.[32–34] OX-40 (CD134, TNFRSF4) is a marker of activated $CD4^+$ T cells.[32,34,35] OX-40 is up-regulated 24-48 hours post-stimulation and functions to promote T cell proliferation and augment cytokine secretion in activated T cells.[34,35] CD40L (CD154) is another member of the TNFR family and is similar to CD137 and OX40.[36] CD40L is highly expressed on $CD4^+$ T cells between 2 and 6 hours after activation.[37] CD40L binds to CD40, typically expressed on naïve B cells, and engagement leads to B cell activation and enhances the development of a T_H2 humoral-mediated immune response.[38] CD137 (4-1BB, TNFRSF9) is expressed on both activated $CD4^+$ and $CD8^+$ T cells.[33,39] CD137 is maximally up-regulated 24-48 hours post-stimulation[40] and functions to promote proliferation, survival, cytokine secretion, and effector function in activated T cells.[33] Due to its low background expression on non-activated T cells and its rapid and specific up-regulation following antigen stimulation,[10,40,41] studies on both $CD4^+$- and $CD8^+$-mediated anti-tumor responses have favoured the use of CD137 as a marker of activated T cells *in vitro*.

1.2 Tumor Antigens

Tumor antigens are a diverse category of proteins that allow immune-mediated discrimination between tumor and normal cells. Tumor antigens were first described in chemically-induced tumors in mice.[42] In this model, tumors induced using methylcholanthrene could be removed and transplanted into syngeneic mice, or re-transplanted into the original mouse, and in both cases full immunological rejection of the tumor was observed. In contrast, allogeneic recipients had full tumor progression and died due to disease.[42] Since this early study, numerous tumor antigens have been identified and exploited in the pursuit of immunotherapies.[10,11,43] In humans, three main categories of tumor antigens have been identified: i) viral antigens, in cases of virally-induced cancers like Human Papilloma Virus (HPV)-induced cervical carcinoma,[44] ii) self-antigens that the immune system recognizes due to incomplete tolerance and tissue-restricted expression,[45] or iii) mutant proteins expressed specifically by the tumor.[46] As described in more detail below, each of these classes of tumor antigen has been shown to elicit T cell-mediated anti-tumor immune responses.[43,47–49]

1.2.1 Viral Antigens

In virally-induced tumors, viral antigens are an obvious immunological target. Virally-induced tumors can arise from numerous viral infections such as: liver cancer from hepatitis B and hepatitis C infections,[50] Hodgkin's lymphoma and head and neck cancers from Epstein-Barr Virus (EBV) infections,[51,52] and Kaposi's sarcoma from either human herpesevirus-8[53] or human cytomegalovirus (CMV).[54] Perhaps the most well-known virally-induced cancer types are HPV-induced cervical, anogenital, and head and neck cancers.[55] HPV infects epithelial cells and integrates its genome into the genome of the host. HPV proteins E6 and E7 are oncogenes that inactivate p53[56] and retinoblastoma protein,[57] respectively, leading to the development of cancers.[58] Despite their role in oncogenesis, HPV E6 and E7 are also antigens that can elicit T cell responses. Notably, many patients with HPV^+ tumors harbour T cells specific for either E6 or E7 proteins.[44,47,59] Indeed, a clinical trial studying adoptive cell therapy (ACT) using TIL with confirmed HPV reactivity found 3 of 9 cervical cancer patients had objective responses, with two having complete durable responses to ACT.[10] Taken together, these data suggest viral antigens represent a tumor target antigen that can elicit strong, durable anti-tumor responses in humans.

1.2.2 Cancer Testis Antigens and Shared Tumor Antigens

Cancer testis (CT) antigens have long been an attractive target in the study of anti-tumor immunity. CT antigens are normal proteins with highly specific, tissue-restricted distribution in germline cells. Because these antigens are not expressed in adult somatic cells, they are not presented to immature T cells in the thymus. Therefore, CT-antigen-specific T cells are not deleted from the T cell repertoire during thymic selection. Cancers have been shown to reactivate expression of these genes,[60–62] and as a result CT antigens have been studied extensively with the aim to exploit them in immunotherapy for CT-antigen expressing tumors. Numerous examples have been discovered, including melanoma antigen-1 (MAGE), BAGE,[63] and GAGE[64] proteins, and NY-ESO-1.[60] Notably, NY-ESO-1 has been shown to be expressed in 40.7% of ovarian cancers, and its expression is associated with poor prognosis.[65] Both $CD4^+$ and $CD8^+$ T cell responses against NY-ESO-1 have been identified in HGSC patients.[66–68] Further, a vaccine clinical trial using an MHC class II-restricted NY-ESO-1 epitope was shown to induce long-lived $CD4^+$ and $CD8^+$ T cell responses, as well as NY-ESO-1-specific antibodies in 18 NY-ESO-1^+ HGSC patients. Together, these data suggest that NY-ESO-1 is an attractive target for immunotherapy in HGSC.

1.2.3 Neoantigens

Perhaps the most important class of tumor antigens are mutant proteins that elicit non-self T cell reactivity, so-called tumor neoantigens. Because these mutant proteins are distinct from wild type proteins, they are not expressed in the thymus. Therefore, T cells that recognize these antigens are not deleted from the T cell repertoire during thymic selection. Because they escape central tolerance, the pool of neoantigen-reactive T cells is expected to be large,[69] making neoantigens an attractive target in anti-tumor immune responses. There have been many examples of human T cell responses to mutations encoded by tumors.[48,49,70,71] Studies have shown neoantigens are largely responsible for mediating clinical responses in patients treated with immunotherapy.[72–74] For example, one study showed patients who responded to anti-PD-1 therapy had higher numbers of total mutations (synonymous, nonsynonymous, indels, and frameshifts) compared to patients who did not respond. Similarly, melanomas with higher mutational load responded better to anti-CTLA-4 therapy compared to tumors with lower mutational load.[74] Additionally, one study reported that patients who responded to either anti PD-1 therapy or anti-CTLA-4 therapy were more likely to have homogeneous tumors with clonal

nonsynonymous mutations.[72] Poor responders showed higher Tumor heterogeneity, as marked by high subclonal nonsynonymous mutation burden (such as mutations that are private to tumor cells or shared by only a few tumor cells) .[72] Further, a recent study showed a patient with HPV$^+$ cervical cancer who had a complete durable tumor regression had a higher frequency of neoantigen-reactive TIL compared to HPV-reactive T cells in the TIL,[47] further highlighting the significance of neoantigens in anti-tumor immune responses.

1.3 High-Grade Serous Carcinoma

High-grade serous carcinoma (HGSC) of the ovary is a deadly disease. Fewer than 40% of women with HGSC survive longer than 10 years post-diagnosis.[75] Serum levels of cancer antigen-125 (CA-125) are measured to track disease progression and response to treatment.[76] CA-125 protein in the mucin family, which function to protect the mucosa from pathogens, including in the female reproductive tract.[77,78] At diagnosis, CA-125 serum levels are elevated in 80% of epithelial ovarian cancer patients.[76] Following cytoreductive surgery and subsequent platinum-based chemotherapy, patients who respond well to treatment typically have a large reduction in serum CA-125 levels. Post-diagnosis, CA-125 levels are routinely monitored, and post-treatment increases are indicative of insensitivity to chemotherapy (chemoresistance) or tumor recurrence.[76] Approximately 80% of patients with advanced HGSC will either have progressive disease or tumor recurrence, and survival rates have not changed in nearly 40 years.[75,79] Therefore, there is a desperate need for better treatment options that induce long-term disease control in HGSC patients.

1.3.1 Effect of TIL on HGSC Prognosis

Despite overall poor outcomes in HGSC patients,[75] the presence of intra-epithelial TIL is associated with a positive prognostic outcome.[7,80,81] Zhang *et al* were the first to correlate prognosis with the presence of intratumoral CD3$^+$ TIL in HGSC.[7] They found the five-year overall survival rate of patients who had TIL within epithelial tumor islets was 38%, while for patients without TIL it was just 4.5%.[7] This striking difference has led to numerous studies evaluating multiple aspects of the immune response to cancer in attempts to directly harness the effects of the immune response to HGSC. These include studies attempting to identify whether patient outcomes are impacted by the subtype of T cells,[82–84] the functional status of T cells,[85–88] or other markers or cell types in the epithelium or stroma.[89–91] Sato *et al* found intra-epithelial CD8$^+$ TIL were associated with longer survival in epithelial ovarian cancer

patients.[84] Further, they found patients with high $CD8^+/CD4^+$ TIL ratios had improved survival.[84] The authors suggest this effect is due to the infiltration of not just $CD4^+$ T helper cells, but also $CD4^+$ $CD25^+$ $FoxP3^+$ T regulatory cells, which have an immunosuppressive effect on active $CD8^+$ T cell responses.[84] However, despite the prognostic benefit of TIL in HGSC, survival rates remain low. This would suggest that other factors may thwart the anti-tumor immune response, leading to poor survival despite T cell infiltration.

1.3.2 Clonal Evolution and Intratumoral Heterogeneity

It is widely accepted that tumors exhibit clonal evolution due to their extreme genetic instability.[92,93] Genetic instability is a hallmark of tumors,[94] as mutations in DNA repair and replication mechanisms are nearly ubiquitous in tumors. Thus, without high fidelity DNA replication, altered gene expression patterns may emerge over time, leading to progressively different phenotypes in tumor subclones (reviewed in McGranahan and Swanton, 2015).[95]

Clonal evolution requires selective pressure. Indeed, there is evidence of Darwinian-type selection in tumor cell populations.[96] This selective pressure may be from various factors, such as nutrient competition in the tumor microenvironment,[97] chemotherapy,[98–102] and the anti-tumor immune response.[103–105] These pressures can contribute to spatial intratumoral heterogeneity (ITH) in tumors,[92,106] as well as temporal changes induced by pressure on tumor subclones over time.[107]

1.3.2.1 Spatial Heterogeneity of HGSC Tumors

Spatial ITH has been described in nearly every tumor type, as reviewed in Calderwood[106] and Jacoby *et al*.[92] One seminal study of three HGSC patients revealed striking differences in the subclonal architecture across several tumor sites in each patient.[108] On average only 51.5% of mutations were shared between tumor sites within each patient. Further, gene expression profiles, copy number, and mutation variation was high between tumor sites. In fact, one patient had such high ITH between the right and left ovary, each of these sites looked as if it was a distinct tumor. A second case had 8 distinct tumor subclones present within five separate tumor sites in the peritoneal cavity.[108]

In addition to genetic heterogeneity, HGSC tumors may also exhibit phenotypic variation. For example, one study showed certain regions within an HGSC tumor appear epithelial, while other regions from the same tumor displayed either mesenchymal or mixed phenotypes.[109] These phenotypic differences may affect the expression of cell-surface markers, including those that impact anti-tumor

immune responses. For example, the expression of the immunosuppressive ligand, PD-L1, is associated with a state of epithelial-to-mesenchymal-transition (EMT).[110,111] Further, selective pressure from chemotherapy, radiation, or the host immune system may lead to temporal changes in tumor antigen expression, which could directly impact the anti-tumor immune response.

1.3.2.2 Temporal Dynamics of HGSC Tumors

In addition to spatial ITH, HGSC patients can have a high degree of temporal variation. Evolutionary pressures may act over time to select tumor cells that resist treatment-induced apoptosis or cytolysis,[112] evade the immune system through antigen loss or acquisition of an immunosuppressive phenotype,[113] or accumulate additional mutations in genes contributing to tumorigenesis and tumor survival.[93,114] Although some mutations may lead to gene expression patterns that confer resistance to immune responses,[115] it may be possible that tumors also gain immunogenic mutations or undergo reactivation of CT antigens, bolstering anti-tumor immune responses. Therefore, it is possible that the antigenic landscape and immunogenicity of tumors may be very different between primary and recurrent disease.

One notable example was discussed by Castellarin *et al*, where one HGSC patient was identified who experienced a strong response to chemotherapy, denoted by a sharp and complete reduction in serum CA-125 levels, followed by tumor recurrence.[107] Interestingly, this tumor had large mutational differences between primary and recurrent disease.[107] By recurrent disease, this patient lost a tumor subclone that expressed a set of mutations. However, another tumor subclone became very prominent by recurrence.[107] A subsequent study on this patient revealed an immunogenic mutation in the hydroxysteroid dehydrogenase like-1 (HSDL-1) gene emerged between primary disease and first recurrence,[49] suggesting chemotherapy may play a role in the expression of mutations that can be targeted by the anti-tumor immune response in HGSC.

Studies show chemotherapy can put extensive selective pressure on tumor cell populations (reviewed in Lake *et al*).[116] First, studies in multiple tumor types suggest chemotherapies can induce specific mutational signatures.[117–119] For example, platinum-based chemotherapy in esophageal adenocarcinoma leads to the accumulation of C>A mutations in CpG islands due to preferential cross-linking of C-G bases and improper DNA repair,[119] which could lead to increased mutations and hence tumor-specific neoantigens. This finding is highly relevant to HGSC tumors, which are also treated with platinum-based chemotherapies. Notably, in a study on one HGSC patient, post-chemotherapy recurrent

tumor had a higher degree of clonal diversity compared to her primary, untreated sample.[108] These results further implicate chemotherapy in the development of ITH over time in HGSC tumors. Second, chemotherapy can induce increased MHC class I and class II expression compared to chemo-naïve tumors, suggesting chemotherapy-induced differences in antigen presentation may occur in HGSC.[98] Further, platinum-based chemotherapy, specifically cisplatin, can induce increased expression of MHC Class I on the surface of tumor cell lines.[99,100,102] Together, these studies suggest chemotherapy may have profound effects on ITH, potentially impacting the immune response to HGSC.

1.3.3 Heterogeneity of the Anti-Tumor Immune Response

For long term disease control, the anti-tumor immune response must not only contend with spatial ITH, but also temporal changes in the tumor, which may result in very different antigen expression and disease characteristics at recurrent disease. Despite numerous studies evaluating ITH in tumors, few have been published on the spatial or temporal heterogeneity of anti-tumor immune responses.[120–122] Nonetheless, they show patterns of TIL infiltration in several tumor sites within a patient are different between HGSC and renal cell carcinoma.[120–122] Additionally, there are several selective pressures that may act on immune cells within the tumor microenvironment (TME) or the patient themselves. However, there have been few reports investigating the temporal changes to anti-tumor immune responses.[48,49] Therefore, it is largely unknown how these responses mediate long term disease control in HGSC.

1.3.3.1 Spatial Heterogeneity of the Anti-Tumor Immune Response

The spatial heterogeneity of anti-tumor immune responses is largely understudied. However, a few studies have evaluated the complexity and heterogeneity of TIL infiltration of tumors. One study evaluating renal cell carcinoma found the T cell clonal repertoire, as identified by deep sequencing of TCRβ sequences in two to four tumor sites within each patient, found a high degree of immunological heterogeneity with a median of 2394 unique TCR clonotypes found in each tumor site. Further, the top 100 most frequent T cell clones within each site had poor overlap with other tumor sites, indicating each tumor site had a largely unique anti-tumor T cell response.[120] In contrast, a study in HGSC found the infiltration of various TIL subsets were largely homogeneous between tumor sites within most patients.[122] Further, another study in HGSC showed tumor and metastatic sites within a patient contain a homogenous T cell repertoire as compared to peripheral blood.[121] If the same T cells are found in

numerous tumor sites yet the repertoire is distinct from that of peripheral blood, it raises the possibility that TIL may recognize shared features between distinct tumor sites within the patient. Together, this suggests the anti-tumor immune response may contend with high ITH in recurrent disease by targeting shared features of tumor clones.

1.3.3.2 Temporal Dynamics of the Anti-Tumor Immune Response

The same selective pressures that act on tumors can also exert selective pressure on anti-tumor T cells. Tumor genetics influence tumor antigen expression, which subsequently influences anti-tumor T cell populations. Further, chemotherapy and radiation treatment may induce profound effects on the immune response to tumors through improvements in antigen presentation and immune cell recruitment to the tumor microenvironment, or alternatively, inducing immune cell death and suppressing anti-tumor immune responses.

Chemotherapy agents lead to extensive cell death in chemoresponsive tumors. Apoptotic bodies from dying tumor cells can express antigens.[123] Further, apoptotic bodies likely get phagocytosed by APCs, which traffic to the lymph nodes to present antigens to T cells and stimulate an anti-tumor immune response.[123] Notably, in a murine ovarian cancer model, cisplatin improved recruitment of macrophages and CD8+ tumor-reactive TIL and also reduced the overall immunosuppression in the tumor microenvironment.[124] Further, one study showed that gemcitabine, a common chemotherapy agent used for treating recurrent tumors, increased tumor-antigen cross-presentation and induced antigen-specific T cell expansion *in vivo*.[123] This suggests that chemotherapy may increase the amount of antigen presented to the adaptive immune system and raises the possibility that T cell responses to the tumor may become more robust and polyclonal following chemotherapy.

A recent study from our lab described changes to the immune infiltrate in HGSC cases with matched pre- and post-chemo samples.[125] Following platinum- and taxane-based chemotherapy, patients who had immune infiltrate prior to treatment had an increase in $CD3^+$, $CD8^+$, and $CD20^+$ TIL subsets. Further, TIL expressed increased levels of functional makers such as TIA-1 and PD-1.[125] Tumors that had no TIL prior to chemo had no change in immune infiltrate post-chemotherapy. These results suggest that chemotherapy may bolster an existing anti-tumor immune response, however this improved infiltration could be due to trafficking of non-tumor-specific immune cells to a highly inflamed environment. Thus, tumors may express barriers to TIL infiltration that are not circumvented by chemotherapy.

Radiation is also known to induce *de novo* anti-tumor immunological responses. A number of reports have demonstrated that radiation treatment of target lesions can also lead to the regression of non-irradiated lesions (reviewed in Kalina *et al*).[126] This phenomenon is called the abscopal response and has been observed in numerous tumor types, such as lymphoma,[127] hepatocellular carcinoma,[128] melanoma,[129] renal cell carcinoma,[130] and lung cancer.[131] It has been hypothesized that the abscopal response is mediated by a systemic anti-tumor immune response.[132] Indeed, there are numerous reports showing that radiotherapy improves responses to immunotherapies such as checkpoint blockade or vaccination.[133–136] Even with treatment only to metastatic lesions (such as occurred with one of our study patients, IROC 106) systemic anti-tumor immune responses may be unleashed that shape the T cell landscape within the patient over time.

1.3.4 Co-Evolution of Tumors and the Anti-Tumor Immune Response

Tumor clonal evolution and the evolution of the associated anti-tumor immune response are dependent on one another. The immune system can exert pressure on the tumor by eliminating highly immunogenic tumor cell clones, while poorly immunogenic tumor cell clones remain. Additionally, tumor cells may exert pressure on immune cells by developing an immunosuppressive phenotype or recruiting immunosuppressive cells to the TME. This may lead to the deletion of tumor-reactive T cell clones from the patient repertoire. Therefore, changes to both populations of tumor cells and reactive T cells are intimately related, suggesting they may co-evolve. These concepts are exemplified in the concept of immunoediting and tumor-mediated immunosuppression, which are discussed below.

1.3.4.1 Immunoediting

The concept of immunoediting builds upon the foundational concept of immunosurveillance. It has long been hypothesized that tumors should be much more common in immunocompromised members of long-lived species, such as humans.[113,137,138] Indeed, in mice with impaired interferon responses and perforin deficiencies, spontaneous tumors are more prevalent.[139,140] Further, tumors grown in immunocompromised mice had a greater number of antigens than tumors grown in immunocompetent mice.[141] These results helped to highlight the importance of the immune system in tumor development, and gave rise to the idea of immunoediting. Immunoediting is the process by which the immune system shapes the tumor through elimination of more immunogenic tumor cell clones, while selecting for less immunogenic clones. For example, immunoediting has been implicated in tumor

progression of a human tumor following vaccination against the CT antigen, NY-ESO-1.[142] Thus, immunoediting is a significant challenge for immunotherapy.

The process of immunoediting is divided into three phases: elimination, equilibrium, and escape.[103] First, in the elimination phase, the tumor secretes multiple types of danger signals, such as IL-2, TNF-α, and type I interferons, which elicit both an innate and adaptive immune response that leads to destruction of immune cells in the TME. Elimination is contingent on both the presence of antigen, and anti-tumor T cells that are capable of eradicating tumor cells. Once tumors reach a certain size they start to invade surrounding tissue, which leads to the subsequent release of multiple signals, including inflammatory signals that recruit innate immune cells, along with additional adaptive immune cells into the TME, further promoting anti-tumor immunity. However, the immune response places selective pressure on the tumor, fostering the development of tumor cells that are poorly immunogenic, and this leads to the equilibrium phase.[104,105,113] During the equilibrium phase, there is a no change in the number of highly immunogenic tumor cells versus poorly immunogenic tumor cells, because the rates of tumor cell proliferation and immune-mediated tumor cell killing are in balance.[103] However, as chronic antigen stimulation abrogates the anti-tumor immune response, and/or as tumor cells acquire features that may allow for rapid growth of tumor cells that evade the immune response, the tumor enters the last phase, immune escape.[104,105,113] Immune escape can be through various mechanisms, such as antigen-loss[142] or down-regulation of the antigen processing[143] and presentation[144] machinery.

Immunoediting is a challenge for immunotherapy because it is hypothesized that what is often observed upon initial diagnosis is the immunoedited, "escaped" tumor.[105,113] As such, in patients with a late stage, aggressive tumor, such as those with HGSC,[75] it is possible that due to complete immune-mediated elimination of highly immunogenic tumor cell clones few cells remain that can be recognized by T cells. This presents challenges for developing immunotherapies for more advanced, or recurrent, forms of HGSC. Further, it highlights the importance of understanding the dynamic relationship between tumors and anti-tumor T cells, to give the best possible chance of mediating clinical responses using immunotherapy.

1.3.4.2 Tumor-Mediated Immune Suppression

Immune suppression can occur through various mechanisms that fall under two broad categories: (a) the triggering of inhibition through immunological checkpoints and (b) creation of an immunosuppressive TME. These two concepts are described below.

1.3.4.2.1. Immunological Checkpoints

Various immunological "checkpoints" exist to stop the development of potentially damaging, over-exuberant immune responses.[145,146] Many checkpoint molecules are part of the B7 family of molecules. Two of the most well-studied in the field of cancer immunology are PD-1 with its ligands PD-L1 and PD-L2,[29] and cytotoxic T-lymphocyte-associated antigen-4 (CTLA-4).[147] Both molecules function to attenuate immune responses, and in particular they help to maintain peripheral tolerance.[145] However, these checkpoints can be exploited as immune-evasion strategies by malignant cells. Therefore, much attention has been paid to studying these proteins in cancers, in order to develop robust cancer therapies.[148–150]

CTLA-4 and PD-1 share similar overall functions, however, the mechanisms by which each suppress the immune response are different. Like PD-1, CTLA-4 functionally suppresses T cells. It directly inhibits co-stimulation by blocking the interaction between the co-stimulatory molecule CD28 and its ligands CD80 (B7-1) and CD86 (B7-2) due to higher affinity over CD28. On effector T cells, CTLA-4 is upregulated rapidly and peaks at 6 hours following T cell activation.[151] In contrast, CTLA-4 is constitutively expressed on Tregs. Tregs expressing CTLA-4 have been shown to cause down-regulation of CD80 and CD86 on DCs, thus abrogating APC-mediated activation of effector T cells.[152] Mice deficient in CTLA-4 have severe immune dysregulation that leads to a fatal wasting disease,[153,154] demonstrating that CTLA-4 has a critical role in the maintenance of peripheral tolerance.

PD-1 is an inducible regulatory molecule that functions to indirectly suppress T cell effector functions by preventing phosphorylation of CD28. PD-1 is upregulated following TCR stimulation and peaks around 48-hours post-stimulation. To mediate suppression, PD-1 interacts with its own specific ligands, PD-L1 and PD-L2. Interactions between PD-1 and its ligands are thought to mediate peripheral tolerance. For example, mice that are PD-1 deficient develop lupus-like proliferative arthritis, as well as glomerulonephritis.[155] PD-L1 can be expressed on normal epithelial and endothelial cells,[31,156] as well as tumor cells and macrophages found within the tumor microenvironment. PD-L1 is up-regulated through the IFN-γ response pathway,[156] and as such it is often expressed on cells found in areas of inflammation.[157] PD-L2 expression is also IFN-γ inducible; however, expression patterns appear more restricted to DCs and mast cells.[30] When PD-1 interacts with its ligands, it activates SHP-2, which in turn dephosphorylates CD28, thereby preventing the necessary co-stimulation required for T cell activation.[26–28] Further, PD-L1 can be significantly up-regulated on tumor cells, including melanoma, non-

small cell lung carcinoma, and colorectal cancer.[158] Additionally, APC within the microenvironment can express PD-L1, particularly in ovarian cancer.[88]

PD-1 expression may also demarcate tumor-reactive T cells. Three studies have shown prospective identification of tumor-reactive T cells by selection of PD-1$^+$ TIL or peripheral T cells.[47,159,160] The first study found PD-1$^+$ TIL were highly enriched for both tumor- and neoantigen-specific T cells.[160] The second study found circulating PD-1$^+$ T cells from 4 melanoma patients were highly enriched for neoantigen-specific and germline-antigen-specific T cells in 3 of 4 patients studied.[159] The third study from the same group used TCRβ deep sequencing on HPV$^+$ cervical cancer patients' peripheral blood and found HPV-reactive, neoantigen-reactive, and CT-antigen-reactive T cells were all enriched within the PD-1$^+$ subset of peripheral T cells.[47]

Checkpoint blockade has been gaining fast ground in the clinic due to the striking survival benefit seen in patients.[161] Many of these therapies are in various stages of development and/or clinical trials. The two most prevalent types of therapies target either the PD-1/PD-L1 interaction or the CTLA-4/B7-1 interaction. Clinical success of both PD-1/PD-L1 and CTLA-4 blockade has largely been reported in melanoma.[161] Despite this success, clinical responses in other tumor types have been much more moderate, such as in HGSC,[162] or even completely absent, as seen in a recently published clinical trial in advanced non-small cell lung cancer.[163] Nonetheless, since February of 2017, there have been 7 FDA-approvals for use of checkpoint blockade in numerous cancer settings,[164] highlighting both the reality and promise of checkpoint blockade therapies for cancer.

Recently, several papers have been published highlighting a few mechanisms involved in resistance to checkpoint blockade.[165–169] First, Zaretsky *et al* studied four cases of advanced melanoma, which had initial responses to anti-PD-1 therapy followed by delayed relapses.[165] In three of the four cases there was impairment of an immune response pathway. Two patients had mutations in either the Janus kinase (JAK) 1 or JAK2 genes that resulted in an impaired IFN-γ response pathway. The third patient had a truncating mutation in the β2-microglobulin gene resulting in a loss of surface MHC class I expression. In the fourth patient, a mechanism of resistance could not be specifically identified.[165] A second, more recent study also found loss-of-function mutations in both JAK1 and JAK2 that contributed to PD-1 blockade resistance in both melanoma and mismatch repair-deficient colorectal cancers.[168] A third study found melanoma tumors that were resistant to anti-CTLA-4 therapy were deficient in IFN-γ pathway genes such as IFNG1 and IFNG2, the IFN-γ receptor components, interferon response factor 1 (IRF1), and JAK2. A fourth study found resistance to anti-PD-1 therapy in lung cancers was due to the

upregulation of an alternate immunosuppressive pathway, T-cell immunoglobulin mucin-3 (TIM-3).[167] TIM-3 mediates T cell suppression by recruiting SH2-domain binding Src kinases Bat3 and Fyn that subsequently suppress TCR signaling.[170,171] Last, a study on sequential CTLA-4 and PD-1 blockade found resistance to both checkpoint blockades was associated with high copy number loss and decreased expression of various immune related genes.[169] In summary, triggering robust immune responses in patients using checkpoint blockade can mediate changes to the tumor that may prevent further T cell recognition and thus may have profound implications on anti-tumor immunity.

1.3.4.2.2 Immunosuppressive Tumor Microenvironment

The tumor microenvironment can be highly immunosuppressive. One mechanism tumors utilize to mediate this is attracting cells such as Tregs,[172] myeloid-derived suppressor cells (MDSC),[173] plasmacytoid dendritic cells (pDC),[174] and tumor-associated macrophages (TAMs).[175] Tregs,[172] which are particularly found in tumors that also have $CD8^+$ T cell infiltration,[176] can lead to direct inhibition of effector T cell responses in the TME through expression of CTLA-4 and TGF-β.[83,177] Further, tumors can have dense infiltration of MDSC,[173,178–180] which suppress $CD8^+$ and $CD4^+$ effector T cells through the release of arginase and reactive oxygen species such as iNOS.[181,182] Plasmacytoid DCs[174,183,184] are also found in tumors and mediate immunosuppression through various mechanisms including secretion of indolamine 2,3-dioxygenase 1 (IDO-1),[185] promotion of Treg development,[183] and stimulation of a regulatory phenotype in $CD8^+$ T cells.[184] TAMs have also been implicated in promoting an immunosuppressive TME. TAMs secrete cytokines, such as IL-10, which in turn suppress T cell responses.[175] In fact, TAMs have been associated with acquired resistance to checkpoint blockade therapy, highlighting their role in immunosuppression of anti-tumor T cell responses.[186] Further, tumors may also contain suppressive cells of non-hematopoietic origin, such as cancer-associated fibroblasts (CAF)[187,188] and mesenchymal stem cells (MSC).[189,190] CAF promote immune suppression through the expression of CXCL12 and subsequent exclusion of T cells from the TME,[188,191] whereas human MSC promote immune suppression through secretion of IDO-1.[192,193]

Tumor cells themselves can also express immunosuppressive molecules including IDO-1 and TGF-β.[194,195] IDO-1 is one of two enzymes responsible for the degradation of tryptophan. Tryptophan catabolism leads to the production of metabolites called kynurenines, which may be toxic to T cells.[195] Further, tryptophan is an essential amino acid and depletion from the TME limits the metabolism of all cells, including TIL.[196] IDO-1 is mainly expressed by pDCs as a consequence of inflammation,[185] but it can

also be expressed by tumor cells to mediate immune suppression.[197] TGF-β is an immunosuppressive cytokine that can be secreted by both cancer cells and immune cells. TGF-β is known to both promote the differentiation of Tregs[198] and suppress the effects of $CD8^+$ T cells.[199,200] In summary, there are numerous mechanisms tumors utilize to escape immune-mediated killing and these all may hinder attempts at targeting tumors with immunotherapies.

1.3.5 HGSC Ascites

Many studies of recurrent HGSC are limited by lack of recurrent tumor specimens.[75] Most HGSC patients have a single cytoreductive surgery which is performed shortly after initial diagnosis. It is uncommon for HGSC patients to undergo surgery at relapse because there is no expected clinical benefit.[201] However, patients with advanced HGSC often develop ascites. Malignant ascites consists of peritoneal fluid, various soluble factors, antibodies, and cells including tumor cells, lymphocytes, and leukocytes such as macrophages, monocytes, and dendritic cells.[202] The composition of malignant ascites can vary between patients as well as between disease time points within a single patient. There is a high variability in tumor cell content, with some patients having minimal (<1%) tumor cell content while others have high levels of tumor cells in the ascites (>30%). Further, many of these tumor cells are part of large floating aggregates of tumor cells called tumor rafts.[202,203] Therefore, malignant ascites can be used as a source of recurrent tumor and tumor-associated lymphocytes (TAL).

There is evidence suggesting ascites tumor cells are representative of solid epithelial tumor cells in HGSC. First, tumor cells from the ascites display abnormal p53 expression, a hallmark of ovarian cancer.[204] Second, ascites cells can express high levels of epithelial markers, such as epithelial cell adhesion molecule (EpCAM) and E-cadherin, and exhibited epithelial morphology.[203] Further, these cells developed into invasive intraperitoneal tumors in nude mice after intraperitoneal injection of single cell suspensions.[203] Together, this shows ascites can be used as a source of tumor cells for studying HGSC.

There is evidence that TAL are enriched for tumor-reactivity. Notably, Ye *et al* identified tumor-reactive T cells within the TAL population in ovarian cancer patients, with some patients' TAL containing up to 12% tumor-reactive T cells.[40] Although the enrichment of tumor-reactive T cells in TAL was less than the enrichment identified in TIL, both TIL and TAL were highly enriched for tumor-reactive T cells compared to peripheral blood.[40] Additionally, a separate study in HGSC identified tumor-reactive T cells in the ascites of one patient.[49] Therefore, ascites is a good source of tumor and TAL to study anti-tumor T cell responses in HGSC.

There has been a focus on $CD8^+$-mediated anti-tumor immune responses. This is largely due to the direct cell killing mediated by CD8+ T cells, as well as the ability of $CD8^+$ T cells to recognize antigen in the context of MHC class I^+. Despite this, some studies have highlighted the importance of tumor-specific $CD4^+$ T cells.[11,43,47] Notably, Tran *et al* described a case where a patient with a relapsed cholangiocarcinoma tumor following ACT was re-treated with a >95% CD4+ T_H1 mutation-specific T cell population and experienced a second tumor regression.[11] A significant challenge for studying tumor-specific $CD4^+$ T cells is the reduced expression or lack of MHC class II expression on tumor cells. To overcome this barrier, malignant ascites, which contains MHC class II^+ antigen-presenting cells,[202,203] could be used to elicit and observe tumor-specific CD4+ T cell responses that are otherwise undetected by assessing recognition of tumor cells only.

1.4 Adoptive Cell Therapy

1.4.1 Successes of ACT

Adoptive cell therapy (ACT) for cancer involves the transfer of large numbers of immune cells (10^9-10^{11}) with cancer-specific reactivity. ACT in human tumors has yielded mixed results. The first trial in humans was conducted in 15 melanoma patients by Dr. Steven Rosenberg in 1988.[205] This study observed objective clinical responses that lasted between 2 and 13 months in 9 out of the 15 patients and was the first indication that adoptive transfer of cells could mediate tumor regressions in the context of metastatic melanoma.[205] The success of ACT was substantially improved after the adoption of pre-ACT lymphodepletion, which significantly improved TIL persistence *in vivo* post-infusion.[206] Subsequent clinical trials between 1998 and 2013 in melanoma have yielded objective responses in 34-56% of patients.[12] Such success in melanoma has spurred the development of ACT for other types of tumors. In fact, a search of www.clinicaltrials.gov for "TIL Therapy," resulted in 98 active studies in many different tumor types, 79 of which are actively recruiting. However, previous clinical trials in non-melanoma tumors show other tumor types do not seem as amenable to ACT therapy, as trials in colorectal cancer,[207] renal cell carcinoma,[208] ovarian cancer,[209–212] and cervical cancer[10] have all had more modest response rates. Particularly, two reports of ACT of TIL in ovarian cancer have shown encouraging initial responses, however complete responses to TIL have been few. In the first study, one of seven patients had a complete response and four of seven patients had an over 50% reduction in tumor size.[209] However, these results were relatively short-lived, lasting only three to five months.[209] This study also evaluated concurrent chemotherapy and ACT and found it mediated robust clinical

responses lasting over 15 months in some patients.[209] A second study from the same institution found ACT of TIL following chemotherapy induced long periods of remission compared to patients treated with chemotherapy only.[212] Despite these encouraging preliminary results, TIL alone failed to elicit long-term clinical responses. Therefore, improved strategies for treating HGSC with ACT are needed.

1.4.2 Approaches to ACT

ACT has been conducted in several ways. The classical ACT protocol uses TIL propagated from fresh tumor digests or fragments using high-dose IL-2.[213] This method builds on the fact that T cells require antigen stimulation and growth signals from IL-2 to proliferate.[2] Therefore, by adding only exogenous IL-2 at high doses, this method of expansion is thought to allow for preferential expansion of tumor-reactive TIL. Following high-dose IL-2 expansion, cultures that recognize either autologous tumor cells or tumor antigens are selected and further expanded to high numbers using the Rapid Expansion Protocol (REP).[213] However, these approaches lead to terminally differentiated T cells that may not be ideal for mediating long term responses to ACT.[214]

Other trials have attempted to improve ACT by using TIL that display a less differentiated phenotype. Approaches to generating "young" T cells include limiting culture time to 3-fold less than the culture time for classical TIL generation or the addition of cytokines that may maintain less-differentiated phenotypes.[215,216] Clinical trials using less-differentiated TIL have elicited more robust clinical responses compared to treatment with classical TIL.[217,218] The success of these approaches has led to ongoing research to find additional approaches to limiting terminal differentiation of TIL *in vitro* and subsequently maximizing clinical responses to ACT.

Other studies have used TCR sequences identified from tumor-reactive T cell clones and engineered autologous peripheral T cells to express these TCRs.[43,219] For example, T cells engineered to express TCRs that recognize NY-ESO-1 were used to treat NY-ESO-1^{+} multiple myeloma tumors and mediated encouraging clinical responses in 80% of patients.[220] Another trial used engineered T cells that expressed a TCR specific for "melanoma antigen recognized by T cells-1" (MART-1) elicited durable clinical responses in 2 of 15 patients treated.[221] Together, these results suggest ACT using engineered T cells represent a promising option for improving ACT.

Clinical trials of chimeric antigen receptor (CAR)-expressing T cells have been incredibly successful in the setting of acute lymphoblastic leukemia (ALL), achieving complete response rates reaching 90%.[222,223] CARs are engineered molecules that contain an external single-chain variable

fragment (scFv) linked to one or more signaling domains of costimulatory molecules such as CD137 or CD28, and the TCR intracellular signaling domain CD3ζ. The scFv molecule is a fusion protein of the heavy and light chain variable regions from an antibody that confers antigen specificity of the CAR molecule.[224] The most commonly used CAR construct recognizes CD19, a B-cell specific antigen,[225] and has been used in the setting of B cell malignancies such as ALL and chronic leukocytic leukemia (CLL).[222] Current research is directed to identifying new CAR T cell targets, such as carboxy-anhydrase-IX (CAIX) and mesothelin, however responses to these CAR T cells have been limited.[226,227] Therefore, despite the diversity of approaches used for ACT, and the resounding successes seen in CD19-CAR T cell therapy of ALL and TIL therapy of melanoma, clinical responses in the majority of tumor types are rare, modest, and short-lived.

1.4.3 Challenges of ACT

Despite clinical trials of ACT starting nearly two decades ago, challenges remain for mediating durable, complete tumor regressions. First, some patient's TIL expand poorly *in vitro* and therefore fail to yield enough cells for infusion.[208] Second, TIL can have poor persistence post-infusion. This is thought to be due to the terminally differentiated phenotype of typical TIL for infusion[214]. Third, some tumors lack good T cell targets, particularly HGSC, due to low or moderate mutation burden.[228] Therefore, efforts should be made to identify targets amenable to immunotherapy that do not rely on the overall mutation burden of tumors. Fourth, with engineered T cell strategies, there have been numerous severe toxicities reported. In CAR T cell therapy, cytokine release syndrome is nearly ubiquitous,[222] and several off-target toxicities have been reported, including some that have been fatal.[229,230] Further, there are reports of severe and fatal neurotoxicity in patients who received engineered T cells specific for MAGE-A3.[231] Perhaps the biggest challenge for ACT is the fact that these clinical trials are done on recurrent or refractory disease. These patients will likely have failed numerous prior therapies, suggesting their tumors may be treatment resistant, have limited tumor antigen expression, and/or display a highly immunosuppressive phenotype.[107,112] Therefore, optimal protocols for the treatment of recurrent disease using ACT are required.

1.5 Previous literature on temporal changes to anti-tumor immune responses

It is important to understand the mechanisms used by T cells to control ITH to improve ACT therapies of recurrent disease. Two studies have shown that tumor-reactive T cells emerge over time concomitantly with their cognate tumor antigen. However, they also found that both neoantigens and neoantigen-reactive T cell clones were lost over time. Despite this finding, Verdegaal *et al* (Nature 2016)[48] determined that TIL from all disease time points were able to recognize tumor from all disease time points in two melanoma cases.[48] Further, as described above, the T cell responses to spatially distinct tumor sites in HGSC patients, irrespective of ITH, are largely homogeneous.[121,122] Together, these results suggest the anti-tumor T cell response may target common features shared by primary and recurrent disease to contend with ITH. Indeed, if this is the case, ACT using primary TIL to treat recurrent tumors should elicit strong, durable clinical responses in HGSC. However, in previous ACT trials of HGSC, this was not the case,[209,210] suggesting other factors may contribute to T cell responses to heterogeneous tumors. To develop improved protocols for ACT of recurrent tumors that elicit stronger, more durable clinical responses, I aimed to determine the predominant mechanisms by which tumor-reactive T cells respond to ITH in HGSC.

1.6 Chapter 1 Summary, Aims, and Hypothesis

In summary, T cells can produce specific, robust immune responses against tumors. These anti-tumor T cell responses are mediated by tumor antigens, such as viral proteins, CT antigens, and neoantigens. Further, the presence of TIL in tumors, such as HGSC, confer prognostic benefit, highlighting the important role of T cells in tumor control. Despite the positive prognostic effect of TIL in HGSC, the survival rate remains low, suggesting T cells encounter challenges in controlling tumors completely.

One possible explanation for this is the high rate of ITH in HGSC tumors. Indeed, studies have shown HGSC tumors may lose tumor antigens over time and display phenotypes and contain cells that are associated with immunosuppression.[49,88,109,176,180,184] Further, two studies found tumor-reactive T cells are dynamic over time,[48,49] perhaps to contend with the increased immunosuppression and varied antigen expression. Based on these studies in HGSC and melanoma,[48,49] I hypothesized that new T cell clones would emerge over time to respond to ITH. In this study, I had two specific aims. The first aim

(chapter 2) was to identify differences in anti-tumor T cell responses between primary and recurrent disease to determine how patterns of tumor-recognition change over time in HGSC patients. The second aim (chapter 3) was to profile the clonal repertoire of purified populations of tumor-reactive T cells from primary and recurrent disease to determine how these T cell populations change over time.

ACT for HGSC is conducted on recurrent disease, yet it is unknown what the best T cell population is for mediating complete and long-lived clinical responses. This study will illuminate potential mechanisms utilized by TIL for long-term tumor control. Using the results from this study, we will be able to design optimal ACT protocols for the treatment of recurrent tumors to improve the chances of eliciting more complete and durable responses in HGSC patients. Ultimately, with optimized ACT protocols, we aim to improve survival rates for patients with HGSC.

Chapter 2: Changes in Tumor-Reactive T Cell Populations from Primary and Recurrent HGSC Ascites

Nicole S. Little[1,2], Spencer D. Martin[2,3], Victoria P. Hodgson[2], David R. Kroeger[2], Julie S. Nielsen[2], Darin A. Wick[2], John R. Webb[2], and Brad H. Nelson[1,2]

[1]Department of Microbiology and Biochemistry, University of Victoria, Victoria, B.C., Canada

[2]Trev and Joyce Deeley Research Centre, BC Cancer Agency, Victoria, B.C., Canada

[3]Faculty of Medicine, University of British Columbia, Vancouver, B.C., Canada

BHN and NSL conceptualized the study. NSL conducted the project. VPH assisted with some tissue culture and some ELISPOT development. SDM, DRK, JSN, DAW, JRW, and BHN contributed to both experimental design and scientific suggestions. NSL wrote the chapter. All specimens were collected by The Tumour Tissue Repository (TTR) and were accessed retrospectively for this study.

2.1 Abstract

Background: There is a strong association between tumor-infiltrating lymphocytes (TIL) and survival in high-grade serous carcinoma (HGSC). However, HGSC can change dramatically between primary and recurrent disease due to various selective pressures that lead to extensive intratumoral heterogeneity (ITH). Previous studies in melanoma and HGSC showed tumor-reactive T cell clones fluctuate over time with their cognate tumor-antigens. Therefore, I hypothesized patients would share a common mechanism of T cell evolution to contend with ITH in HGSC. If this is so, I expect to see similar patterns of tumor recognition between primary and recurrent disease.

Methods: Tumor-associated lymphocytes (TAL) were expanded from primary and recurrent ascites samples using high-dose IL-2 and a rapid-expansion protocol (REP). Following expansion, TAL were assessed for recognition of autologous tumor by IFN-γ ELISPOT and flow cytometry for CD137.

Results: Patient TAL recognized tumor in two out of three cases. In patient IROC 060, the tumor became more immunogenic between primary and recurrent disease, which may reflect expression of new antigens and/or loss of an immunosuppressive phenotype. In patient IROC 106, the tumor remained immunogenic between primary and recurrent disease, which may reflect maintenance of stable antigen expression and immune-sensitive phenotype. Patient IROC 034 did not exhibit any tumor-reactivity, suggesting tumor-reactivity is not ubiquitous in HGSC.

Conclusions: Anti-tumor T cell responses from ascites are diverse between patients and dynamic within a patient, suggesting various mechanisms of T cell evolution to respond to ITH in HGSC.

Future Directions: Individual tumor-reactive TAL clonotypes will be tracked over time by sequencing T cell receptors of FACS-purified $CD137^{+}$ tumor-reactive subpopulations.

Significance: This study provides early insights into how TAL contend with ITH in HGSC. Ultimately, these results will inform the design of adoptive T cell therapy for recurrent HGSC.

2.2 Introduction

Despite the low survival rate of HGSC,[75] the presence of $CD3^+$ and $CD8^+$ tumor-infiltrating T lymphocytes (TIL) is associated with superior prognosis.[7,84] There have been several reports of direct T cell recognition of tumor antigens and tumor cells,[49,67,68] indicating the immune system can play a direct role in mediating tumor control in HGSC patients. Further, immunotherapies have elicited clinical responses in some HGSC patients.[210,212,232,233] Despite the success in some patients, it is unknown why clinical responses to immunotherapy have been rare and modest in HGSC.

One possible explanation for these modest responses lies in the high spatial and temporal intratumoral heterogeneity (ITH) of HGSC tumors. One study evaluated multiple tumor sites within three HGSC patients and found gene expression profiles, copy number, and mutation variation was high between tumor sites.[108] For example, one patient had eight distinct tumor subclones that were present within five separate tumor sites throughout the peritoneal cavity.[108] Despite the heterogeneity between tumor sites, the immune infiltrate in each tumor site seems to be relatively homogeneous,[121,122] suggesting the immune response to HGSC may respond to shared features shared by each tumor subclone, rather than unique subclonal features. Further, HGSC tumors can exhibit temporal ITH.[107] In particular, one study described an HGSC patient, who had dramatic responses to platinum-based chemotherapy, lost an entire tumor subclone while concomitantly gaining a new, prominent, tumor subclone between primary and recurrent disease.[107] Further study on this patient found the co-emergence of a neoantigen and cognate T cell pair at first recurrence.[49] Another study of two melanoma patients also found neoantigens and their cognate T cell clones emerged together between primary and recurrent disease.[48] However, the predominant mechanisms by which anti-tumor T cells contend with ITH in HGSC is unknown.

In this study, I investigated the dynamics of anti-tumor T cell responses in three HGSC patients. I expanded tumor associated T lymphocytes (TAL) from primary and recurrent ascites and evaluated their reactivity to both primary and recurrent tumor from ascites using IFN-γ ELISPOT and flow cytometry for CD137. Based on previous studies, I hypothesized patients would share a common mechanism of T cell evolution to contend with ITH in HGSC. Here I show tumor recognition patterns are diverse between to HGSC patients and dynamic within a patient over time, suggesting the anti-tumor T cell response utilizes various mechanisms to respond to ITH in HGSC.

2.3 Methods

Patient Selection and Recruitment

Patient specimens and clinical data were collected with informed written consent through a prospective study in partnership with the BC Cancer Agency's Tumour Tissue Repository (TTR) called the Immune Response to Ovarian Cancer (IROC). Study ethics approval was granted by the BC Cancer Agency and University of British Columbia Research Ethics Board. All patients had a diagnosis of HGSC and had ascites specimens available from primary and recurrent disease timepoints. Patients IROC 060, IROC 106, and IROC 034 underwent standard surgical debulking followed by carboplatin-based chemotherapy. After recurrence, patients were treated with additional cycles of carboplatin-based chemotherapy and one patient (IROC 106) was additionally treated with radiation treatment for metastases.

Specimens used in this study were accessed retrospectively through the TTR and IROC. Ascites was collected by the TTR at time of primary surgery or through palliative paracentesis. Isolation of ascites cells was done by centrifugation. Ascites cells were cryopreserved in 50% fetal bovine serum (FBS), 40% freezing media (RPMI 1640 (Gibco cat no. 22400-089), 10% FBS, 25 mM HEPES, 300 mg/L L-glutamine, and 50 µM β-mercaptoethanol), and 10% dimethyl sulfoxide (DMSO). Peripheral blood was collected by the TTR prior to surgery and chemotherapy treatment. Peripheral blood mononuclear cells (PBMC) were prepared by Ficoll density centrifugation using SepMate tubes (StemCell Technologies; Cat No. 15465) and cryopreserved. Samples with a high density of erythrocyte contamination were subjected to ammonium-chloride-potassium (ACK) lysis prior to cryopreservation. Both ascites cells and PBMC were stored in the vapour phase of liquid nitrogen.

Cell Lines and Culture

To generate tumor-associated lymphocyte (TAL) cell lines, bulk ascites cells were thawed and cultured in complete media (RPMI 1640 (Gibco cat no. 22400-089), 10% pooled human AB male serum, 100 µg/mL penicillin-streptomycin, 50 µg/mL gentamicin, and 50 µM β-mercaptoethanol) at $1x10^6$ cells/mL in the presence of 6,000 U/mL human interleukin-2 (IL-2; Novartis; DIN 02130181) at 37°C and 5% CO_2. Cultures were maintained by adding fresh complete media with IL-2 every 2-3 days and split when concentrations rose above $2x10^6$ cells/mL. After 14 days, IL-2 expanded TAL lines were rested in complete media supplemented with 300 U/mL IL-2 and 10 ng/mL interleukin-7 (IL-7; Peprotech cat no.

200-07) for 2-3 days before cryopreservation in 50% human AB male serum, 40% complete media, and 10% DMSO.

Following high-dose IL-2 expansion, TAL were thawed and further expanded *in vitro* using the rapid expansion protocol (REP^{234}) in complete media with 30 ng/mL OKT3 (eBioscience cat no. 16-0037) and 300 U/mL IL-2. Cultures were maintained by adding fresh complete media with IL-2 every 2-3 days and cultures were split when concentrations rose above $1x10^6$ cells/mL. After 14 days, TAL lines were rested in complete media supplemented with 1 U/mL IL-2 and 10 ng/mL IL-7 for 2-3 days before cryopreservation. Additional REPs were performed as needed.

OVCAR8 cells and HeLa cells were cultured separately in high-glucose Dulbecco's Modified Eagle Medium (DMEM; Gibco cat no. SH30022.01) supplemented with 10% fetal bovine serum (FBS), and 100 µg/mL penicillin-streptomycin. Cells were grown at 37°C and 5% CO_2 and were split when they reached confluency. When indicated, cells were incubated with 100 U/mL recombinant human IFN-γ (Peprotech cat no. 200-02) for 24 hours at 37°C and 5% CO_2 prior to trypsinizing and flow cytometric analysis of HLA expression.

Ascites and tumor cell lines from IROC 060 and IROC 106 were kindly donated by Dr. Maartje Wouters. To generate tumor cell lines from ascites and disaggregated tumor, bulk ascites or bulk disaggregated tumor cells were washed in PBS, pelleted, and resuspended in Renaissance Essential Tumor Media (Cellaria cat no. CM-0001) supplemented with RETM-supplement (Cellaria), 0.25 µg/mL cholera toxin (Sigma cat no. C8052), 1% FBS, and 1% penicillin streptomycin. Cells were seeded into a T25 flask and once the cells reached confluency, split into a T75 flask. If the culture had significant fibroblast contamination, a partial trypsinization was performed. Briefly, following a short trypsinization period (approximately 2 minutes), any detached cells, which were highly enriched for fibroblasts, were removed. All remaining attached cells were left in culture. Once a clean tumor culture was established, the FBS was slowly raised in 1% increments up to 5% final FBS concentration.

Flow Cytometric Analysis of TAL Lines, Tumor Lines, and Ascites Samples

Bulk ascites and TAL lines obtained following the high-dose IL-2 expansion and REP were assessed by flow cytometry for expression of CD3 (Biolegend cat no. 317332), CD56 (BD cat no. 560361; eBioscience cat no. 11-0566), CD8 (Biolegend cat no. 300906 or 301036), CD4 (Biolegend cat no. 357404 or 317444), CD103 (eBioscience cat no. 11-1037), CD137 (Biolegend cat no. 309810), and PD-1 (eBioscience cat no. 25-2799). Samples were run on a Becton Dickinson FACSCalibur.

Purity of tumor cells from bulk ascites following the CD45 depletion (below) was assessed by flow cytometry for the following markers: EpCAM (eBioscience cat no. 12-9326 or 46-9326), CD45 (Biolegend cat no. 304012, eBioscience cat no. 12-9459, or 46-0459), CD14 (Biolegend cat no. 301842), PD-L1 (eBioscience cat no. 25-5983), HLA-ABC (BD cat no. 561346 or 565291), and HLA-DR,DP,DQ (Biolegend cat no. 361706 or BD cat no. 564244). Tumor cell lines were analyzed following pre-treatment with IFN-γ for expression of HLA-ABC (BD cat no. 561346 or 565291), HLA-DR,DP,DQ (Biolegend cat no. 361706 or BD cat no. 564244), and PD-L1 (eBioscience cat no. 25-5983).

Purification of Tumor Cells from Bulk Ascites

To isolate tumor cells, $CD45^+$ cells were depleted from bulk ascites using magnetic beads (Miltenyi MACS cat no. 130-045-801) according to the manufacturers' protocol with the following exceptions: (a) to prevent column clogging, samples were filtered through a 100 µm filter followed by a 40 µm filter prior to loading the column to remove any large tissue clumps and tumor rafts.[202,203] Samples were pelleted and resuspended at $2x10^7$ cells/mL, and (b) a maximum of 10^7 cells were loaded per LS column to prevent clogging.

Following the separation, the $CD45^-$ and $CD45^+$ fractions were each pooled, centrifuged, and resuspended in complete media. To increase tumor cell expression of HLA molecules prior to assessing tumor reactivity of TAL, the $CD45^-$ fraction was seeded at 10^5 cells/mL in complete media containing 100 U/mL recombinant human IFN-γ (Preprotech cat no. 200-02) and incubated for 24 hours at 37°C and 5% CO_2. The $CD45^+$ fraction of ascites was plated at 10^6 cells/mL in complete media without IFN-γ and incubated for 24 hours at 37°C and 5% CO_2. Prior to plating the tumor and TAL co-culture, the $CD45^-$ and $CD45^+$ fractions were washed three times in AIM-V serum-free media (Gibco cat no. 12055-083) and resuspended in AIM-V serum-free media at $3.5x10^5$ cells/mL.

Assessing Tumor Reactivity by IFN-γ ELISPOT and Flow Cytometry

Standard IFN-γ ELISPOT assays were performed as described previously[235] using the following reagents: MabTech IFN-γ primary coating antibody cat no. 3420-3-1000, MabTech IFN-γ secondary biotinylated antibody cat no. 3420-6-1000, Vectastain Elite ABC Kit Vector Labs cat no. PK6100, Vectastain AEC Substrate Reagent Vector Labs cat no. SK4200. TAL lines were thawed, washed in AIM-V serum free media (3 x 10mL washes; Gibco cat no. 12055-083), and plated in AIM-V serum free media at $5x10^5$ cells/well of a 96-well ELISPOT plate with or without $3.5x10^4$ target cells per well. Wells containing

anti-CD3/anti-CD28 coated beads (Dynabeads; Gibco cat no. 11131D) were used as a positive control. Co-cultures were incubated for 20 hours at 37°C and 5% CO_2. Spots were enumerated using an ELISPOT plate reader (AID GmbH). Wells with spot counts greater than 2X background were deemed positive.

When sample availability allowed, separate TAL co-cultures, identical to those in the IFN-γ-ELISPOT assay, were set up in U-bottom 96-well plates for flow cytometry. After a 20-hour incubation at 37°C and 5% CO_2, cells were harvested and stained for viability (Fixable Viability Dye V450 eBioscience cat no. 65-0863), CD3 (Biolegend cat no. 317332), CD8 (Biolegend 300906), CD4 (Biolegend cat no. 357404), and CD137 (Biolegend 309810). Flow cytometry samples were run on a BD Influx Cell Sorter or BD FACSAriaII.

Immunohistochemical Analysis of Primary FFPE Tumor Specimens:

Fresh, surgically resected tumor specimens were placed in 10% neutral buffered formalin and subsequently embedded in paraffin wax to create formalin-fixed paraffin-embedded (FFPE) tissue blocks. Staining was performed on 4 μm thick sections. Chromagens used were DAB, Ferengi Blue, and Warp Red.

For the CD3, CD8, CD20 triple stain panel, deparaffinization was done using xylene followed by a series of ethanol and dH_2O washes and slides were stained in an Intellipath FLX (Biocare Medical, Pacheco, CA). Heat-based antigen retrieval was performed in Diva Decloaker (Decloaking Chamber Plus, Biocare Medical, Concord, CA; Biocare cat no. BC-DV2004) with the following settings: P1 = 110°C for 15 minutes; P2= 100°C, fan on; fan off = 80°C. Following antigen retrieval, slides were washed in dH_2O and placed in an Intellipath FLX rack. Peroxidase blocking was done using a 5 minute peroxidased-1 wash (Biocare cat no. BC-PX968) followed by 10 minutes of non-specific blocking in background sniper (Biocare cat no. BC-BS966). Slides were washed in TBS buffer (Biocare cat no. BC-TWB945) and first round staining for CD3 (1/500, clone SP7) and CD8 (1/250; clone C8/144B) was conducted for 30 minutes in the Intellipath FLX followed by a 30-minute incubation with MACH2 anti-rabbit double stain polymer (Biocare cat no. BC-MRCT525H). Following first-round staining, slides were washed with dH_2O and incubated with SDS-glycine for 45 minutes. The diluent used was DaVinci Green (Biocare cat no. BV-PD900). Slides were again washed with TBS buffer and stained for CD20 (1/300, clone L26) for 30 minutes followed by a 30-minute incubation with MACH2 Mouse-AP polymer (Biocare cat no. BC-MALP521H). Finally, slides were counterstained using hematoxylin (1/5 dilution with dH_2O; Biocare cat no. BC-CATHEM), dried, and cover-slipped using Ecomount (Biocare cat no. EM897L).

For the PD-L1, PD-1, CD8 triple stain panel, IHC was performed as described above with the following exceptions: Antibodies used for staining were PD-L1 (1/100, clone SP142), PD-1 (1/100, clone NAT105), PD-1 and PD-L1 were stained in the first round for 60 minutes and CD8 was stained in the second round for 30 minutes.

MHC class I and class II single stains were done in a Ventana Discovery XT autostainer (Ventana, Tuscon, AZ). The protocol is the same as described above with the following exceptions: decloaking was done with the following settings: P1 = 125°C for 30 seconds; P2= 100°C, fan on; fan off = 80°C and antibodies used for staining were either MHC class I (clone EMR8-5) or MHC class II (clone CR3/43) for 30 minutes followed by a 30-minute incubation with MACH2 anti-mouse HRP polymer (Biocare cat no. MHRP520H).

2.4 Results

2.4.1 Clinical courses of the HGSC cohort

It is unknown how tumor immunogenicity and the anti-tumor T cell response change over time in HGSC patients. To evaluate this, it was necessary to select patients with multiple disease time points. Therefore, I assessed CA-125 levels from clinical data for HGSC patients and selected three patients for this study who had primary and recurrent disease. All three patients in our study cohort presented with high levels of serum CA-125 (Figure 1). IROC 060 (Figure 1A) and IROC 034 (Figure 1C) had suboptimal cytoreductive surgery (>1cm residual disease) at the time of diagnosis, whereas IROC 106 (Figure 1B) had optimal cytoreductive surgery (<1cm residual disease). All three patients received first round carboplatin and paclitaxel chemotherapy and experienced significant tumor regressions, as shown by complete reductions in serum CA-125 levels post-treatment. Despite good clinical responses, all three patients relapsed (Figure 1). Following relapse, IROC 060 had additional cycles of carboplatin with gemcitabine but developed platinum resistance and died 16-months post-diagnosis (Figure 1A). IROC 106 (Figure 1B) also was treated with additional cycles of carboplatin and doxorubicin post-relapse, but ultimately developed platinum resistance. She had further treatment with letrozole and radiation on metastatic lesions, however she died over 2 years post-diagnosis. IROC 034 (Figure 1C) was the only patient to have two tumor recurrences. At first recurrence, she was treated with carboplatin and doxorubicin, which induced another strong tumor regression. However, she relapsed a second time and with no further treatment she succumbed to her disease nearly three years post-diagnosis. At both primary and recurrent disease, all three patients developed ascites, which was collected and cryopreserved for evaluation in this study.

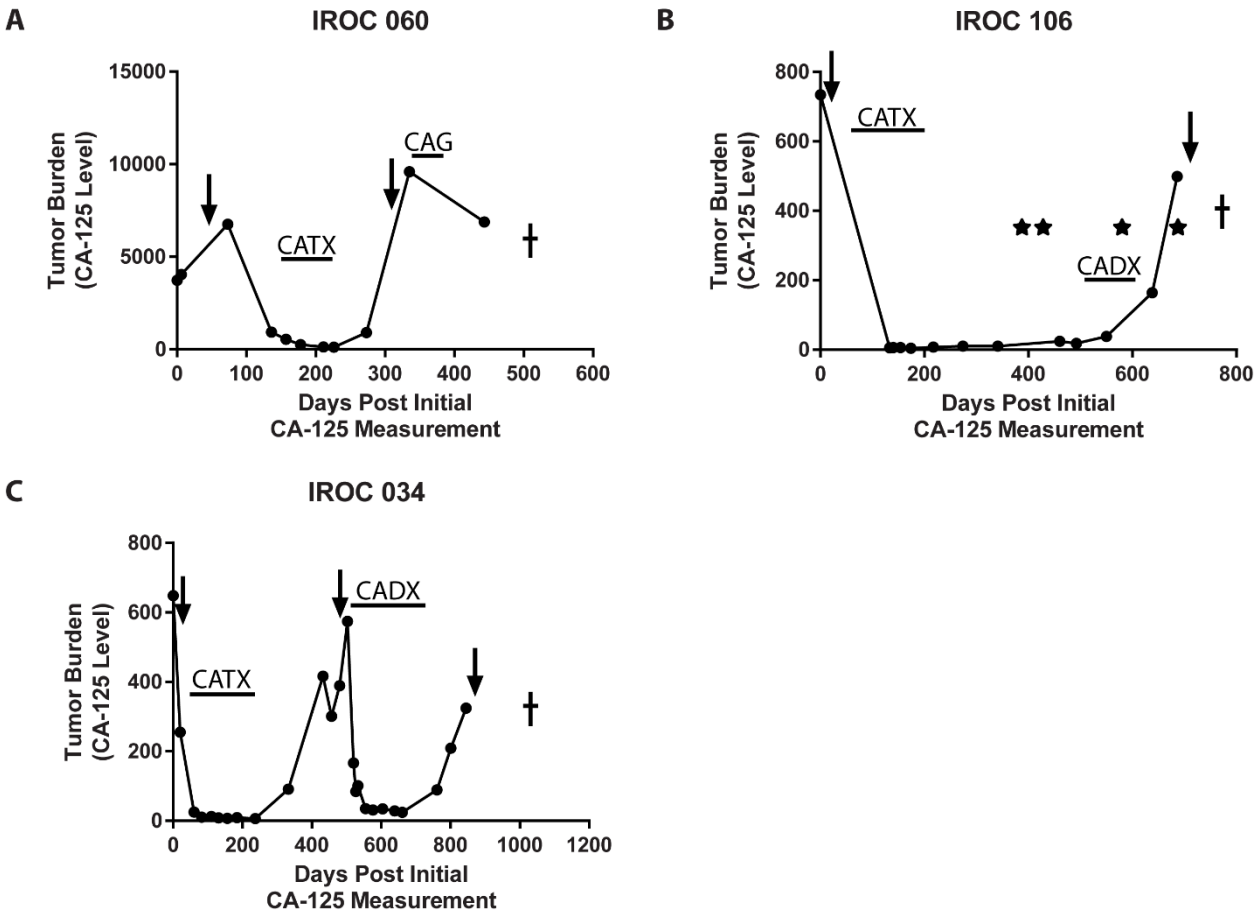

Figure 1. Clinical courses of three HGSC patients studied (A) IROC 060, (B) IROC 106, and (C) IROC 034. Three patients were diagnosed with HGSC and underwent primary debulking surgery followed by a standard course of platinum-based chemotherapy. Tumor burden is indicated by CA-125 measurements (black dots). CA-125 U/mL was measured in blood serum as standard of care. Chemotherapy cycles are denoted with black bars and patients were treated with: CATX, carboplatin and paclitaxel; CAG, carboplatin and gemcitabine; CADX, carboplatin and doxorubicin. Down arrows represent ascites taps where ascites fluid was collected and ascites cells were harvested. Stars represent radiation treatment. Cross represents time of death.

2.4.2 CD137 identifies recently activated, TCR-stimulated CD4⁺ T cells better than OX-40

Given my aim to assess the tumor reactivity of $CD4^+$ and $CD8^+$ T cells from mixed TAL populations, I sought to find a cell surface marker that would identify recently activated T cells of the $CD4^+$ and $CD8^+$ subsets. CD137 is a well described activation marker on recently activated antigen-specific CD8+ T cells,[32,236] whereas the more canonical $CD4^+$ activation marker is OX-40, or CD134.[35] Despite this, many other studies have used CD137 to identify recently activated $CD4^+$ tumor-antigen-specific T cells.[11,40,47,48] To systematically assess which marker is best to identify recently activated $CD4^+$ cells, I evaluated expression levels of OX-40, CD137, and two other activation markers (CD69 and CD40L) on $CD4^+$ T cells in a REP-expanded healthy donor T cell population by flow cytometry over 6 days following various polyclonal stimuli: plate-bound anti-CD3 antibody, phytohemagglutinin (PHA), phorbol 12-myristate 13-acetate and ionomycin (PMA/IM), and anti-CD3 and anti-CD28-coated Dynabeads.

When analyzing potentially rare anti-tumor responses, it is important that background expression is very low. CD69 had the highest background expression on non-activated T cells (Figure 2A) and was therefore unsuitable for detecting rare antigen-specific $CD4^+$ TAL. Despite low background, CD40L had the lowest expression level of any marker following stimulation (Figure 2) and accordingly was also unsuitable for detecting antigen-specific $CD4^+$ T cells. Both CD137 and OX-40 had high expression levels post-TCR-stimulation (Figures 2B, 2C). However, CD137 had much lower background on unstimulated cells compared to OX-40 (Figure 2A). Due to limiting sample for tumor recognition experiments, it was sometimes necessary to harvest T cells for flow cytometry directly from the ELISPOT plate after 20 hours of co-culture. Therefore, although levels of OX-40 rose substantially higher than CD137 by 48-hours post-stimulation, CD137 had the highest expression on $CD4^+$ T cells at 24 hours (Figures 2B, 2C). Further, CD137 was the most specific marker for identifying T cells activated through their TCR rather than by aggregation by a mitogen. In contrast to OX-40, which was up-regulated following PHA stimulation, CD137 was up-regulated robustly following TCR stimulation (Figures 2B, 2C) yet was low after stimulation with either PMA/IM or PHA (Figures 2D, 2E). Therefore, CD137 was determined to be the best activation marker to evaluate potentially rare, antigen-activated $CD4^+$ TAL.

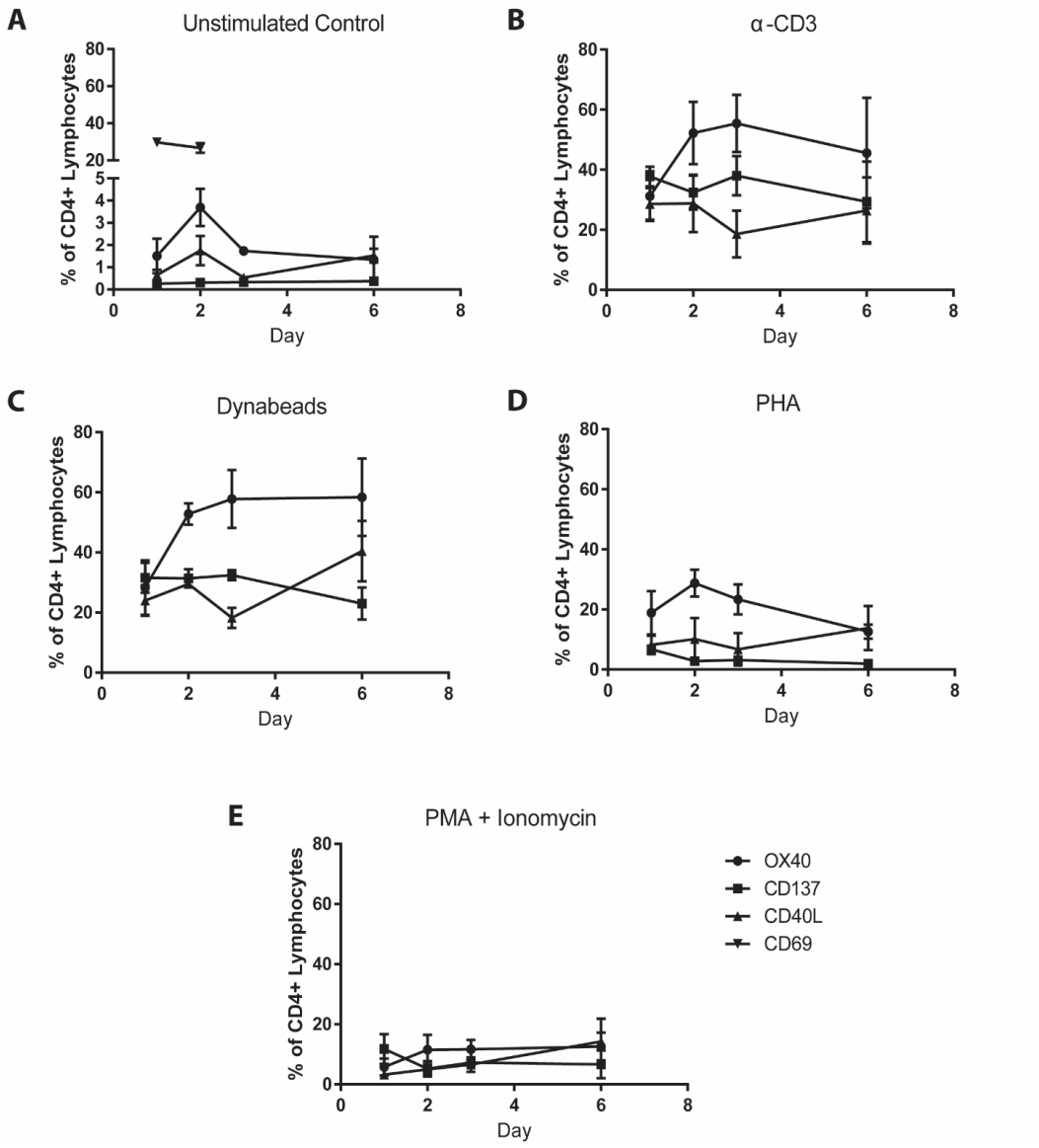

Figure 2. CD137 is the optimal activation marker to detect $CD4^+$ T cells recently activated through the T cell receptor. REP-expanded T cells from healthy donor PBMC were left unstimulated (A), stimulated with (B) plate-bound α-CD3 monoclonal antibody, (C) α-CD3, α-CD28-coated Dynabeads, (D) phytohemagglutinin (PHA), or (E) phorbol myristate acetate (PMA) and ionomycin and the levels of the activation makers CD137 (squares), OX40 (circles), CD40L (up-facing triangles), and CD69 (down-facing triangles) were compared. Each data point is the mean of three T cell lines expanded from the same healthy donor and standard error is reported. $CD4^+$ lymphocytes were gated on lymphocytes by FSC and SSC.

2.4.3 Ex vivo expression levels of HLA class I and II molecules on tumor cells

Expression of MHC molecules is necessary for T cell recognition[237] but can be highly variable on tumor cells[238,239]. To determine the baseline MHC class I expression on tumor cells in primary and recurrent ascites, bulk ascites cells were analyzed by flow cytometry for expression of EpCAM and MHC class I and II. All three patients had high MHC class I expression on both primary and recurrent $EpCAM^+$ ascites cells (Figure 3). IROC 060 had high MHC class II expression on $EpCAM^+$ tumor cells (Figure 3A), while both IROC 106 and IROC 034 had low MHC class II expression (Figures 3B, 3C). However, these results may be biased, as only a few cells were analyzed for MHC expression directly *ex vivo* due to sample limitation. For example, only 32 events fell within the $EpCAM^+$ gate when analyzing IROC 106 primary ascites (Figure 3B). Nonetheless, the results clearly indicate that MHC class II expression was not ubiquitous on tumor cells in ascites, raising the possibility that tumor-reactive $CD4^+$ T cells may not be able to recognize autologous tumor cells. Therefore, to increase the likelihood of identifying potentially rare tumor-reactive T cells, I sought to increase MHC expression by pre-treating $CD45^-$ ascites cells with IFN-γ.

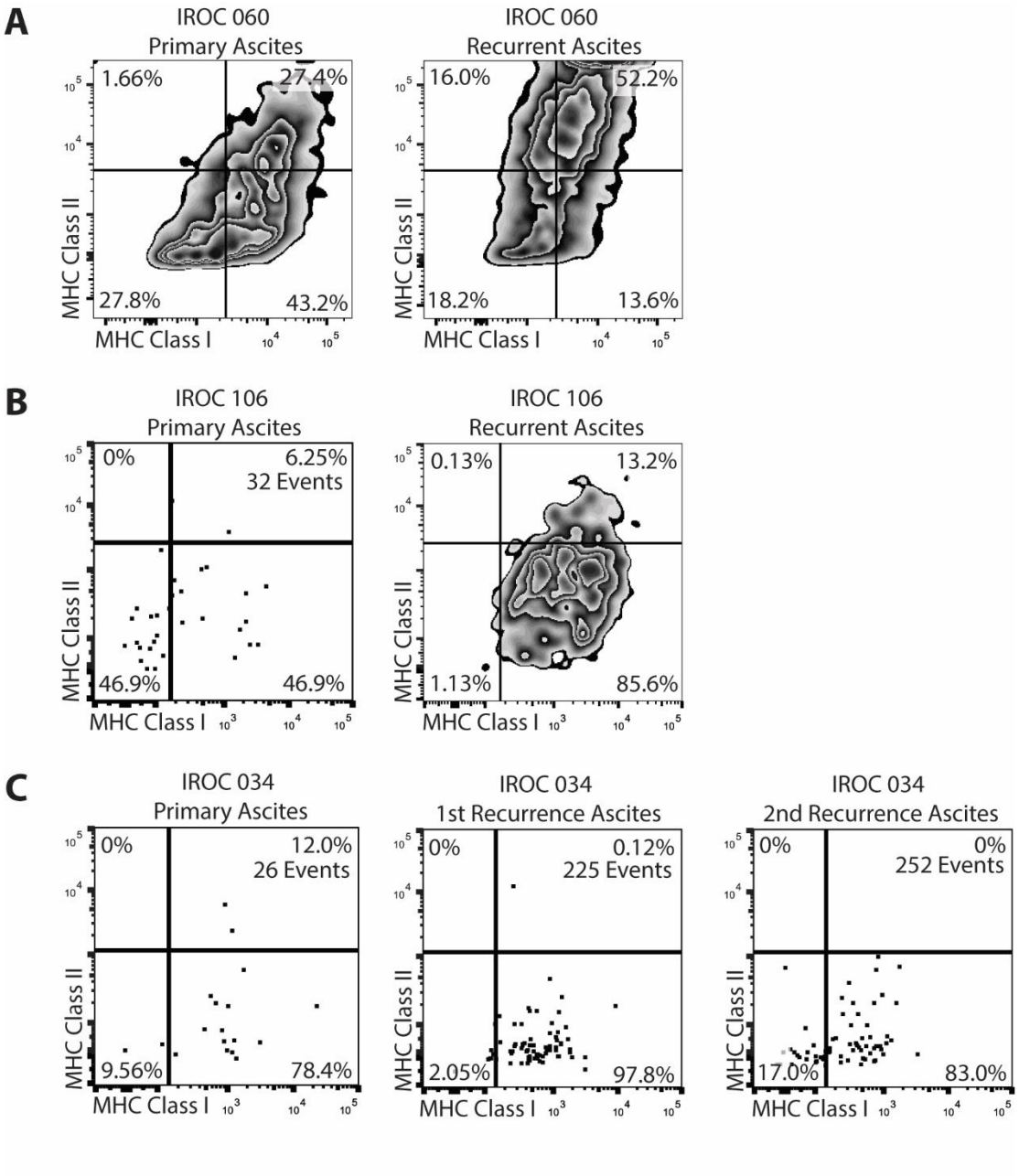

Figure 3. *Ex vivo* expression levels of MHC Class I and Class II on EpCAM^{+} tumor cells from bulk ascites of (A) IROC 060, (B) IROC 106, and (C) IROC 034. Gating strategy is shown in Figure A1.

2.4.4 IFN-γ pre-treatment has little effect on MHC and PD-L1 expression on EpCAM$^+$ ascites cells

IFN-γ is well known to increase expression of MHC molecules on the surface of many cell types, including tumor cells.[240,241] However, some tumors have mutations that result in resistance to IFN-γ signaling and thus prevent IFN-γ-induced MHC up-regulation.[166,168] Therefore, it was uncertain whether EpCAM$^+$ ascites cells from each of the three HGSC patients would up-regulate MHC following IFN-γ pre-treatment. To address this, I stimulated primary cell lines (derived from either IROC 060 bulk ascites or IROC 106 bulk disaggregated tumor) with IFN-γ for 24 hours and assessed expression of MHC class I and II by flow cytometry. On IROC 060 ascites tumor cells, IFN-γ treatment induced robust up-regulation of both MHC class I and II (Figure 4A). On IROC 106 tumor cells, IFN-γ also induced up-regulation of MHC class I, while MHC class II expression was unchanged (Figure 4B). IFN-γ signaling can also induce up-regulation of the inhibitory cell surface protein PD-L1.[156,241] Indeed, on both IROC 060 and IROC 106 tumor cells, PD-L1 expression increased 10-fold following treatment with IFN-γ (Figure 4A,B).

In contrast to the cell lines, primary human ascites cells did not respond as robustly to IFN-γ directly *ex vivo*. EpCAM$^+$ tumor cells from IROC 060 and IROC 106 failed to up-regulate MHC class I or class II following IFN-γ treatment compared to untreated controls (Figures 5A-B, 6A-B, top row). Likewise, PD-L1 expression was high on untreated EpCAM$^+$ tumor cells and failed to increase following IFN-γ pre-treatment (Figures 5A-B, 6A-B, bottom row). The lack of MHC upregulation was unexpected. Therefore, to confirm IFN-γ was active, I evaluated up-regulation of MHC and PD-L1 on the surface of CD45$^+$ cells from parallel cultures of IROC 060 and IROC 106 bulk ascites. MHC expression levels on CD45$^+$ cells were already high after 24 hours of *in vitro* cell culture, and as such, IFN-γ treatment failed to induce increased expression (Figures 5C-D, 6C-D, top row). However, PD-L1 expression did increase substantially (Figure 5C-D, 6C-D, bottom row), indicating IFN-γ was indeed functional. Although *ex vivo* expression levels of MHC class I expression was high on IROC 060 and IROC 106 EpCAM$^+$ tumor cells and MHC class II expression levels were high on IROC 060 EpCAM$^+$ tumor cells (Figure 3A,B), following 24 hours of *in vitro* cell culture in the absence of IFN-γ, expression levels of MHC class I decreased. For example, 70% of IROC 060 primary EpCAM$^+$ cells were MHC class I$^+$ directly *ex vivo* while only 55% were MHC class I$^+$ following 24-hour culture (Figure 5A). Likewise, IROC 060 recurrent EpCAM$^+$ cells and both primary and recurrent IROC 106 EpCAM$^+$ cells experienced a similar reduction in MHC class I expression levels following 24 hours of *in vitro* cell culture (Figure 5B, 6A,B) compared to directly *ex vivo* (Figure 3A,B). In contrast, MHC class II expression levels on IROC 060 were maintained following *in vitro* culture (Figures 3A, 5A,B). Therefore, because MHC class I levels decreased following *in vitro* culture in the

absence of IFN-γ, yet did not increase after IFN-γ treatment, it suggests both IROC 060 and IROC 106 tumor cells may have a resistance mechanism to IFN-γ signaling.

In contrast to IROC 060 and IROC 106, IROC 034 did not have sufficient tumor cells to pre-treat tumor cells with IFN-γ for use in TAL reactivity assays and keep an aliquot as an untreated control. Therefore, for IROC 034, MHC and PD-L1 expression levels on IFN-γ pre-treated cells were compared with tumor cells directly *ex vivo*, rather than to an untreated control. Unexpectedly, IROC 034 MHC and PD-L1 expression levels were substantially lower in the IFN-γ treated group compared to the direct ex vivo sample (Figures 3C, 7A-C). This apparent reduction in MHC and PD-L1 expression could have been due to reduced tumor cell viability following overnight culture, as was seen for IROC 060 and IROC 106 (data not shown), rather than a biological response to IFN-γ. Thus, $EpCAM^+$ tumor cells from all three patients failed to up-regulate MHC molecules in response to IFN-γ treatment. Nevertheless, regardless of IFN-γ treatment, $EpCAM^+$ cells from IROC 060 and IROC 106 did express MHC class I, and some cells also expressed class II. This suggests MHC expression may not be a barrier to T cell recognition of $EpCAM^+$ tumor cells for two of three study patients.

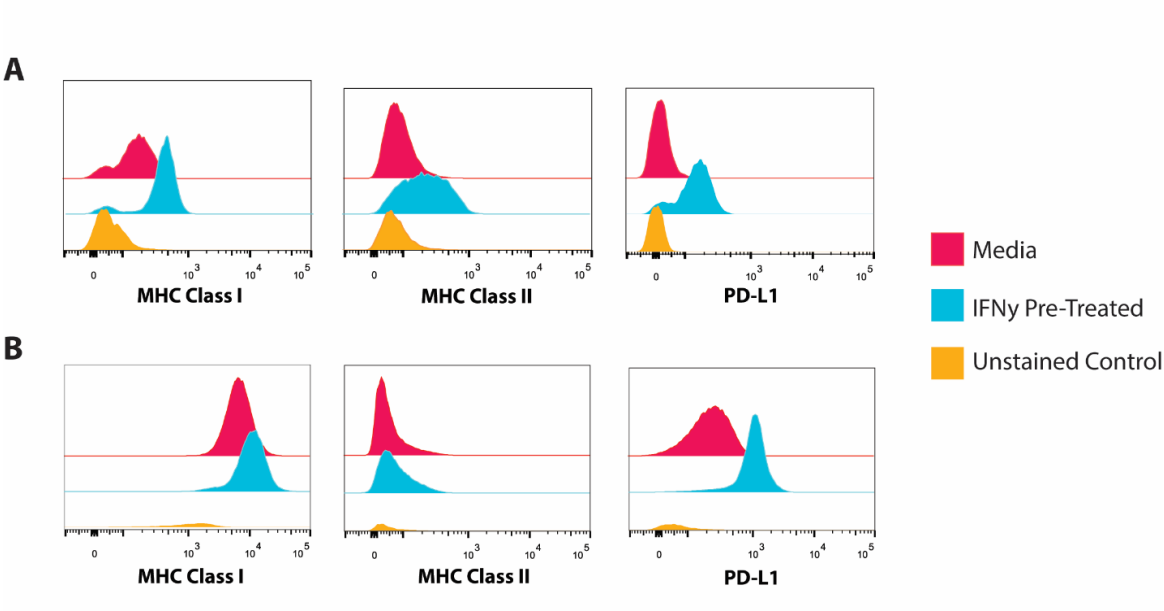

Figure 4. IFN-γ pre-treatment results in up-regulation of MHC class I, MHC class II, and PD-L1 on primary human cell lines. (A) IFN-γ pre-treatment of an ascites tumor cell line grown from IROC 060 primary bulk ascites. (B) IFN-γ pre-treatment of a tumor cell line grown from IROC 106 disaggregated tumor. Both cell lines express cytokeratin and are $CD45^-$. Yellow histograms represent unstained controls, red histograms represent un-treated cell lines, and blue histograms represent IFN-γ-treated cell lines.

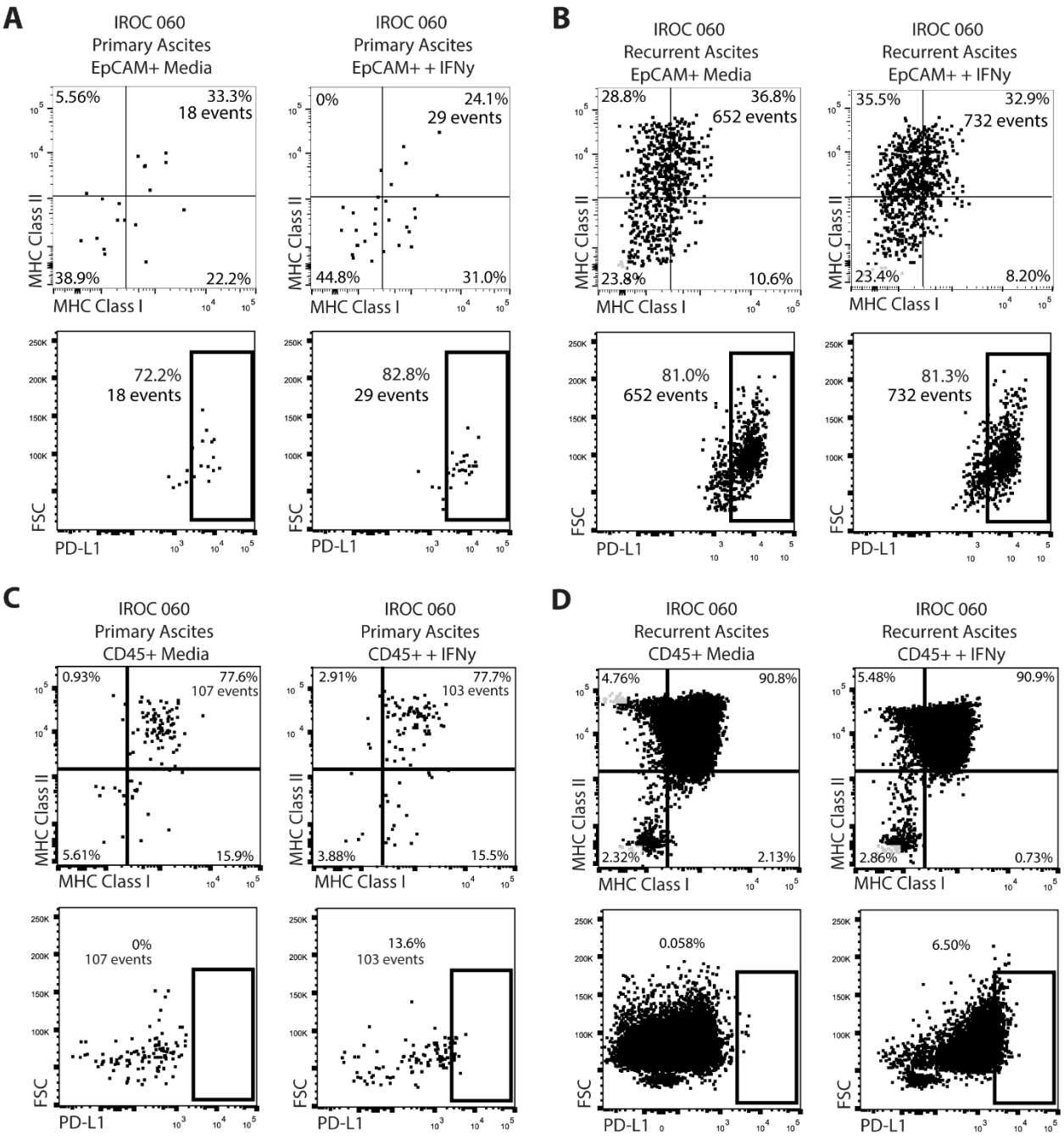

Figure 5. Effect of IFN-γ pre-treatment of IROC 060 EpCAM$^+$ tumor cells and CD45$^+$ cells from bulk ascites. (A,C) IROC 060 primary and (B,D) recurrent ascites cells were treated with IFN-γ for 24 hours. Post-treatment, (A,B) EpCAM$^+$ tumor cells and (C,D) CD45$^+$ ascites cells were analyzed for expression of MHC Class I, MHC Class II, and PD-L1. Gating strategy is shown in Figure A1.

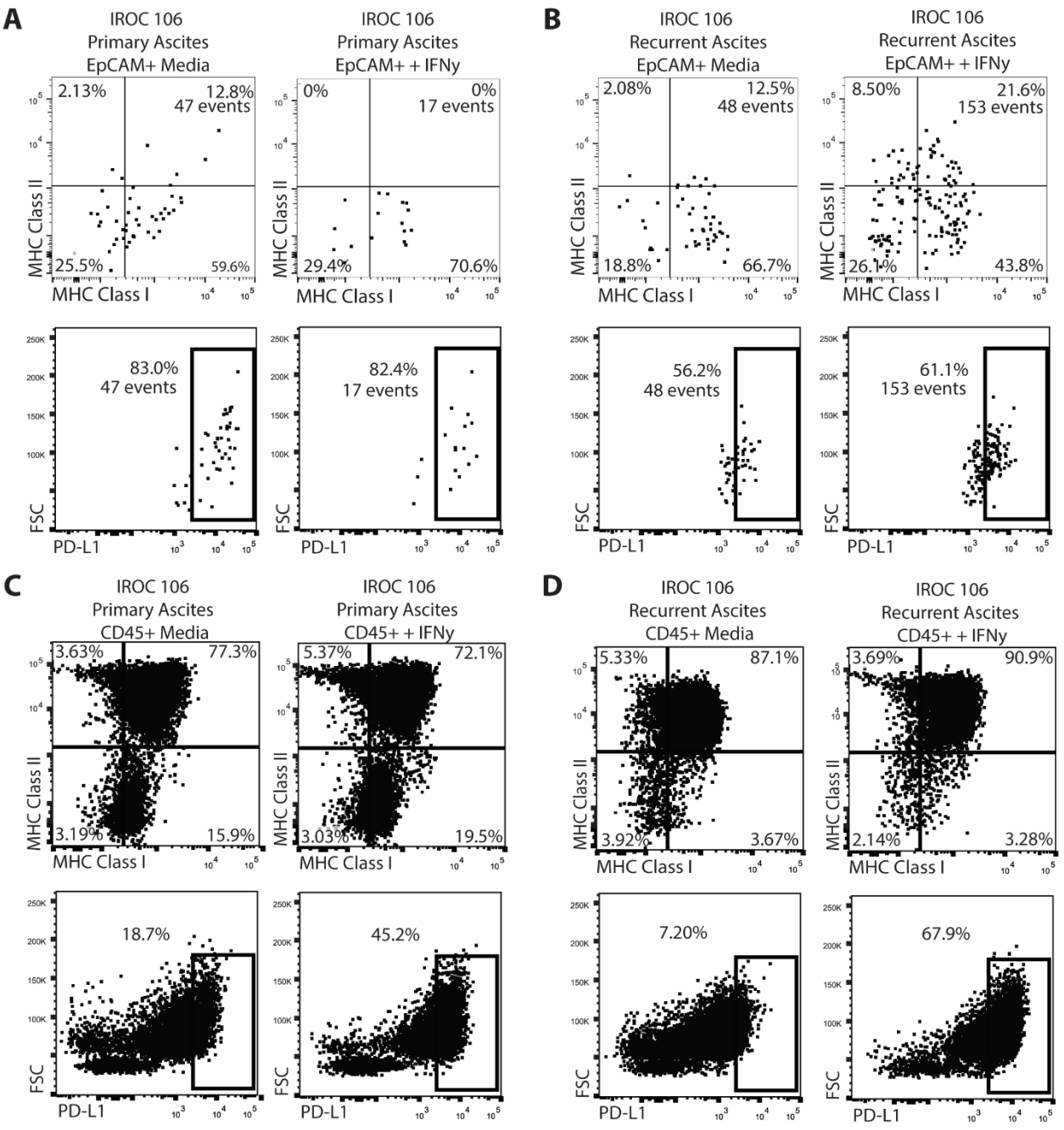

Figure 6. Effect of IFN-γ pre-treatment of IROC 106 ascites EpCAM$^+$ tumor cells and CD45$^+$ cells. (A,C) IROC 106 primary and (B,D) recurrent ascites cells were treated with IFN-γ for 24 hours. Following treatment, (A,B) EpCAM$^+$ tumor cells and (C,D) CD45$^+$ ascites cells were analyzed for expression of MHC Class I, MHC Class II, and PD-L1. Gating strategy is shown in Figure A1.

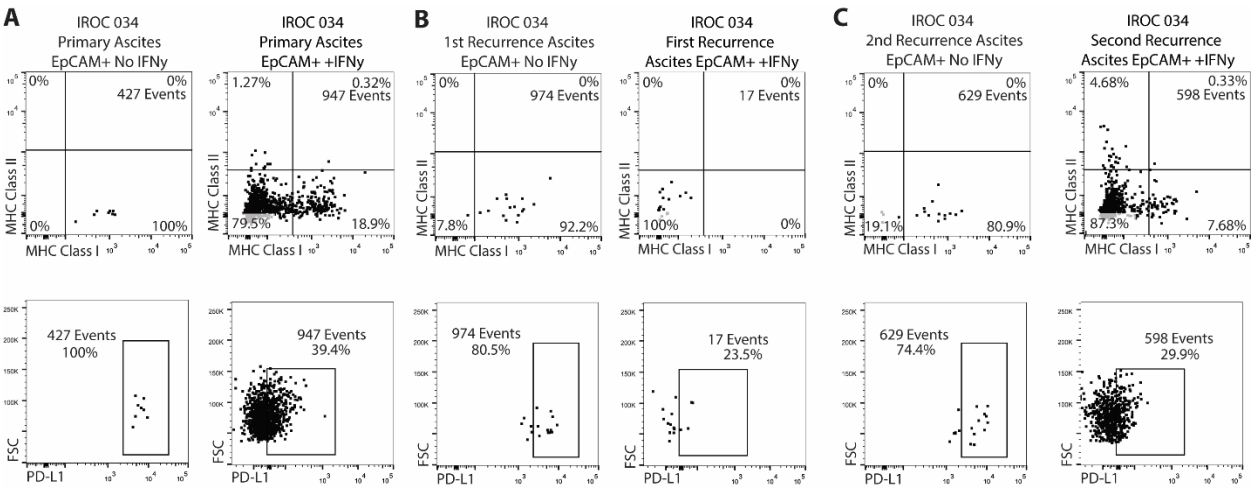

Figure 7. Effect of IFN-γ pre-treatment of IROC 034 ascites EpCAM$^+$ tumor cells. (A) IROC 034 primary, (B) first recurrence, and (C) second recurrence CD45$^-$ ascites cells were treated with IFN-γ for 24 hours. EpCAM$^+$ and CD45$^-$ ascites cells were analyzed for expression of MHC Class I, MHC Class II, and PD-L1. Gating strategy is shown in Figure A1.

2.4.5 Assessment of tumor reactivity by TAL

Using the methods described in the preceding sections, I evaluated the ability of $CD4^+$ and $CD8^+$ TAL to recognize primary and recurrent disease. TAL reactivity was assessed to three different cellular populations from primary and recurrent disease: (a) bulk ascites, consisting of a heterogeneous cellular mixture including $EpCAM^+$ tumor cells, monocytes, and lymphocytes (subsequently called ascites), (b) $CD45^-$ ascites cells purified from ascites using a $CD45^+$ microbead depletion, and highly enriched for $EpCAM^+$ tumor cells (subsequently called $CD45^-$ cells) and (c) $CD45^+$ ascites cells isolated by harvesting all cells bound to the magnetic column following a $CD45^+$ microbead-based depletion of ascites (subsequently called $CD45^+$ cells). Each patient exhibited a different pattern of ascites evolution and corresponding change in anti-tumor T cell response over time, and are therefore described separately in the following sections:

2.4.5.1 IROC 060 ascites reactivity by TAL

I first assessed primary TAL for recognition of primary and recurrent tumor from ascites. Primary TAL did not recognize primary ascites but strongly recognized recurrent ascites (i.e. 1% versus 8% of $CD3^+$ T cells up-regulated CD137; Figures 8A, 8B). The response to recurrent ascites was predominantly mediated by the $CD8^+$ subset of TAL (Figure 8A). These results were further supported by IFN-γ ELISPOT, which showed primary TAL secreted IFN-γ only in response to recurrent ascites (Figure 8B). I next assessed recurrent TAL for recognition of primary versus recurrent ascites. Similar to primary TAL, recurrent TAL did not recognize primary ascites, but recognized recurrent ascites (i.e. 0.5% versus 3% of $CD3^+$ T cells up-regulated CD137; Figures 8C,D). Again, this was supported by ELISPOT results showing recurrent TAL secreted IFN-γ only in response to stimulation with recurrent ascites (Figure 8D). In contrast to primary TAL, the responding recurrent TAL involved nearly equal proportions of $CD4^+$ and $CD8^+$ T cells (Figure 8C), suggesting either the loss of a $CD8^+$ T cell response or the emergence of a $CD4^+$ T cell response between primary and recurrent disease.

When primary and recurrent TAL were assessed for reactivity to the $CD45^-$ and $CD45^+$ cell fractions from ascites, it was clear that all reactivity was directed towards $CD45^+$ cells (Figure 9). To ensure TAL were not recognizing a ubiquitous auto-antigen expressed on $CD45^+$ cells, TAL were screened for reactivity to autologous PBMC. Despite robust reactivity to recurrent ascites and $CD45^+$ cells, there was no reactivity to autologous PBMC from either primary or recurrent TAL (Figures 8, 9), suggesting TAL were not auto-reactive. Rather, TAL likely recognized a tumor-associated antigen presented by $CD45^+$

cells. In summary, IROC 060 ascites did not elicit an immune response at primary disease yet induces a robust immune response at disease recurrence. Concomitantly, TAL became a mixture of $CD8^+$ and $CD4^+$ T cells over time.

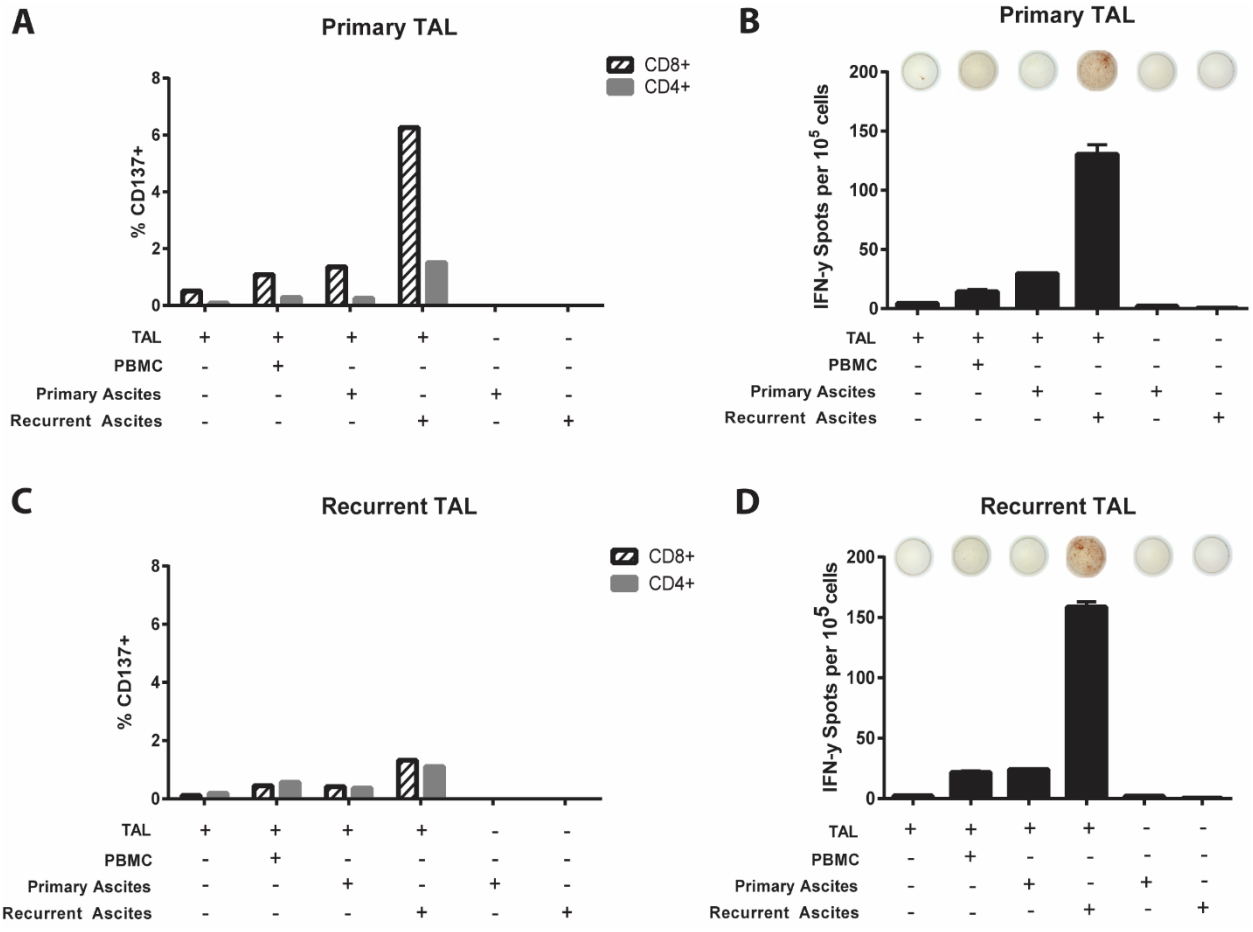

Figure 8. Ascites reactivity of IROC 060 TAL. IL-2 and REP expanded primary (A, B) and recurrent (C, D) TAL were stimulated with autologous primary and recurrent ascites cells. Reactivity was called positive when it was at least two times the level of reactivity to autologous PBMC in the IFN-γ ELISPOT (B, D) and by CD137 expression (A, C). The frequency of $CD8^+CD137^+$ TAL is represented by hatched bars while the frequency of $CD4^+CD137^+$ TAL is represented by solid grey bars. The gating strategy for $CD137^+$ TAL and representative dot plots are shown in Figure A2. Representative images of the IFN-γ ELISPOT wells are shown above each bar in the graphs (B, D).

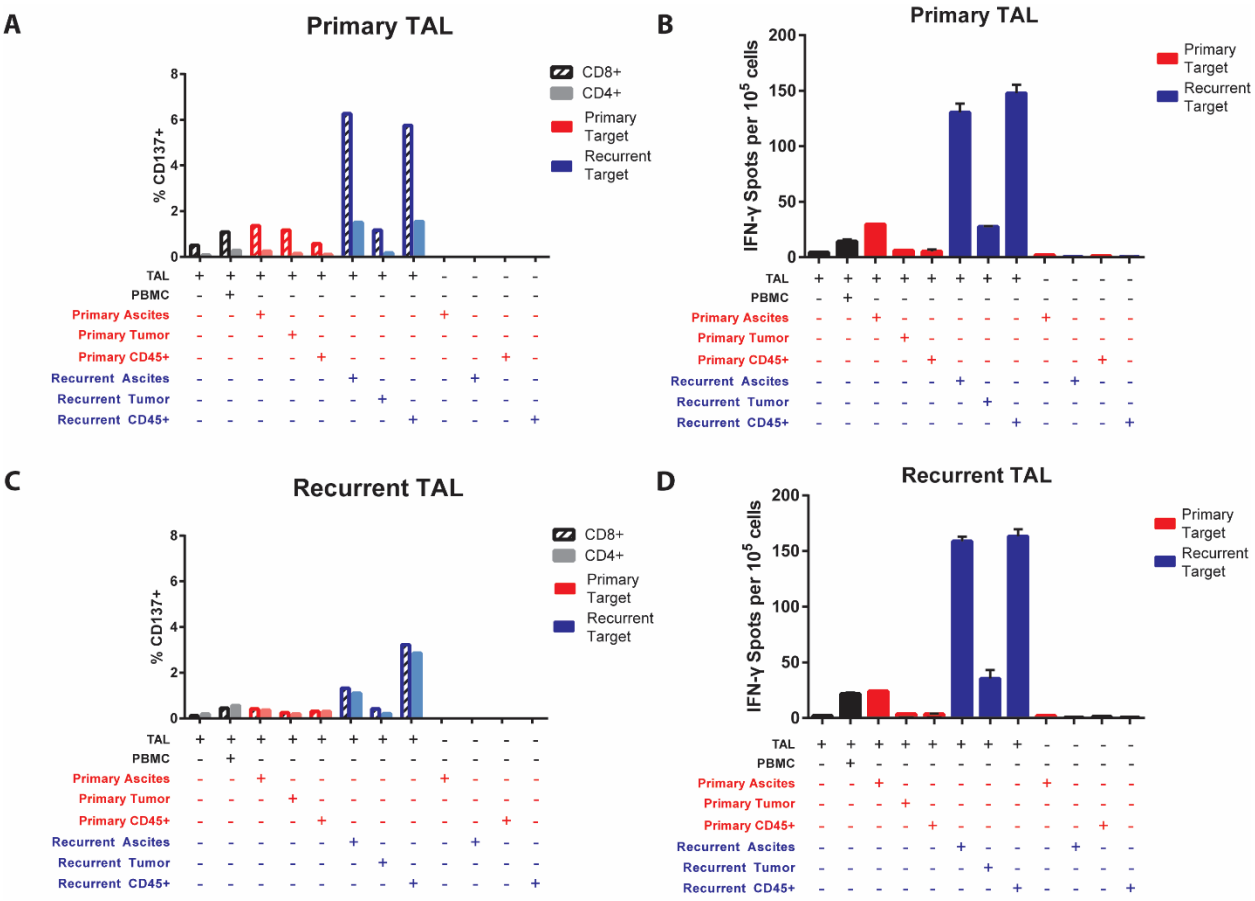

Figure 9. Tumor and ascites reactivity of IROC 060 TAL. IL-2 and REP expanded primary (A, B) and recurrent (C, D) TAL were stimulated with autologous primary and recurrent bulk ascites cells, CD45- tumor cells, and $CD45^+$ ascites cells. Reactivity was called positive when it was at least two times the reactivity to autologous PBMC in the IFN-γ ELISPOT (B, D) and by CD137 expression (A, B). The frequency of $CD8^+CD137^+$ TAL is represented by hatched bars while the frequency of $CD4^+CD137^+$ TAL is represented by solid bars. Assessment of TAL recognition of primary ascites, tumor, or $CD45^+$ cells is represented by red bars while assessment of TAL recognition of recurrent ascites, tumor, or $CD45^+$ cells is represented by blue bars. The gating strategy and representative dot plots are shown in Figure A2.

2.4.5.2 IROC 106 ascites reactivity by TAL

In contrast to IROC 060, primary TAL from IROC 106 demonstrated robust recognition of primary or recurrent tumor from ascites. Nearly 75% of the responsive primary TAL were $CD4^+$; Figures 10A,B). Recurrent TAL also recognized primary or recurrent ascites (Figures 10C, 10D). In contrast to primary TAL, responding recurrent TAL were 50% $CD4^+$ and 50% $CD8^+$ (Figure 10C). There was significant background IFN-γ secretion when primary TAL were co-cultured with autologous PBMC. However, representative ELISPOT images show substantially more IFN-γ secretion when TAL were cultured with either primary or recurrent ascites (Figures 10B,D) compared to autologous PBMC, suggesting despite potential background auto-reactivity, TAL exhibit specific recognition of tumor-associated antigen. Further, flow cytometry results showed TAL express very little (<1%) CD137 following stimulation with autologous PBMC (Figures 10A,C) compared to stimulation with ascites (3-8% $CD137^+$). TAL also showed no reactivity to autologous B cells, further indicating TAL recognize a tumor-associated antigen rather than a self antigen ubiquitously expressed on blood cells.

When I assessed TAL reactivity to the $CD45^-$ or $CD45^+$ fractions, it was clear ascites-reactivity of IROC 106 TAL was entirely directed towards $CD45^+$ cells, rather than tumor-enriched $CD45^-$ cells (Figure 11). Again, despite the lack of response to $CD45^-$ cells, background reactivity to autologous PBMC and B cells was low (Figures 10, 11). Therefore, TAL likely recognized a tumor-associated antigen presented by $CD45^+$ cells, rather than an auto-antigen expressed on blood cells. In summary, results suggest IROC 106 ascites elicited T cell responses at primary and recurrent time points, whereas tumor-reactive TAL changed from predominantly $CD4^+$ to a nearly equal mixture of both $CD4^+$ and $CD8^+$ T cells.

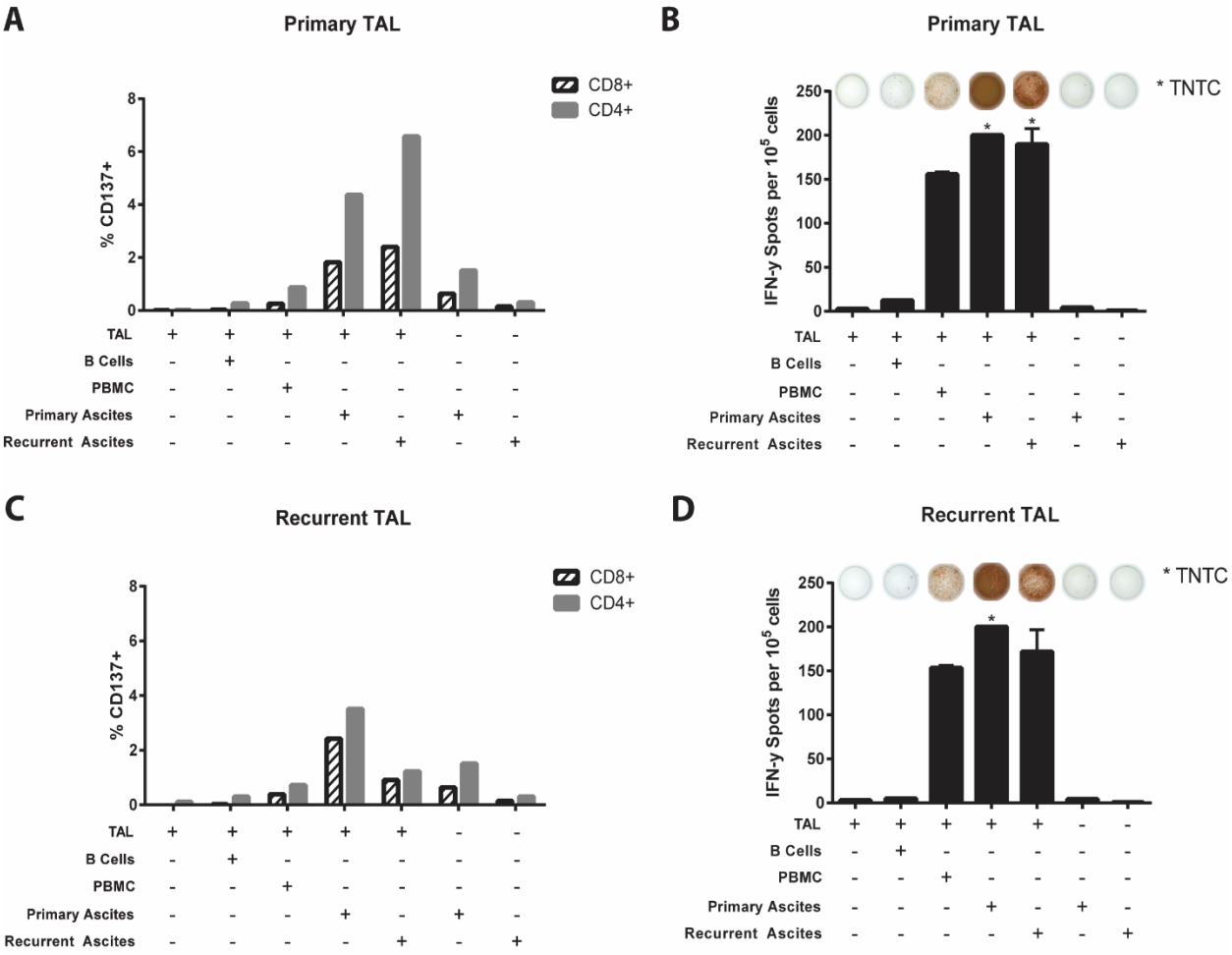

Figure 10. Ascites reactivity of IROC 106 TAL. IL-2 and REP expanded primary (A, B) and recurrent (C, D) TAL were stimulated with autologous primary and recurrent ascites cells. Reactivity was called positive when it was at least two times the level of reactivity to autologous PBMC and autologous B cells in the IFN-γ ELISPOT (B, D) and by CD137 expression (A, C). The frequency of $CD8^{+}CD137^{+}$ TAL is represented by hatched bars while the frequency of $CD4^{+}CD137^{+}$ TAL is represented by solid grey bars. The gating strategy for $CD137^{+}$ TAL and representative dot plots are shown in Figure A3. Representative images of the IFN-γ ELISPOT wells are shown above each bar in the graphs (B, D).

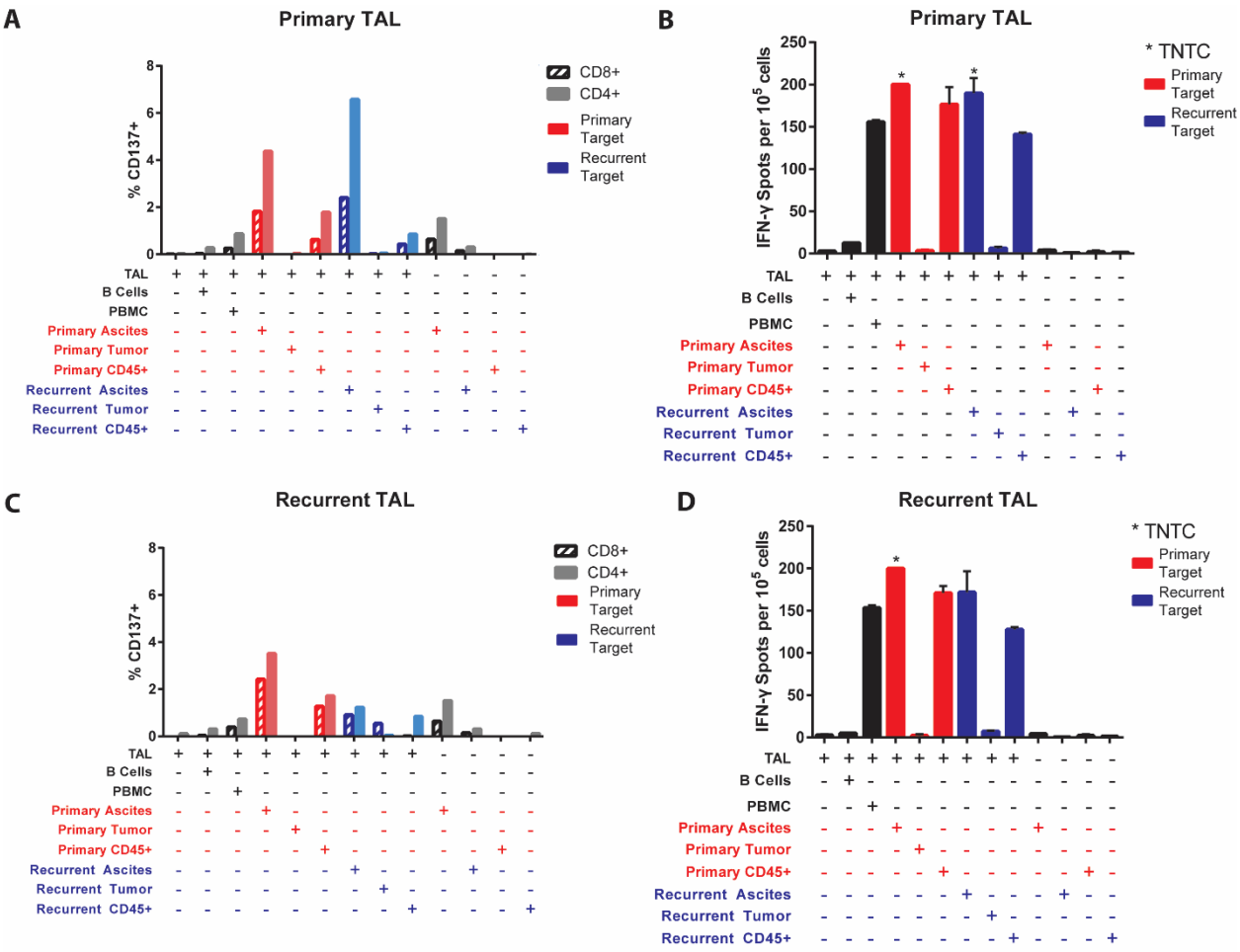

Figure 11. Tumor and ascites reactivity of IROC 106 TAL. IL-2 and REP expanded primary (A, B) and recurrent (C, D) TAL were stimulated with autologous primary and recurrent bulk ascites cells, CD45- tumor cells, and CD45+ ascites cells. Reactivity was called positive when it was at least two times the reactivity to autologous PBMC and autologous B cells in the IFN-γ ELISPOT (B, D) and by CD137 expression (A, B). The frequency of $CD8^+CD137^+$ TAL is represented by hatched bars while the frequency of $CD4^+CD137^+$ TAL is represented by solid bars. Assessment of TAL recognition of primary ascites, tumor, or $CD45^+$ cells is represented by red bars while assessment of TAL recognition of recurrent ascites, tumor, or $CD45^+$ cells is represented by blue bars. The gating strategy and representative dot plots are shown in Figure A3. IFN-γ ELISPOT TNTC values were estimated to be 200 spots based on the highest countable number of spots on the ELISPOT plate.

2.4.5.3 IROC 034 ascites reactivity by TAL

IROC 034 presented a unique opportunity to evaluate anti-tumor T cell responses from ascites over two disease recurrences (Figure 1C). However, TAL from primary, first recurrence, or second recurrence time points failed to respond to tumor from ascites from any disease time point (Figure 12). While IROC 034 did not up-regulate CD137 or secrete IFN-γ in response to ascites, they did up-regulate CD137 and secrete IFN-γ in response to stimulation with anti-CD3/anti-CD28-coated Dynabeads, a polyclonal stimulant (Figure 13). Further, both primary and 2^{nd} recurrence TAL had weak reactivity to autologous PBMC (more than 2X background spots in the media control) and 1^{st} recurrence TAL have weak reactivity to both autologous B cells and PBMC (Figures 12,13), indicating TAL may have low-level specificity to an autologous antigen found on blood cells. At all time points, ascites reactivity was equal or lower than reactivity to autologous PBMC or B cells (Figure 12), suggesting IROC 034 TAL are capable of activation, yet do not specifically recognize autologous ascites from any disease time point.

Patterns of primary and recurrent ascites reactivity in IROC 060, IROC 106, and IROC 034 were diverse. IROC 060 primary ascites did not elicit a T cell response while her recurrent ascites elicited a robust T cell response (Figure 8). In contrast, both IROC 106 primary and recurrent ascites elicited a strong T cell response (Figure 10). Further, IROC 034 ascites was incapable of eliciting a T cell response at any disease time point (Figure 12). In both cases with tumor reactivity, IROC 060 and IROC 106, tumor-reactive TAL became mixtures of both $CD4^+$ and $CD8^+$ T cells over time. Although results from IROC 060 and IROC 106 were encouraging, results from IROC 034 show tumor-reactivity is not ubiquitous in HGSC patients. In summary, patterns of tumor recognition were diverse between patients, with evidence of both $CD8^+$-mediated and $CD4^+$-mediated anti-tumor T cell responses, as well as complete absence of an anti-tumor T cell response from ascites. Despite this, both IROC 060 and IROC 106 tumor-reactive TAL became a mixture of $CD8^+$ and $CD4^+$ T cells, indicating a potential shared mechanism of T cell evolution within HGSC patients.

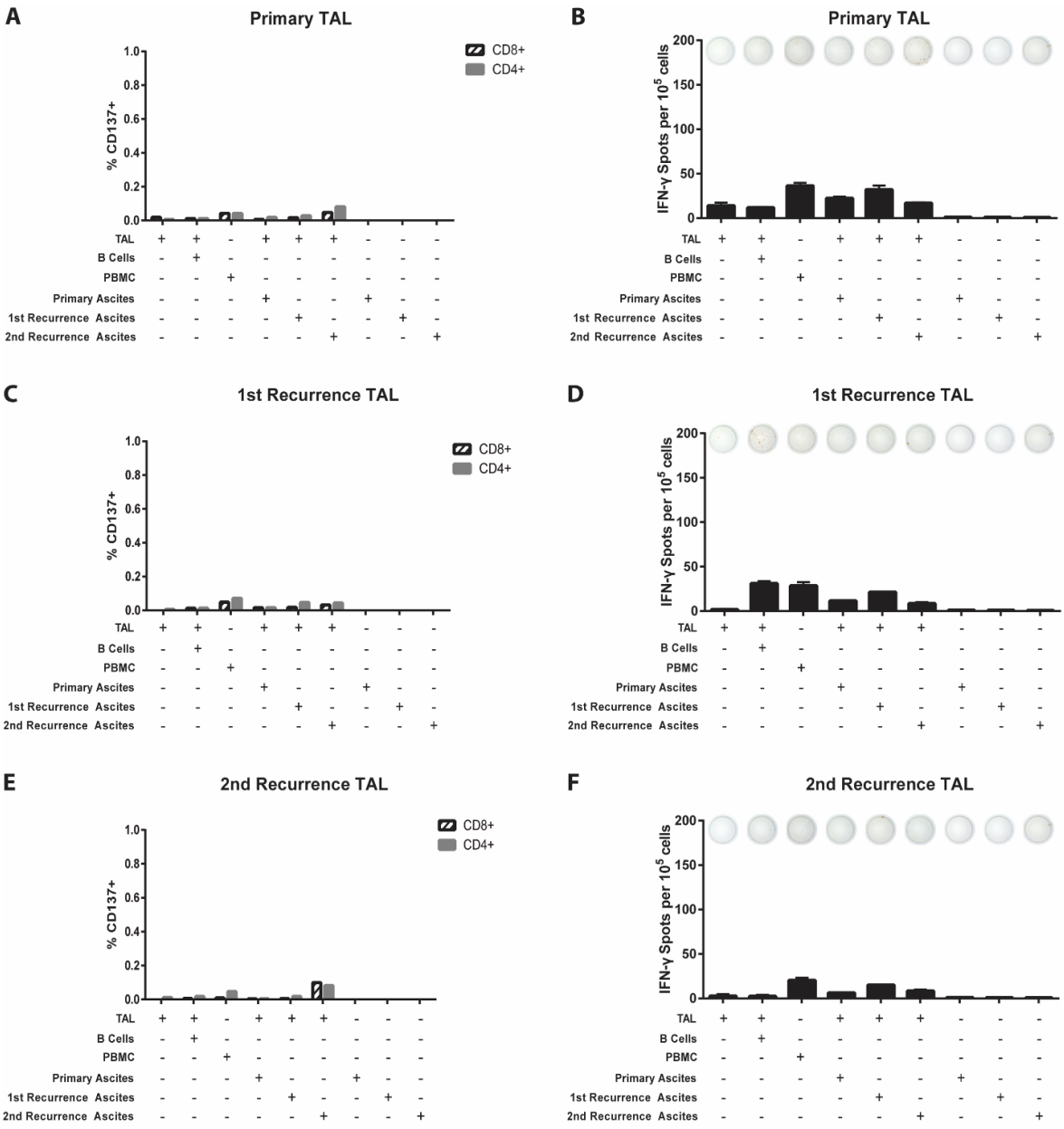

Figure 12. Ascites reactivity of IROC 034 TAL. IL-2 and REP expanded primary (A, B) 1st recurrence (C, D), and 2nd recurrence (E, F) TAL were stimulated with autologous primary and recurrent ascites cells. Reactivity was called positive when it was at least two times the level of reactivity to autologous PBMC and autologous B cells in the IFN-γ ELISPOT (B, D, F) and by CD137 expression (A, C, F). The frequency of $CD8^+CD137^+$ TAL is represented by hatched bars while the frequency of $CD4^+CD137^+$ TAL is represented by solid grey bars. The gating strategy for $CD137^+$ TAL and representative dot plots are shown in Figure A4. Representative images of the IFN-γ ELISPOT wells are shown above each bar in the graphs (B, D, F).

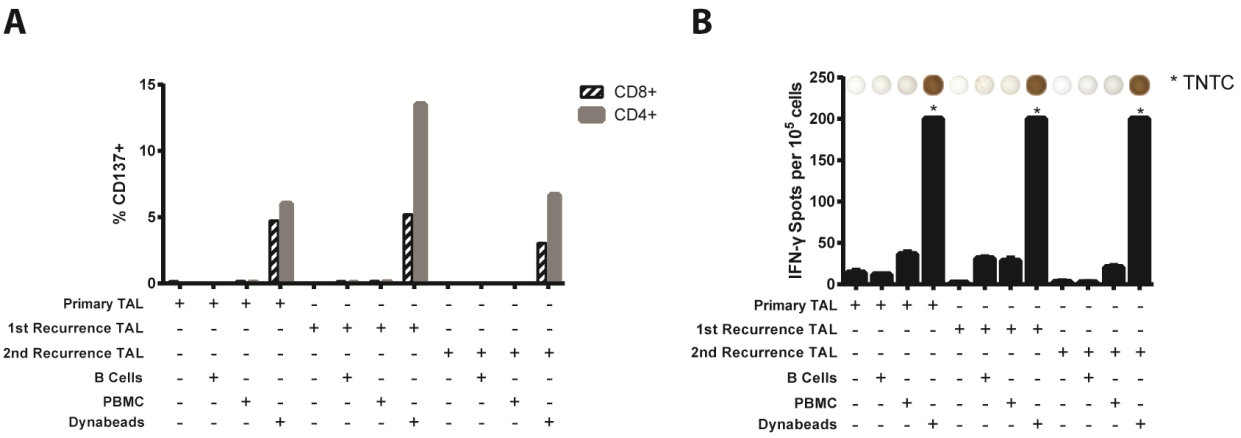

Figure 13. IROC 034 TAL responses to both negative and positive controls. (A) Flow cytometry analysis of CD137 expression and (B) IFN-γ ELISPOT results of primary, 1st recurrence, and 2nd recurrence TAL either unstimulated (media) or stimulated with autologous PBMC, B cells, or Dynabeads. The frequency of $CD8^+CD137^+$ TAL is represented by hatched bars while the frequency of $CD4^+CD137^+$ TAL is represented by solid grey bars. The gating strategy for $CD137^+$ TAL and representative dot plots are shown in Figure A4. Representative images of the IFN-γ ELISPOT wells are shown above each bar in the graphs. IFN-γ ELISPOT TNTC values were estimated to be 200 spots per 100,000 cells based on the highest number of countable spots in ELISPOT plates from assessing IROC 106 TAL (Figures 11,12).

2.4.6 Characteristics of immune infiltrate and tumor phenotype in primary tumors

The infiltration of various T cell subsets are associated with prognosis in ovarian cancer.[7,80,82,242,243] However, it is unknown whether TIL infiltration or tumor phenotype in primary tumor is associated with an anti-tumor TAL response in HGSC. Therefore, retrospective analysis of immunohistochemistry for CD3, CD8, MHC class I, and MHC class II was done on all three patients. Further analysis of PD-1, and PD-L1 was done on IROC 060 and IROC 106, but due to insufficient tumor tissue these analyses were not possible on IROC 034. Because of the positive prognostic effect of $CD3^+$ and $CD8^+$ TIL in HGSC, I expected presence of TIL would be associated with an anti-tumor TAL response for each of the patients studied.

Both IROC 060 and IROC 106 had strong anti-tumor TAL responses (Figures 8-11), however only IROC 060 had infiltrating $CD3^+$, $CD8^+$, and $CD4^+$ ($CD3^+CD8^-$ were presumed $CD4^+$) T cells (Figure 14). Surprisingly, IROC 106 had no TIL (Figure 15A) except for one tissue section in which 3 $CD8^+$ T cells were visible (Figure 15B). In contrast, IROC 034 had no observed anti-tumor T cell response yet had dense intratumoral infiltration of $CD3^+$, $CD8^+$, and $CD4^+$ T cells (Figures 16A-C). Thus, TIL infiltration patterns in primary tumors are not associated with an anti-tumor TAL response in HGSC patients. Likewise, all three patients' tumors expressed MHC class I on epithelial and stromal cells (Figures 14C, 15C, 16D). IROC 060 expressed very high levels of MHC class I, while expression in IROC 106 and IROC 034 was lower and had a patchier distribution across the tumor epithelium (Figures 15C, 16D). The only tumor that had epithelial expression of MHC class II was IROC 060 (Figure 14D), yet the primary TAL response to tumor was predominantly $CD8^+$-mediated (Figure 8A). In IROC 106 and IROC 034, expression of MHC class II was limited to stromal cells that had morphological characteristics of macrophages (Figures 15D, 16E). IROC 106 primary TAL response to tumor was predominantly $CD4^+$-mediated, which suggests tumor infiltrating macrophages may be associated with a $CD4^+$-mediated anti-tumor response; however, IROC 034 had no tumor-reactive TAL (Figure 12), which suggests tumor infiltrating macrophages have no association with the presence of tumor-reactive TAL within the ascites. Finally, neither IROC 060 nor IROC 106 had any substantial PD-L1 staining (Figures 14B, 15B), suggesting PD-L1 expression, like MHC class I, class II, or TIL infiltration, is not associated with the presence of tumor-reactive TAL in ascites.

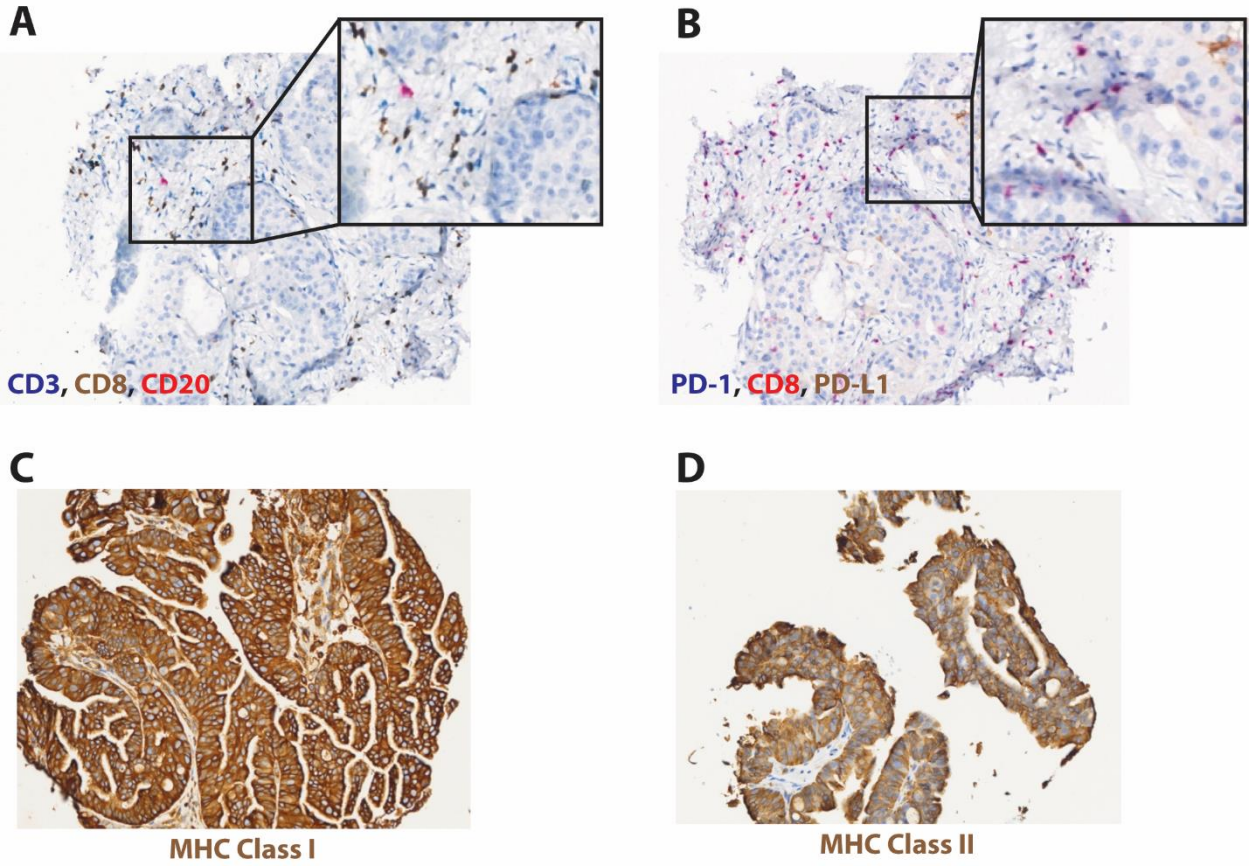

Figure 14. IHC analysis of IROC 060 surgically resected primary tumor stained for (A) CD3 (blue), CD8 (brown), and CD20 (red), (B) PD-1 (blue), CD8 (red), and PD-L1 (brown), (C) MHC class I (brown), and (D) MHC class II (brown).

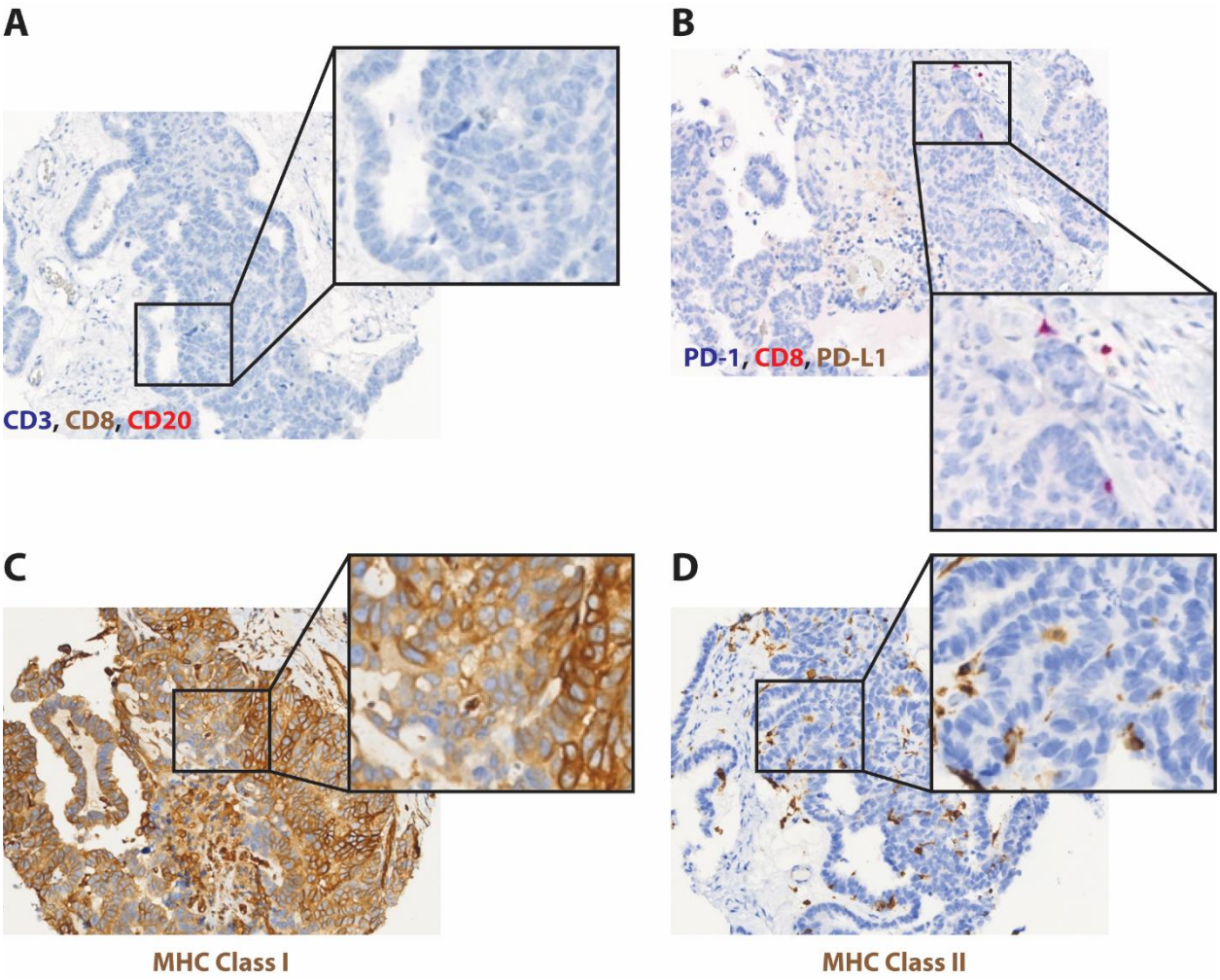

Figure 15. IHC analysis of IROC 106 surgically resected primary tumor stained for (A) CD3 (blue), CD8 (brown), and CD20 (red), (B) PD-1 (blue), CD8 (red), and PD-L1 (brown), (C) MHC class I (brown), and (D) MHC class II (brown).

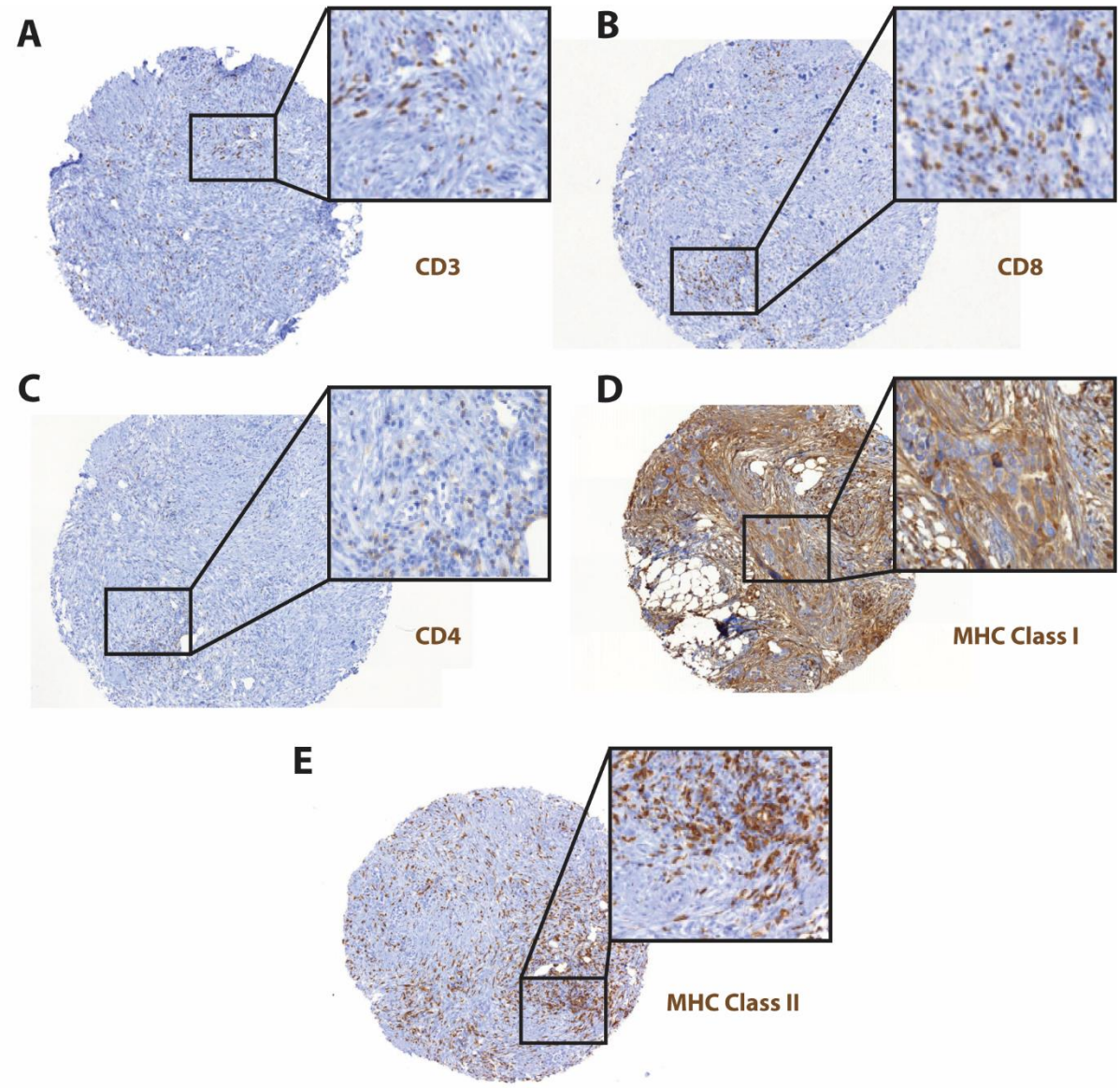

Figure 16. IHC analysis of IROC 034 surgically resected primary tumor for (A) CD3, (B), CD8, (C) CD4, (D) MHC class II, and (E) MHC class II. All markers were stained individually and visualized using DAB (brown) chromogen.

2.4.7 Cellular characteristics of primary and recurrent ascites in HGSC

It is unknown whether differences in ascites cellular composition between primary and recurrent disease can be used to predict ascites reactivity. Therefore, retrospective analysis of ascites from all three HGSC patients was performed by analyzing flow cytometry data for tumor content using EpCAM and for monocyte and lymphocyte content by FSC/SSC to find predictive markers of ascites-reactivity. Only recurrent IROC 060 ascites elicited anti-tumor T cell responses (Figures 8, 9) despite IROC 060 primary and recurrent ascites having high $EpCAM^+$ tumor cell content (31% and 35.5% $EpCAM^+$ cells, respectively; Figure 17A). Between IROC 106 and IROC 034, only IROC 106 exhibited any ascites-reactivity (Figures 10, 11, 12), however both patients had increasing $EpCAM^+$ tumor cell content from primary to recurrent ascites (Figures 17B,C). Therefore, ascites-reactivity could not be predicted simply based on $EpCAM^+$ tumor cell content of ascites.

In contrast, there were some evident trends between tumor-reactive TAL and the presence of monocytes in ascites. IROC 060 recurrent TAL had a greater proportion of responding $CD4^+$ TAL compared to primary TAL (Figures 8A,C). Concordantly, IROC 060 recurrent ascites had a larger monocyte population compared to primary ascites (Figure 18A). Likewise, IROC 106 primary TAL ascites-reactivity was predominantly $CD4^+$-mediated (Figure 10A), and indeed IROC 106 primary ascites had a larger monocyte population compared to recurrent ascites (Figure 18B). IROC 034 ascites had an increase in monocytes over time (Figure 18C) however, it had a lack of tumor-reactive TAL at any time point (Figure 12). Therefore, these results suggest that in patients who demonstrate ascites-reactivity, the presence of monocytes in ascites is associated with an increased population of $CD4^+$ tumor-reactive TAL compared to $CD8^+$ TAL.

The presence of lymphocytes in ascites was associated with the overall frequency of tumor-reactive TAL. IROC 060 and IROC 106 had an overall decrease in the frequency of $CD3^+$ tumor-reactive TAL. Over 8% of primary $CD3^+$ TAL were tumor reactive, compared to only 3% of recurrent TAL (Figures 8A,C). Consequently, the population of lymphocytes in recurrent ascites was smaller compared to primary ascites (29.8% vs. 19.8%; Figure 18A). Likewise, the overall proportion of tumor-reactive T cells was reduced in recurrent TAL compared to primary (Figures 10A,C) and accordingly, the lymphocyte population of recurrent ascites was reduced compared to primary ascites (53.9% vs. 14.3%; Figure 17B). IROC 034 lymphocyte content of both primary and 1^{st} recurrence ascites was very similar; however, it had reduced by over 20% by 2^{nd} recurrence (Figure 18C). Nonetheless, IROC 034 had no tumor-reactive

TAL and therefore, any association of lymphocyte content with tumor-reactive TAL may be specific to cases with demonstrated ascites-reactivity.

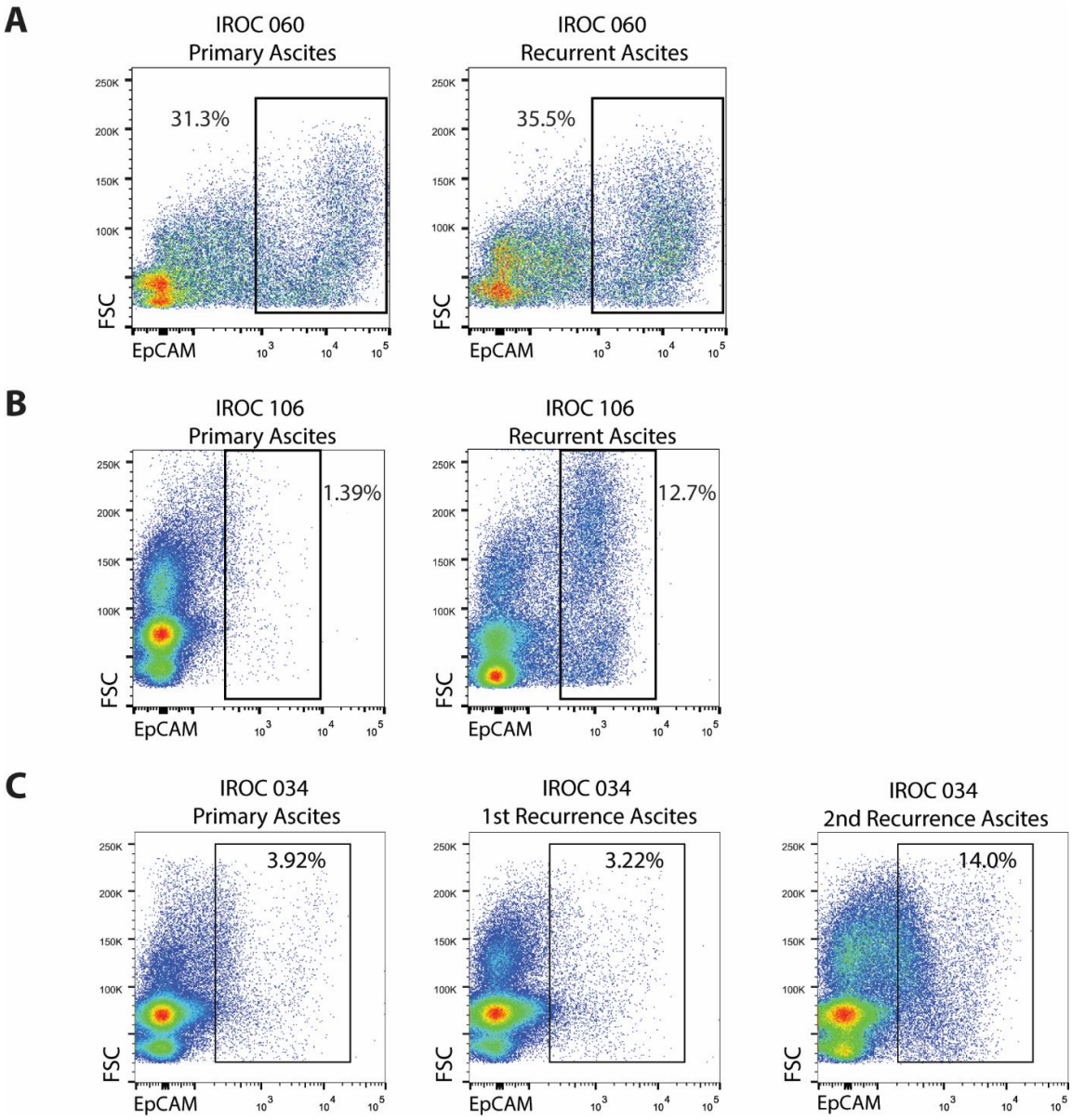

Figure 17. *Ex vivo* proportions of EpCAM$^+$ tumor cells in bulk ascites for the three HGSC patients studied, (A) IROC 060, (B) IROC 106, and (C) IROC 034. The percentage of EpCAM+ cells are indicated inside the rectangular gate within each dot plot. Each patient's ascites samples were analyzed together, however samples between patients were analyzed at different times. Therefore, the EpCAM$^+$ gate is unique to each patient. Cells were gated on singlets and the gating strategy is outlined in Figure A5.

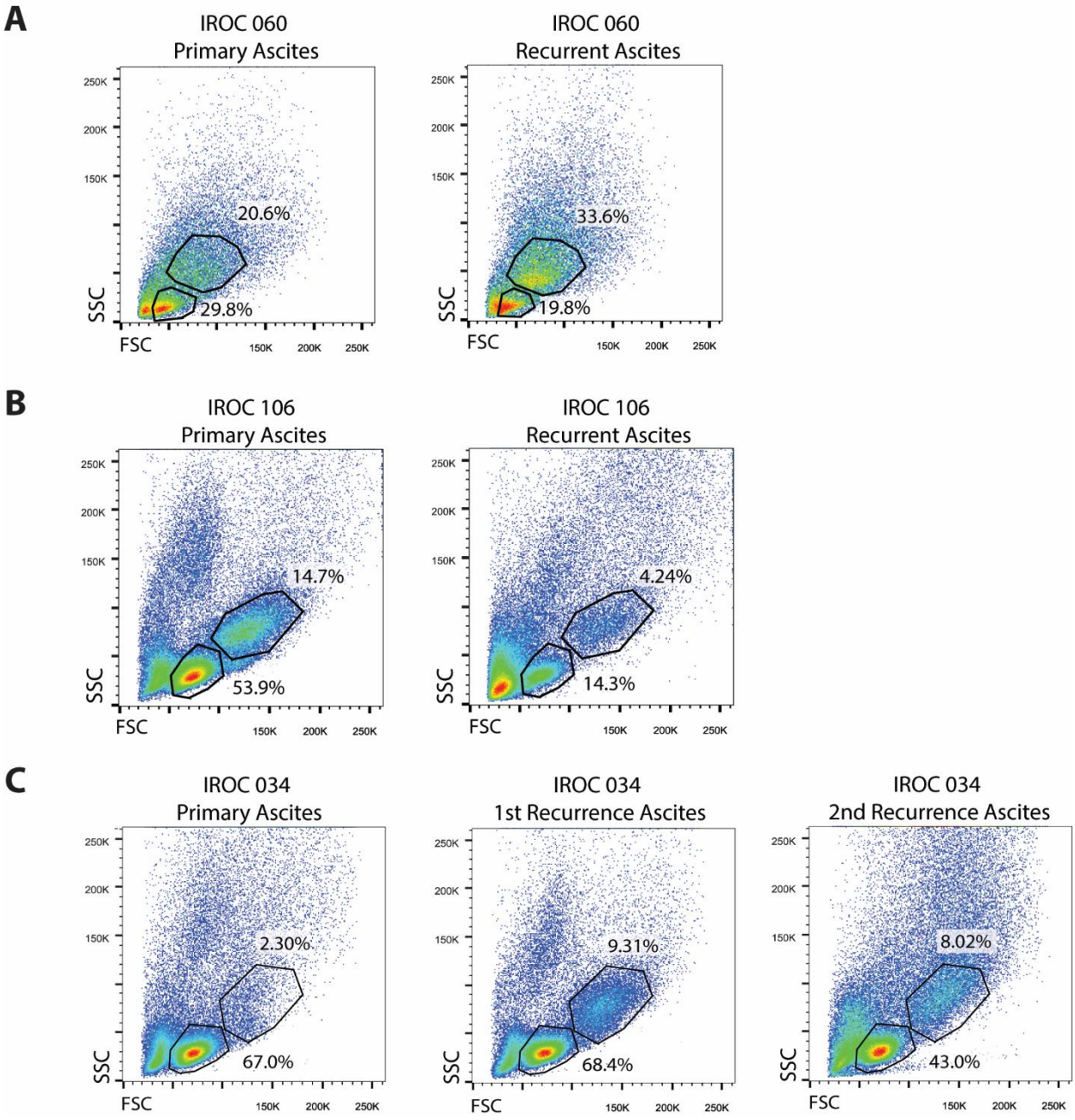

Figure 18. *Ex vivo* proportions of lymphocytes and monocytes in bulk ascites for the three HGSC patients studied: (A) IROC 060, (B) IROC 106, and (C) IROC 034. Lymphocytes and monocytes were gated based on FSC and SSC and the percentage of both populations are indicated beside the gate within each dot plot. Each patient's ascites samples were analyzed together, however samples between patients were analyzed at different times. Therefore, the gates are unique to each patient. Cells were gated on singlets and the gating strategy is outlined in Figure A5.

2.4.8 Ex vivo TAL phenotypes from primary and recurrent ascites in HGSC

Retrospective analysis of primary and recurrent ascites from all three patients was performed by analyzing flow cytometry data for CD3, CD8, CD4, PD-1, CD103, and CD137. For both IROC 060 and 106, PD-1 expression on TAL *ex vivo* as higher on the subset of TAL that mediated anti-tumor reactivity. Indeed, IROC 060 primary $CD8^+$ TAL mediated the anti-tumor response (Figure 8A) and had 2-fold higher PD-1 expression compared to primary $CD4^+$ TAL (i.e. 8.6% vs 4.78% $PD\text{-}1^+$; Table 1). By the time of first recurrence, equal proportions $CD8^+$ and $CD4^+$ TAL mediated the anti-tumor response (Figure 8C) and accordingly, PD-1 expression was comparable on both $CD8^+$ and $CD4^+$ T cells (i.e. 5.97% vs 4.43% $PD\text{-}1^+$; Table 1). This same trend was evident for IROC 106 TAL (Table 1, Figures 10A,C). In primary disease, $CD4^+$ T cells mediated the anti-tumor immune response (Figure 10A) and correspondingly had over 2-fold higher PD-1 expression compared to $CD8^+$ TAL (Table 1). This correlation was not perfect, as recurrent $CD4^+$ TAL *ex vivo* had 3-fold higher PD-1 expression compared to $CD8^+$ TAL (Table 1) despite having an equal mixture of $CD8^+$ and $CD4^+$ T cells mediated the anti-tumor response (Figure 10A,C). IROC 034 had no tumor-reactive TAL at any disease time point (Figure 12). Consistent with this, PD-1 expression levels were similar on both $CD8^+$ and $CD4^+$ TAL (Table 1). In contrast, expression of CD137 and CD103 was low and similar between primary and recurrent disease in all three patients (Table 1), suggesting no association between *ex vivo* expression levels of either CD137 or CD103 on T cells from ascites and ascites-reactivity.

Table 1. Characteristics of TAL *ex vivo* and post-expansion from each of the three HGSC patients studied. *Ex vivo* TAL gating strategies are shown in Figure A6, IL-2 expanded TAL gating strategies are shown in Figure A7, and REP-expanded TAL gating strategies are shown in Figure A8. Samples were stained for CD3, CD8, CD4, PD-1, CD137, and CD103. *Ex vivo* and IL-2-expanded TAL PD-1, CD103, and CD137 values are represented as the percentage of either the total $CD4^+$ and $CD8^+$ T cells (IROC 060) or the total $CD3^+$ T cells (IROC 106 and IROC 034). REP-expanded TAL PD-1, CD103, and CD137 values are represented as the percentage of total singlet lymphocytes by FSC and SSC

			IROC 060		IROC 106		IROC 034		
			Primary	Recurrent	Primary	Recurrent	Primary	1st Recurrence	2nd Recurrence
Ex Vivo	CD8+	**Total**	**48.5%**	**44.0%**	**29.2%**	**20.8%**	**41.1%**	**28.0%**	**28.2%**
		PD-1+	8.61%	5.97%	11.0%	9.49%	9.46%	6.25%	6.95%
		CD137+	0.35%	0.096%	0.069%	0.096%	0.052%	0.029%	0.11%
		CD103+	8.89%	6.07%	2.54%	5.90%	1.10%	0.93%	1.67%
	CD4+	**Total**	**48.8%**	**53.6%**	**63.7%**	**74.8%**	**50.1%**	**67.1%**	**68.3%**
		PD-1+	4.78%	4.43%	25.2%	31.6%	5.04%	6.43%	8.29%
		CD137+	0.44%	0.19%	0.064%	0.38%	0.061%	0.044%	0.13%
Post IL-2 Expansion	CD8+	**Total**	**65.6%**	**40.6%**	**29.7%**	**29.9%**	**52.3%**	**34.6%**	**42.0%**
		PD-1+	22.4%	17.4%	7.18%	11.0%	9.28%	5.01%	14.9%
		CD137+	1.90%	0.84%	0.90%	0.53%	1.28%	1.83%	2.67%
		CD103+	4.04%	6.46%	0.28%	1.23%	1.18%	0.87%	8.56%
	CD4+	**Total**	**13.2%**	**44.9%**	**62.9%**	**63.0%**	**35.8%**	**58.1%**	**44.6%**
		PD-1+	4.80%	35.1%	30.2%	33.3%	12.9%	12.9%	12.1%
		CD137+	0%	1.29%	0.10%	0.49%	0.78%	1.92%	1.81%
Post REP Expansion	CD8+	**Total**	**70.1%**	**45.0%**	**7.65%**	**26.0%**	**30.8%**	**22.2%**	**27.0%**
		PD-1+	8.20%	4.90%	3.90%	10.5%	19.6%	13.7%	13.3%
		CD137+	0.39%	0.10%	0.035%	0.15%	0.047%	0.077%	0.032%
		CD103+	0.10%	0.13%	0.012%	0.17%	0.67%	0.056%	0.048%
	CD4+	**Total**	**22.2%**	**46.6%**	**91.6%**	**72.4%**	**54.7%**	**74.9%**	**71.0%**
		PD-1+	5.54%	20.1%	49.4%	46.6%	42.7%	48.9%	42.2%
		CD137+	0.061%	0.096%	0.25%	0.62%	0.071%	0.067%	0.027%

2.4.9 Characteristics of expanded T cells from primary and recurrent ascites

I also assessed the phenotype of expanded TAL using flow cytometry for CD3, CD4, CD8, CD137, PD-1, and CD103. Within each patient, primary and recurrent TAL had similar populations of $CD4^+$ and $CD8^+$ T cell subsets directly *ex vivo* (Table 1). However, certain TAL subsets expanded preferentially following high-dose IL-2 and a REP. For example, IROC 060 primary TAL had a nearly 4-fold greater proportion of $CD8^+$ T cells compared to $CD4^+$ T cells following expansion, despite comparable populations of $CD4^+$ and $CD8^+$ TAL *ex vivo* (Table 1). Consistent with this, ascites reactivity of primary TAL was predominantly $CD8^+$-mediated. Likewise, for all other TAL populations from IROC 060 and IROC 106, the T cell subset that preferentially expanded during the high-dose IL-2 expansion mediated ascites-reactivity. In contrast, expression of PD-1, CD137, or CD103 on expanded TAL showed no consistent association with ascites-reactivity (Table 1). Collectively, monocyte and lymphocyte content of ascites as well as *ex vivo* expression of PD-1 on TAL and the high-dose IL-2 and REP expansion patterns were associated with tumor-reactive TAL and therefore may represent markers that can be used for predicting ascites reactivity in HGSC.

2.5 Discussion

To determine how the anti-tumor immune response changes over time to respond to intratumoral heterogeneity in HGSC, I evaluated changes in the T cell response to primary and recurrent disease in three HGSC patients. The three patients showed different patterns of ascites recognition. In the case of IROC 060, primary ascites did not elicit a T cell response, but recurrent ascites elicited a robust T cell response (Figure 8), indicating ascites changed from non-immunogenic to highly immunogenic during the progression from primary to recurrent disease. In the case of IROC 106, primary and recurrent ascites elicited robust immune responses, demonstrated by TAL from primary and recurrent disease recognizing ascites from primary and recurrent disease (Figure 10), indicating ascites remained immunogenic during progression from primary to recurrent disease. Finally, in the case of IROC 034, neither primary nor recurrent ascites elicited a T cell response, indicating this patient's cancer remained relatively non-immunogenic over time (Figure 12). As discussed below, these three different response patterns provide unique insights into the co-evolution of tumors and the immune response in human cancer patients.

It is not clear why ascites-derived tumor cells from IROC 060 primary disease or IROC 034 primary and recurrent disease did not elicit T cell responses. An explanation could be the moderate mutation burden of HGSC compared to other tumor types in which T cell reactivity is more commonly found.[244] Recently, Martin *et al*[228] found the low mutation burden in a mouse model of epithelial ovarian cancer limited the ability to find neoantigen-reactive T cell clones. In fact, peptide vaccines based on predicted neo-epitopes of the mouse epithelial ovarian tumor line ID8 failed to elicit a therapeutic response and induce tumor regression, despite each mutant peptide activating mutation-specific T cells *in vitro*.[228] Although the mutation burden of IROC 034 and IROC 060 tumors is unknown, it is possible these tumors may not harbour any immunogenic mutations and thus may not elicit an anti-tumor immune response.[245] Further, given the potential for high ITH in HGSC tumors, it is possible that the tumor could express an immunogenic antigen, but only in a low-frequency subclone,[108] thus, lowering the chances of detecting a reactive T cell clone with the threshold of current methods.

The lack of tumor-reactivity found in these patients may be due to limited expansion of tumor-specific T cells. T cell expansion requires growth signals from IL-2 and TCR stimulation,[2] however expansion can be constrained by various factors. For example, an immunosuppressive ascites environment[246,247] may prevent the proliferation of specific TAL and subsequent detection of tumor-

reactivity. Ascites fluid has been shown to suppress T cell function[247] and can contain immunosuppressive cytokines, [246–249] subsets of immunosuppressive cells[172,173,179,180], such as those that express immunosuppressive molecules such as PD-L1[28,29], IDO-1[195], β-catenin[250,251], TGF-β[194], VISTA[149], and CD155[150]. Indeed, in my study, IROC 060 and IROC 034 had high PD-L1 expression on EpCAM$^+$ tumor cells in the ascites (Figures 5A,B, 6A,B, 7A-C) and PD-1 expression on TAL (Table 1). It was unclear why PD-L1/PD-1 interactions blocked T cell expansion in these specific cultures when PD-1 and PD-L1 were also expressed on ascites samples that did have tumor-reactive T cell expansion. Therefore, interactions between PD-1$^+$ T cells and PD-L1$^+$ EpCAM$^+$ tumor cells may be part of a more complex network of other immunosuppressive factors that prevent expansion of tumor-reactive T cell subsets and should be studied further.

I found TAL reactivity in IROC 060 and IROC 106 was directed towards the CD45$^+$ fraction of ascites, rather than towards tumor cells. Cell-intrinsic immune resistance mechanisms may explain the lack of reactivity towards tumor cells. For instance, impaired IFN-γ signaling pathways may lead to reduction in expression of MHC molecules on the cell surface of tumor cells and subsequently impair T cell responses. Recent studies evaluating resistance mechanisms to checkpoint blockade therapy found non-responding tumors had genomic defects in IFN-γ pathway genes such as JAK1, JAK2, as well as truncation of the β-2-microglobulin gene resulting in impaired expression of MHC class I.[165,166] In this study, EpCAM$^+$ ascites cells did not up-regulate either MHC or PD-L1 in response to pre-treatment with IFN-γ (Figures 5A,B, 6A,B, 7A-C), suggesting tumor cells may possess intrinsic mechanisms of IFN-γ resistance. Further, irrespective of IFN-γ pre-treatment, EpCAM$^+$ tumor cells expressed much higher levels of PD-L1 than CD45$^+$ cells in the ascites (Figure 5, 6), suggesting tumor cells could be directly suppressing the T cells and concealing a tumor-specific TAL response.

The lack of TAL reactivity to tumor cells may highlight the requirement of co-stimulation for full T cell activation. For example, CD28 engagement by its ligands, CD80 and CD86 (B7-1 and B7-2), is necessary for full effector T cell activation.[252] Additionally, members of the tumor necrosis factor receptor super family, such as CD137 and OX40, provide pro-survival and proliferative signals upon binding with their ligands.[32,35,253] Non-hematologic tumor cells have been shown to express no, or low levels of costimulatory ligands such as CD80, CD86, and CD137L,[146,254–256] while macrophages and other immune cells express high levels of co-stimulatory ligands.[147,257–259] Therefore, with efficient unimpaired antigen processing and presentation in the context of appropriate co-stimulation, tumor-reactive TAL may be fully activated towards CD45$^+$ cells. Tumor cells, on the other hand, with defects in IFN-γ

response, expression of suppressive molecules, moderate MHC expression, and potentially a lack of co-stimulatory ligands, may not be able to fully activate TAL and therefore direct recognition of purified tumor cells may escape detection.

The ability to specifically identify and select tumor-reactive T cells from polyclonal populations would be helpful for development of immunotherapies, leading to improved tumor-specificity and less *in vitro* manipulation as compared to current protocols. There have been several markers suggested for prospective identification of tumor-reactive T cells,[40] but it is unknown what the best marker is to select such cells from polyclonal populations like peripheral blood, TIL, and TAL. One study by Ye *et al* suggested CD137 was the most accurate identifier of tumor-specific T cells in ovarian cancer.[40] However, rather than assessing CD137 levels directly *ex vivo*, the authors rested bulk disaggregated tumor and ascites samples in IL-7 and IL-15 overnight prior to assessment of CD137 to increase the percentage of positive cells. Because the authors found CD137 levels to be low directly *ex* vivo, CD137 is unlikely the best marker for identification of tumor-reactive TIL directly *ex vivo*.[40] Indeed, in my patient cohort, CD137 levels were very low (<1%) on TAL directly *ex vivo* from all time points (Table 1), suggesting CD137 is a poor marker of tumor-reactive TAL directly *ex vivo*.

A few recent studies from our lab suggested CD103 is another candidate marker for identifying the tumor-reactive subset in ovarian cancer.[87,242,260] CD103 is a marker of tissue-resident memory T cells (T_{RM}) and is up-regulated following antigen-specific activation in the presence of TGF-β.[261] However, CD103 levels on TAL were found to be low across all three patients' ascites samples and therefore, CD103 is unlikely to be a predictive marker of tumor-reactive TAL directly *ex vivo*.

Another set of papers published recently suggested CD27 may be a good marker of prospective identification of tumor-reactive T cell subsets in melanoma or ovarian cancer.[86,262] CD27 is a tumor necrosis family (TNF) receptor family member involved in T cell proliferation, effector function, and development of T cell memory.[263] One study in melanoma evaluated CD27 in TIL subsets used for clinical infusion[262] while the study in ovarian cancer found $CD27^+$ TIL conferred a prognostic benefit.[86] Neither study showed direct evidence that $CD27^+$ T cells were highly enriched for tumor-reactivity, and therefore CD27 was not investigated in this study.

Perhaps the most promising marker for prospectively identifying tumor-reactive T cells is PD-1. Notably, there has been exceptional clinical success using checkpoint blockade therapies that specifically block the suppressive interaction between PD-1 and PD-L1/PD-L2.[161] Additionally, two studies demonstrated the use of PD-1 as a marker of a highly enriched tumor-reactive T cell population in TIL

and peripheral T cells.[159,160] In agreement with earlier studies, I showed *ex vivo* levels of PD-1 expression were higher on the subset of T cells that mediated the anti-tumor response. For example, $CD8^+$ T cells from IROC 060 primary disease mediated the anti-tumor response (Figure 8A) and in line with this, primary $CD8^+$ TAL expressed 2-fold higher PD-1 compared to primary $CD4^+$ T cells (Table 1). These results require validation in a larger cohort of patient; nonetheless, PD-1, more so than CD103 or CD137, may be a useful marker for prospectively identifying tumor-reactive T cells.

I next investigated whether patterns of TIL infiltration in primary solid tumors were indicative of anti-tumor TAL responses using immunohistochemistry analysis of T cell infiltration in primary tumor tissue. Patterns of T cell infiltration in solid tumor were not indicative of anti-tumor TAL responses. In fact, IROC106 had a near complete absence of TIL in primary tumor (Figure 15A,B) despite the presence of tumor-reactive TAL in primary ascites (Figure 10A). These findings may be explained by the differences in T cell infiltration between ascites and tumor. Because of their dense architecture, tumors are likely far more exclusive to T cell infiltration compared to the liquid ascites. For example, tumors can erect barriers to T cell infiltration by promoting the development of extremely dense stroma[264] or through the expression of various molecules that prevent trafficking of immune cells into the TME, such as dipeptidylpeptidase-4,[267] or CXCL12[188,268].[265,266] Therefore, it is not unexpected that tumor-reactive T cells may be present in ascites despite a near complete absence of T cells in the tumor. These results suggest that HGSC patients who lack TIL infiltration in their tumors may still be amenable to ACT using T cells isolated from ascites.

This study had a few limitations. First, only three patients were in the study cohort, which limits any conclusions made about overarching patterns of tumor and anti-tumor T cell evolution. This is particularly true because each patient exhibited different patterns of ascites recognition. Therefore, results should be validated on a larger cohort of HGSC patients. Second, due to the overall low number of $CD45^-$ cells within ascites samples from IROC 060 and IROC 106 primary ascites and IROC 034 ascites (data not shown) and subsequent sample loss during the $CD45^+$ depletion of ascites, almost the entire sample had to be used for assessing TAL reactivity, leaving very little sample available for flow cytometry analysis of MHC class I, class II, and PD-L1. For example, only 29 events fell within the viable, singlet, $EpCAM^+$ gate when analyzing MHC and PD-L1 expression on IROC 060 primary ascites following IFN-γ pre-treatment (Figure 5A). Therefore, conclusions made on the expression patterns of both MHC and PD-L1 may not necessarily represent biological reality. Last, without knowing the specific antigen that

TAL recognize, it is not possible to elucidate more specific mechanisms of T cell evolution, highlighting the importance of profiling tumor-reactive T cell clones by TCRseq, as discussed in chapter 3.

This study highlights potential mechanisms used by the immune system to contend with ITH over time in HGSC. Two recent studies have shown new tumor mutations with concomitant responsive T cell clones emerged over time in ovarian and melanoma patients.[48,49] Wick *et al* studied one ovarian cancer patient and found a non-synonymous point mutation in the hydroxysteroid dehydrogenase-like 1 (HSDL1) gene that emerged over the time between primary disease and first tumor recurrence.[49] Despite maintenance of the HSDL1 mutation at 2nd recurrence, the HSDL1-mutation-reactive T cell clone had been lost from the ascites T cell repertoire.[49] A separate study of two melanoma patients showed similar results.[48] This study found neoantigens and cognate T cell clones were dynamic over time, with both patients' tumors losing neoantigens with their cognate T cell clones while subsequently gaining new neoantigens and cognate T cell clones over time.[48] These studies suggest that the neoantigen landscape and concomitant T cell responses are dynamic, with new T cell clones recognizing new tumor antigens emerging over time. As such, the finding that IROC 060 and IROC 106 tumor-reactive TAL became more equal mixtures of $CD4^+$ and $CD8^+$ T cells by recurrent disease compared to the primary TAL may indicate that in these two patients, T cells adapt to ITH by recognizing a more diverse set of both class-I- and class-II-restricted tumor-associated antigens.

ITH in tumors may induce the immune system to recognize common antigens shared by primary and recurrent disease. For example, despite the overall dynamic nature of neoantigens and neoantigen-reactive T cells in the two melanoma patients studied, Verdegaal *et al* found that T cells from every disease time point recognize tumor cells from all but one disease time point.[48] In IROC 060 and IROC 106, the "evening-out" of $CD4^+$ and $CD8^+$ tumor-reactive T cell populations, together with the overall reduction in the frequency of tumor-reactive T cells by recurrent disease, suggest tumor-reactive T cells were lost over time in both patients. If this is the case, based on the findings from Verdegaal *et al*,[48] it could be argued that the tumor-reactive T cells lost between primary and recurrent disease may have been T cells that recognized neoantigens also lost between primary and recurrent disease, while tumor-reactive T cells recognized common antigens remained from primary to recurrent disease. However, without knowing the antigen specificities or the clonal diversity of these TAL populations, it is not possible to elucidate this. This issue is further addressed by the TCRseq results in chapter 3.

These results have implications for the treatment of HGSC with adoptive cell therapy (ACT). In HGSC, surgically resected primary tumor is often the only source of TIL.[201] Secondary surgeries at

recurrent time points are not associated with prognostic benefit and are therefore not part of standard of care.[269] However, ACT trials are limited to treating recurrent disease. Therefore, given the potential for high ITH in HGSC tumors, it is critical to know whether TIL from primary disease can recognize recurrent disease. If results from this study are confirmed by studying additional HGSC patients, they would indicate primary TAL recognize recurrent disease even more robustly than recurrent TAL, suggesting primary TAL may, in fact, be the best choice to improve the changes of eliciting strong clinical responses in ACT of HGSC. Further, for patients like IROC 106, whose tumors are largely devoid of TIL, ascites may represent a source of tumor-reactive T cells that would otherwise be unattainable using primary tumor specimens. Recurrent ascites also offers an opportunity to expand T cells from disease time points closer to the time of ACT treatment. In summary, this study shows primary TAL recognized recurrent disease and may mediate clinical responses through ACT of recurrent tumors.

This study also illuminated a potential challenge for ACT in HGSC. Namely, TAL specifically recognized the $CD45^+$ fraction of ascites and not purified tumor cells, which raises the possibility that ACT of TAL may not lead to direct tumor killing. However, $CD45^+$ antigen-presenting cells are often found in tumors.[270,271] This raises the possibility that adoptively-transferred T cells may still elicit robust T cell responses despite lacking the ability to directly recognize tumor cells. During robust immune responses, T cells may induce indirect anti-tumor effects through the release of effector molecules such as IFN-γ and TNF-α, which have been shown to suppress tumor cell growth.[272,273] Also, APCs may activate $CD4^+$ helper T cells which in turn may stimulate the humoral immune response, leading to the production of anti-tumor antibodies,[2] further bolstering the anti-tumor immune response and ultimately leading to tumor regression. In fact, a recent study from our lab found the presence of plasma cells in the stroma of HGSC tumors was significantly associated with improved prognosis,[89] highlighting the importance of the humoral arm of the adaptive immune response in HGSC.

In summary, I determined anti-tumor T cell responses from ascites are diverse between HGSC patients and dynamic within a patient. Nonetheless, in cases with demonstrated ascites-reactivity, primary TAL recognized recurrent disease, suggesting ACT of recurrent tumors using TIL from primary disease may mediate clinical responses in HGSC patients.

Chapter 3: T Cell Clonal Dynamics from Primary to Recurrent Disease in HGSC

Nicole S. Little[1,2], Phineas T. Hamilton[2], Spencer D. Martin[2,3], David R. Kroeger[2], John R. Webb[2], Robert A. Holt[4,5], Brad H. Nelson[1,2]

[1]Department of Microbiology and Biochemistry, University of Victoria, Victoria, B.C., Canada

[2]Trev and Joyce Deeley Research Centre, BC Cancer Agency, Victoria, B.C., Canada

[3]Faculty of Medicine, University of British Columbia, Vancouver, B.C., Canada

[4]Canada's Michael Smith Genome Sciences Centre, BC Cancer Agency, Vancouver, B.C., Canada

[5]Department of Medical Genetics, University of British Columbia, Vancouver, B.C., Canada

BHN and NSL conceptualized the study. NSL conducted the project. PTH assisted with sequencing data analysis. SDM, DRK, and JRW assisted with FACS. PTH, SDM, DRK, JRW, RAH, and BHN contributed both to experimental design and scientific suggestions. NSL wrote the chapter.

3.1 Abstract

Background: Intratumoral heterogeneity (ITH) can be high in high-grade serous carcinoma (HGSC). However, it is unknown how anti-tumor T cell responses predominantly respond to ITH in HGSC. Previous studies in melanoma and high-grade serous carcinoma show tumor-reactive T cell clones fluctuate over time with their cognate tumor-antigens. Further, in chapter 2, I demonstrated that the anti-tumor T cell response varies between patients and is dynamic within each patient. Therefore, I hypothesize new tumor-reactive T cell clones emerge over time to contend with ITH. If this is true, I should see differences in the clonal repertoire of tumor-reactive T cells between primary and recurrent disease.

Methods: $CD137^+$ tumor-reactive TAL were FACS-purified following overnight co-culture of TAL with autologous ascites. RNA was extracted and sent for deep sequencing of TCRβ chains (TCRseq) at the Michael Smith Genome Sciences Centre (Vancouver, BC) to profile the tumor-reactive repertoire of both primary and recurrent disease. Raw sequencing reads were analyzed using the MiXCR data analysis suite and TCR clonotypes were compared between primary and recurrent disease to elucidate differences in tumor-reactive populations over time in HGSC.

Results: FACS-purification of $CD137^+$ T cells followed by TCRseq was successfully performed on high- and low-abundance T cell populations, suggesting TCRseq can be performed using very few T cells. IROC 060 and IROC 106 had numerous tumor-reactive T cell clones that were unique to either primary or recurrent disease. Further, IROC 106 had tumor-reactive T cell clones that were shared between primary and recurrent TAL.

Conclusions: I developed a pipeline for the identification of tumor-reactive TCR sequences without the need for *a priori* knowledge of specific antigens. Further, this pipeline is feasible for very low-abundance samples, such as tumor-reactive T cells. For both patients, TCRseq results show some tumor-reactive T cell clones are lost over time, while others emerge between primary and recurrent disease to respond to ITH in HGSC.

Future Directions: Trends observed in patterns of T cell evolution within HGSC patients will be validated across a larger patient cohort. Additionally, the pipeline developed can be used to further study the immune response to HGSC using *in situ* PCR, T cell engineering, and immune monitoring post-adoptive cell therapy (ACT).

Significance: This study provides early insights into how TAL respond to ITH in HGSC. Ultimately, these results will inform the design of adoptive T cell therapy for recurrent HGSC.

3.2 Introduction

Intratumoral heterogeneity (ITH) is a significant challenge for the immune response to tumors. Spatial ITH has been described in nearly every tumor type,[92] including high-grade serous carcinoma (HGSC).[108] One study on spatial ITH in HGSC found that on average only 51.5% of mutations were shared between tumor sites within each patient. Therefore, one can appreciate that the anti-tumor T cell response must take certain approaches to deal with this diversity. First, the anti-tumor T cell response may be comprised of a diverse set of T cell clones that recognize several private tumor antigens expressed by different subclones within the tumor architecture. This was described in renal cell carcinoma, where TCRseq profiling of various tumor sites within a patient revealed poor overlap between the most abundant T cell clones, suggesting a heterogeneous anti-tumor response.[120] Alternatively, T cells could recognize common features of every tumor clone. This approach has been observed in HGSC, where T cell profiling of various tumor sites have shown more homogenous T cell populations.[121,122]

Not as much is known about temporal ITH of tumors and their corresponding anti-tumor T cell responses. One seminal study described large mutational differences between primary and recurrent disease in an HGSC patient who had dramatic responses to platinum-based chemotherapy.[107] Further, the patient lost one tumor while gaining a new, prominent, tumor subclone at recurrence.[107] Subsequently, it was determined that this patient had a new immunogenic mutation that emerged in the first recurrence along with a mutation-specific T cell clone.[49] Another study in melanoma also showed emergence of new T cell clones with their cognate neoantigen over time.[48] However, both studies also found tumor-reactive T cell were lost over time, irrespective of antigen loss.[48,49] Despite these findings, it is largely unknown if there are predominant mechanisms which tumor-reactive T cells use to contend with ITH in HGSC.

In this study, I compare the clonal repertoire of tumor-reactive TAL between primary and recurrent disease. I FACS-purified $CD137^{+}$ tumor-reactive TAL from primary and recurrent disease and sequenced the TCRβ chains in these populations by Illumina-based TCRseq to profile the TCR clonotypes of tumor-reactive TAL. Based on previous studies as well as results from chapter 2, showing tumor-recognition patterns of TAL are diverse between patients and dynamic within patients, I hypothesized that new tumor-reactive T cell clones would emerge over time to contend with ITH in HGSC.

3.3 Methods

Generation of T Cell Mini-lines from Peripheral Blood

T cell clones reactive to cytomegalovirus, Epstein-Barr virus and influenza virus peptide 11 (CEF-11), and melanoma antigen recognized by T cells peptide 1 (MART-1), were generously donated by Dr. David Kroeger. Cryopreserved PBMC from IROC 024 were thawed, washed, and resuspended in 3% fetal bovine serum (FBS; Gibco) in PBS. $CD8^+$ T cells were purified by negative selection using a magnetic $CD8^+$ T cell isolation kit (Miltenyi Cat. No. 130-096-495) according to the manufacturer's protocol. Purity of the $CD8^+$ T cell population was assessed by flow cytometry for CD8-FITC (BioLegend Cat. No. 300906) and CD4-PE (BioLegend Cat. No. 357404) on a FacsCalibur flow cytometer using FlowJo analysis software (Version 7.6.5). $CD8^+$ T cells were washed again, counted using Viacount (EMD Millipore Cat. No. 4000-0130) on a Guava cell counter (EMD Millipore), and resuspended at $2x10^5$ cells/mL in complete media (RPMI 1640 (Gibco cat no. 22400-089), 10% fetal bovine serum (Gibco), 100 µg/mL penicillin-streptomycin, and 50 µM β-mercaptoethanol) supplemented with human IL-2 (300 U/mL) and anti-CD3 antibody (30 ng/mL). To each well of a 96-well round bottom tissue culture plate, 2000 cells were added with $2x10^5$ irradiated (50 Gy) allogeneic healthy donor PBMC feeder cells. On day 5 and every two days following half the media was exchanged with fresh complete media supplemented with 300U/mL human IL-2. Once cell pellets reached 3mm diameter, cells were split into replicate 96-well round bottom plates. After two weeks of expansion, cultures were washed and resuspended in complete media supplemented with 1 U/mL of human IL-2 and 10 ng/mL of human IL-7 and distributed in 96-well flat-bottom tissue culture plates to rest prior to assessment for reactivity to CEF-11, and MART-1 peptides by IFN-γ ELISPOT, as previously described (Chapter 2).

Generation of CEF-11 and MART-1 Reactive T Cell Clones from T Cell Minilines

T cell minilines with reactivity to either CEF-11 peptide or MART-1 peptide were cloned by limited dilution. Briefly, T cell cultures from the miniline expansion with confirmed reactivity to either CEF-11 peptide or MART-1 peptide by IFN-γ ELISPOT were selected and serially diluted down to 1 cell per well of a 96-well round bottom tissue culture plate. Cells were REP-expanded in a "mini-REP". Briefly, to stimulate T cells to proliferate, $2x10^5$ irradiated (50 Gy) allogeneic PBMC feeder cells were added to each well of the 96-well culture plate. T cell cultures were initiated in complete media supplemented with 300 U/mL human IL-2 and 30 ng/mL anti-CD3 antibody (eBioscience eBioscience cat no. 16-0037). At day 5 and every two to three days after, half the media from each well was exchanged

with fresh media supplemented with 300 U/mL human IL-2. Following two weeks of expansion, T cells were rested as described above in media supplemented with 1U/mL human IL-2 and 10 ng/mL human IL-7. Following this rest period, to generate assessable numbers of T cell clones, T cell cultures from wells where the starting cell number was 1 cell/well were seeded into a second full-scale REP-expansion as previously described in Chapter 2. These final REP-expanded cultures were considered clonal and were cryopreserved for future use.

Fluorescence-Activated Cell Sorting of Activated T cells

Following a 20-hour incubation at 37°C and 5% CO_2, cells were harvested and stained for viability (Fixable Viability Dye V450 eBioscience cat no. 65-0863), CD3 (Biolegend cat no. 317332), CD8 (Biolegend 300906), CD4 (Biolegend cat no. 357404), and CD137 (Biolegend 309810). Flow cytometry samples were run on a BD Influx Cell Sorter or BD FACSAriaII. Cells were stained in AIM-V serum free media (Gibco cat no. 12055-083) and collected directly into RLT lysis buffer containing 10 µL/mL 2-mercaptoethanol (Qiagen Cat. No. 79216). Cells were frozen in RLT lysis buffer prior to extraction of RNA, which is outlined below.

T Cell Receptor Sequencing by Cloning

For all samples, RNA was extracted according to manufacturer's instructions using either RNeasy mini kits (Qiagen cat. no. 74106) or AllPrep mini kits (Qiagen cat no. 80204) for extracting RNA and DNA from samples containing >5x10^6 cells and AllPrep micro kits (Qiagen cat no. 80284) for extracting RNA and DNA from samples containing <5x10^6 cells. cDNA synthesis and TCR-β sequence amplification was performed according to the Genome Sciences' Centre (GSC) TCRseq protocol.[274,275] Briefly, first strand cDNA was synthesis proceeded through a 5'-RACE protocol using previously published TCRB primer (5'-CACGTGGTCGGGGAAGAAGC-3')[276] and a previously published template-switching oligo (5'-AAGCAGTGGTAACAACGCAGAGTACGCGGG-3').[277] Primers were mixed at equimolar concentrations (1 µM) with template to up to 9 µL final volume. The solution was incubated at 72°C for 2 minutes and placed on ice immediately. Next, 40 U of RNaseOUT (Invitrogen), 1 mM dNTPs, 2 mM DTT, 10 U SMARTScribe reverse transcriptase (Clontech), and 1X first-strand buffer (Clontech) were added to a final volume of 20 µL. First-strand cDNA synthesis conditions were as follows: 90 minutes at 42°C, 15 minutes at 70°C, and 2 minutes at 4°C. Following first-strand cDNA synthesis, samples were immediately used in the second-strand cDNA synthesis/PCR.

Second-strand cDNA amplification primers are proprietary information of the GSC and can be requested directly from the sequencing core. Primers were added at between 0.2 and 1 µM with 1X HF Phusion Buffer (Invitrogen cat no. F-549S), 0.3 mM dNTPs, 3% DMSO, and 2 U Phusion polymerase (Invitrogen cat no. F-549S) to first-strand cDNA template up to a final volume of 50 µL. Cycling conditions were: 98°C for 30 seconds, 40 cycles of 98°C for 10 second, 72°C for 10 seconds, and 72°C for 20 seconds, followed by a final extension at 72°C for 5 minutes. PCR products were visualized on a 2% low-melt agarose (ThermoFisher cat no. 16520-050) gel and the band at ~550bp was excised for agarose gel purification. Agarose gel purification was performed using agarase (ThermoFisher cat no. EO0461) according to the supplier's protocol with the following exception: 3M sodium acetate was used instead of 2.5M ammonium acetate in step 7 of the protocol and isopropanol was used instead of ethanol in step 9. Purified PCR amplicons were resuspended in 20 µL dH_2O.

Finally, TCR PCR amplicons were further amplified and in a clean-up PCR reaction using additional nested primer-sets from the GSC. Primers were added at between 0.2 mM and 0.1 mM with 1X Taq polymerase buffer, 2 mM $MgCl_2$, 2 mM dNTPs, 10 U Taq polymerase, and cDNA template up to a final volume of 20 µL. Cycling conditions were: 95°C for 2 minutes followed by 40 cycles of 95°C for 30 seconds, 59°C for 30 seconds, and 72°C for 45 seconds, and a final extension at 72°C for 10 minutes. T7 cloning. Products were visualized on a 2% agarose gel run at 120V for 30 minutes and samples with confirmed product were selected for TOPO® TA cloning (Invitrogen cat no. 450071).

The final TCR PCR product was mixed at the maximum volume allowed (4 µL) with the kit's salt solution and the topoisomerase I-activated pCR™4-TOPO® vector according to the manufacturer's protocol. The ligation proceeded for 45 minutes at room temperature and was placed at 4°C for an additional 4 hours prior to transformation of chemically competent DH5α *E. coli* cells. Chemical transformation proceeded as follows: cells were thawed on ice and 5 µL of the ligation reaction was added and gently mixed. Cells and ligation were incubated for 15 minutes on ice. Next, cells were heat-shocked for exactly 60 seconds in a 42°C water bath followed by cold-shock on ice for an additional 60 seconds. Next, 500 µL Luria-Bertani (LB) broth was added gently and cells were incubated at 37°C with shaking for 60 minutes. Finally, 100 µL of cells were plated on LB-agar plates containing ampicillin. After 24-hours, colonies were picked directly into PCR reactions as followed: 1X Taq polymerase buffer, 1 ng/µL each T7 and T3 primers, 2 U Taq polymerase, and 2 mM $MgCl_2$, at a final volume of 20 µL. PCR reaction conditions were as follows: 95°C for 10 minutes followed by 35 cycles of 95°C for 1 minute, 55°C for 1 minute, 72°C for 30 seconds, followed by a final extension at 72°C for 10 minutes. PCR

products were visualized on a 2% agarose gel run for 30 minutes at 120V. PCR products that were of the appropriate size were selected and sent for Sanger sequencing (Genscript). Sequences were analyzed using IMGT/V-QUEST[278] and productive TCR-β sequences were used in further analysis of CDR3 sequences of each T cell clone.

T Cell Receptor Sequencing by Illumina

RNA was extracted using either RNeasy mini kits (Qiagen cat. no. 74106) or AllPrep mini kits (Qiagen cat no. 80204) for extracting RNA and DNA from samples containing >5x10^6 cells and AllPrep micro kits (Qiagen cat no. 80284) for extracting RNA and DNA from samples containing <5x10^6 cells. RNA isolated from FACS-purified T cells or TAL were sent to the Michael Smith Genome Sciences' Centre for TCRseq (Vancouver, BC). For the pilot experiment, first strand cDNA was synthesized from the RNA and subsequently an Illumina sequencing library was constructed. Patient samples underwent first strand cDNA synthesis and the resulting cDNA was split into two samples for sequencing library construction. Libraries were run on one lane of Illumina MiSeq and 250 bp paired-end reads were generated. Raw reads were analyzed using MiXCR,[279] and VDJtools,[280] and subsequent statistical analysis and data plotting on identified clonotypes was done using the R statistical computing application.[281]

3.4 Results

3.4.1 CD137$^+$ T cell purification by FACS followed by TCR sequencing can reveal the correct TCR sequence from a mixture of T cell clones

Although CD137 is well-described as a specific marker for recent activation on T cells and numerous studies have used CD137-selection as enrichment for antigen-specific T cells, it was unknown whether CD137 purification from non-monoclonal populations was sufficiently accurate for purifying T cells and identifying antigen-specific T cells by TCR sequencing (TCRseq). Therefore, I ran a pilot experiment to determine whether FACS-purification of CD137$^+$ T cells from an antigen-stimulated mixture of T cell clones of known reactivity was sufficient to identify and profile TCR sequences from antigen-specific T cell populations. First, to identify the CDR3 sequences of each T cell clone, individual clones were stimulated with their cognate peptide. After 20 hours, CD137$^+$ T cells were sorted, and TCRs were cloned and sent for Sanger sequencing. Both a MART-1 reactive T cell clone (D6) and the CEF-11 reactive T cell clone (F2) from the same patient up-regulated CD137 following stimulation with their cognate peptide (Figure 19). Six identical TCR clones were generated from CD137$^+$-purified clone D6 (N-ASGAGFFTGELF-C; Figure 20A) and two identical TCR clones were generated from CD137$^+$-purified clone F2 (N-ASSEGGMTYYNEQF-C; Figure 20F). Next, clones D6 and F2 were mixed at a 50:50 ratio and the mixture was stimulated with either MART-1 peptide or CEF-11 peptide. After 20 hours of stimulation, CD137+ T cells were FACS-purified, RNA was extracted, TCRs were sequenced. Following MART-1 peptide stimulation, 16.5% of lymphocytes in the mixture were CD137$^+$ and following CEF-11 peptide stim 7.6% were CD137$^+$ (Figure 21). Each of three TCR sequences identified from the purified MART-1 reactive population was identical to the TCR sequence identified from clone D6 (Figures 20A,D). Likewise, each of the 6 TCR sequences from the purified, CEF-11 reactive population were identical to the TCR sequence identified from unmixed clone F2 (Figure 20F,I). These results indicate that CD137$^+$-based FACS purification is sufficient for isolating the target T cells from a bi-clonal mixture, and subsequent TCRseq can identify the correct TCR sequence.

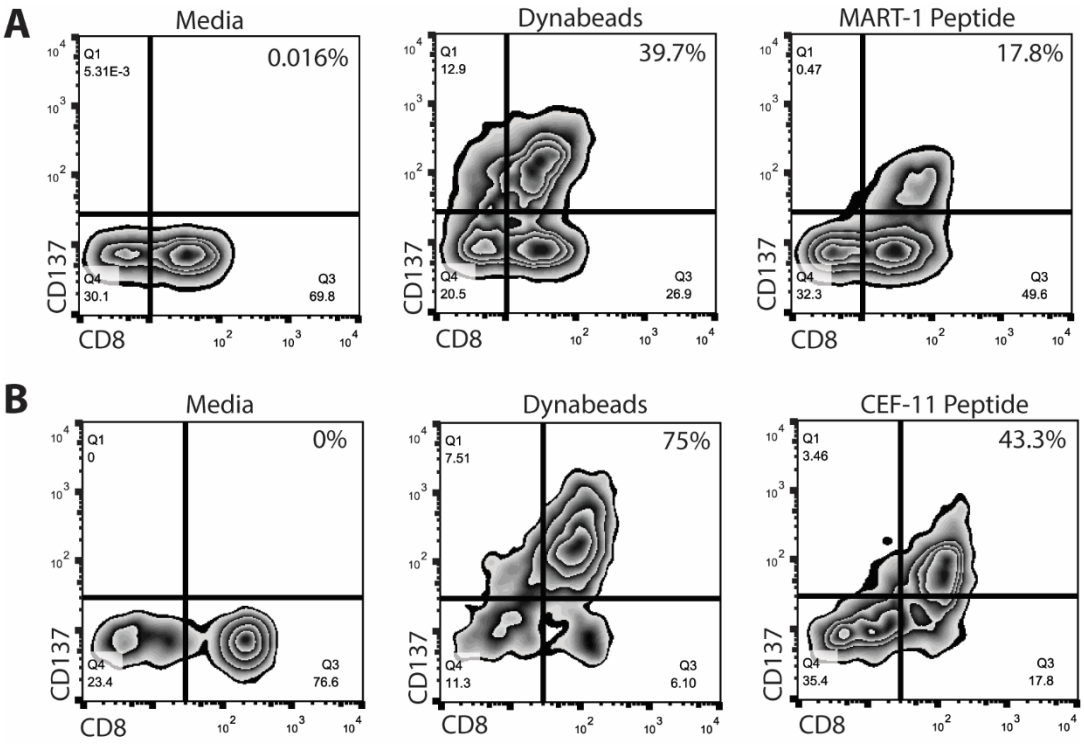

Figure 19. Flow cytometry analysis of T cell clones (A) D6 and (B) F2 stimulated with their cognate peptides MART-1 (clone D6) and CEF-11 (clone F2) or anti-CD3/CD28 coated Dynabeads compared to the unstimulated control. Cells were gated on singlets (Pulse Width by FSC) and lymphocytes (FSC vs SSC). The percentage of $CD137^{+}$ cells are indicated inside upper right-hand quadrant of each plot.

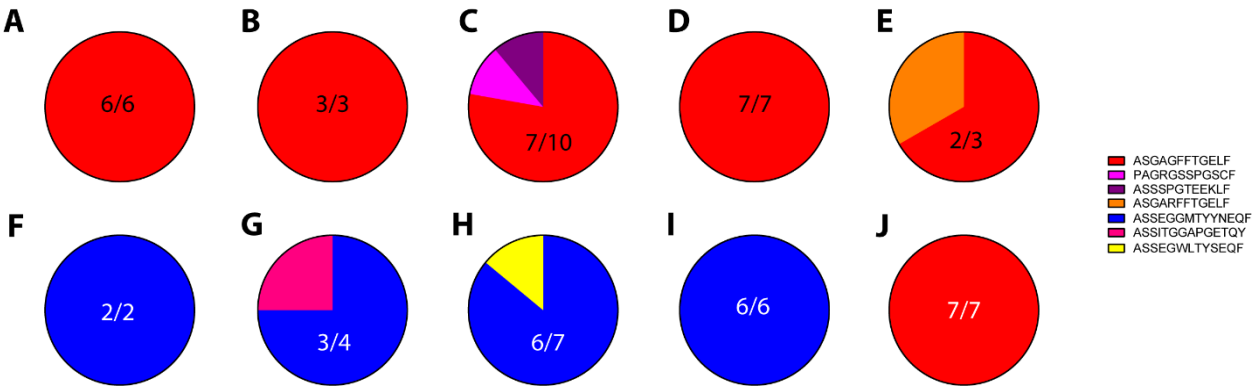

Figure 20. CDR3 sequences of the CEF-11 (F2) and MART-1 (D6) reactive T cell clones from IROC 024 following CD137^{+}-mediated FACS purification from populations of mixed clones. (A) CDR3 sequence of cloned TCRs from an unmixed population of clone D6 stimulated with MART-1 peptide and sorted based on CD137 expression. (B) CDR3 sequence of cloned TCRs from 100 cells from a mixed population of clone D6 and clone F2 stimulated with MART-1 peptide and sorted based on CD137 expression. (C) CDR3 sequence of cloned TCRs from 1,000 cells from a mixed population of clone D6 and clone F2 stimulated with MART-1 peptide and sorted based on CD137 expression. (D) CDR3 sequence of cloned TCRs from 10,000 cells from a mixed population of clone D6 and clone F2 stimulated with MART-1 peptide and sorted based on CD137 expression. (E) CDR3 sequence of cloned TCRs from unstimulated, unsorted clone D6. (F) CDR3 sequence of cloned TCRs from an unmixed population of clone F2 stimulated with CEF-11 peptide and sorted based on CD137 expression. (G) CDR3 sequence of cloned TCRs from 100 cells from a mixed population of clone D6 and clone F2 stimulated with CEF-11 peptide and sorted based on CD137 expression. (H) CDR3 sequence of cloned TCRs from 1,000 cells from a mixed population of clone D6 and clone F2 stimulated with CEF-11 peptide and sorted based on CD137 expression. (I) CDR3 sequence of cloned TCRs from 10,000 cells from a mixed population of clone D6 and clone F2 stimulated with CEF-11 peptide and sorted based on CD137 expression. (J) CDR3 sequence of cloned TCRs from unstimulated, unsorted clone F2. Each colour represents a unique CDR3 amino acid sequence returned by sanger sequencing of cloned TCR-β sequences. The fraction of the dominant CDR3 sequence is represented as a fraction of the total productive TCR sequences returned by Sanger sequencing as identified by IMGT/V-QUEST[278] in its representative fraction of the whole chart.

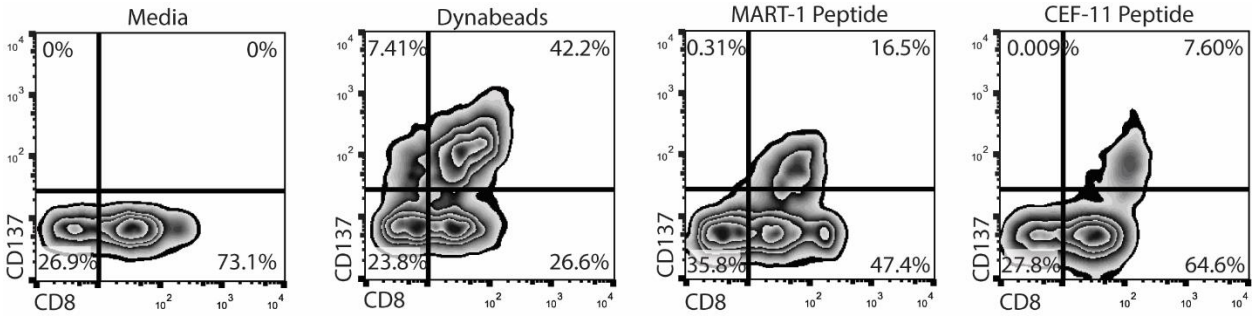

Figure 21. Flow cytometry analysis of bi-clonal mixtures of T cell clones (A) D6 and (B) F2 stimulated with MART-1 peptide, CEF-11 peptide, or anti-CD3/CD28 coated Dynabeads, compared to the unstimulated control. Cells were gated on singlets (pulse width by FSC) and lymphocytes (FSC vs SSC). The percentage of $CD137^{+}$ cells are indicated inside upper right-hand quadrant of each plot.

3.4.2. FACS-purification of as few as 100 cells is sufficient to identify a TCR of interest from a mixture of T cell clones

Tumor-reactive T cells were expected to be rare, particularly because the mutation burden in HGSC is moderate compared to other types of tumors such as melanoma and non-small cell lung carcinoma.[228,244] If, for example, only 1% of TAL were tumor-reactive, under optimal conditions screening $1x10^6$ live TAL would result in only 10,000 $CD137^+$ cells isolated for subsequent TCRseq. To identify the minimum number of cells required to obtain accurate TCR sequencing data, I sorted 100 and 1,000 $CD137^+$ cells from the bi-clonal mixture stimulated with either MART-1 or CEF-11 peptides. From 1,000 sorted $CD137^+$ cells, 70% (7/10) of the TCR sequences identified from the purified MART-1 reactive population (Figure 20C) and 86% (6/7) of the TCR sequences from the purified CEF-11 reactive population (Figure 20H) matched the respective TCR sequences of each clone identified from the unmixed clonal populations (Figures 20A,F). Even as few as 100 $CD137^+$ T cells yielded interpretable TCR sequence (Figures 20B,G). Again, these sequences had high overlap with the sequences identified in the unmixed, $CD137^+$-sorted populations (Figures 20A,F). Together these results suggest FACS purification was highly successful for purifying antigen-specific T cell populations from a mixture, and subsequent TCRseq of biologically relevant cell numbers can identify the correct TCR sequence from purified T cell populations.

3.4.3. Next-Generation TCRseq on low-input RNA samples yields productive and reliable profiling of abundant TCR sequences in a polyclonal population

3.4.3.1 TCRseq with as little as 5ng of RNA is accurate and reproducible for high-abundance T cell clones

The GSC's TCRseq pipeline typically requires 200ng of high-quality RNA for optimal sequencing results. However, tumor-reactive TAL were anticipated to be at low abundance. To determine whether low quantities of RNA were sufficient for TCRseq, an RNA titration was performed. Two RNA samples, TAL-1 and TAL-2, were extracted from two separate vials of one REP-expanded TAL line from IROC 034. RNA was quantified for each sample and titrated from 200ng to 5ng template. From 200 ng of RNA, 1282 unique T cell clonotypes were identified. Results show the sample was very polyclonal, as the top 500 most abundant clones only accounted for 84% of the total sequencing reads. Both samples containing optimal amounts of RNA (200ng) from TAL-1 and TAL-2 were nearly identical for the top 15 most abundant clonotypes (Figure 22). Although the clonotypes that fell below the top 15 most

abundant TCR clones did not have identical frequencies between each of the titrated samples, each clone that fell below the 15th most abundant clonotype represented a small fraction of the total number of sequencing reads. Therefore, small, stochastic differences may account for the differences seen in the relative abundances of TCR clonotypes beyond the top 15 most abundant clones. Further, when RNA was titrated to 75ng, 25ng, or 5ng input, the same 10 to 15 TCR clones were identified at relatively similar frequencies compared to the high-input samples (Figure 22). These results suggest that, even with as little as 5ng of input RNA, TCRseq can be used to accurately profile TCR clonotypes. However, for polyclonal samples, the measured frequencies of rare TCRs are subject to stochastic effects. Therefore, when comparing low-abundance T cell clones between samples, it is more reliable to compare the presence or absence of clones rather than ranked frequencies.

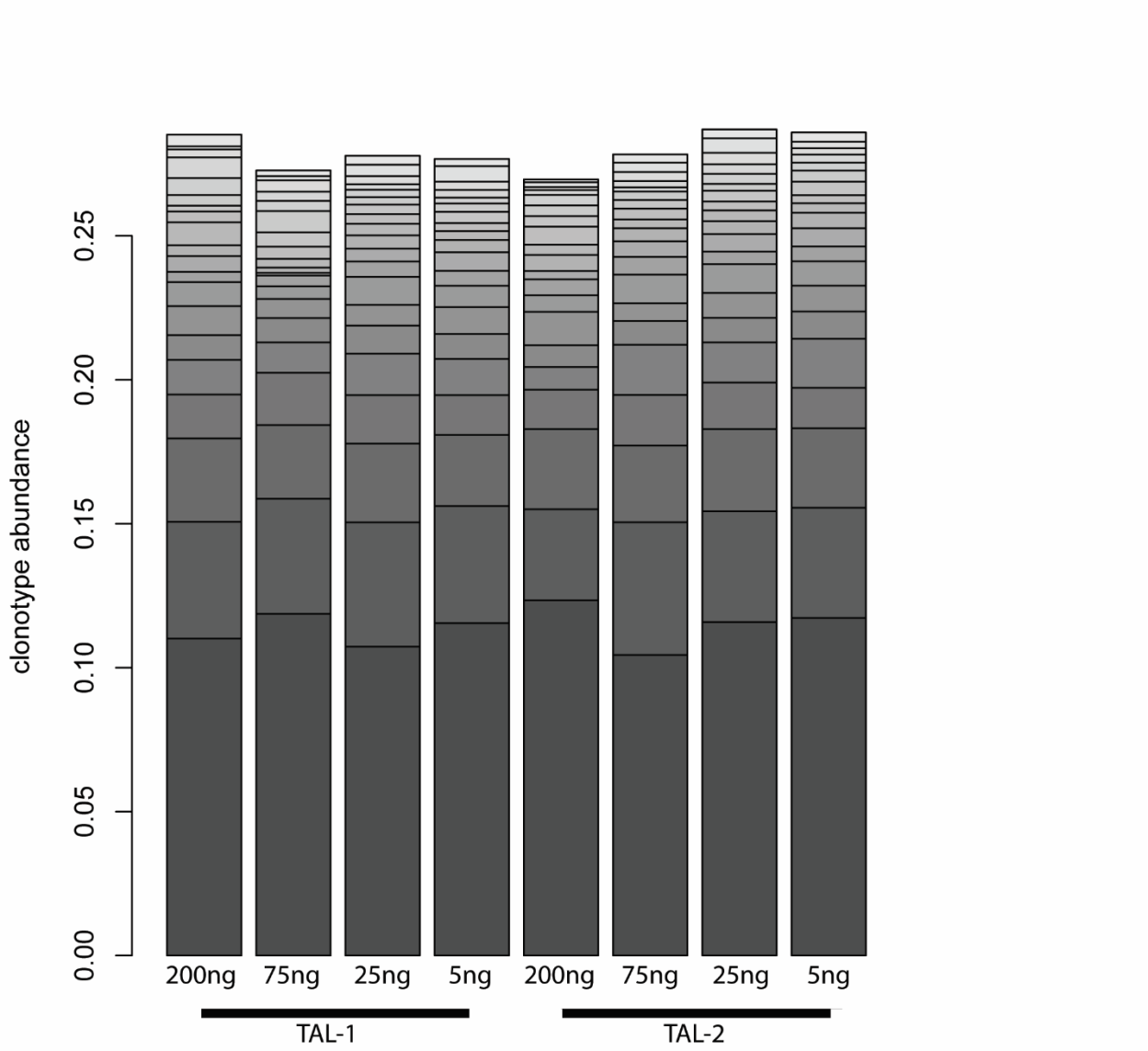

Figure 22. Top 20 most abundant T cell clonotypes from expanded patient T cell samples from ascites. RNA was prepared from two separate vials of the same REP-expanded patient T cells (TAL-1 and TAL-2). Each T cell clonotype is represented by the same shade of grey and the size of each bar represents the abundance of the TCR clonotype based on total number of sequencing reads. RNA was titrated from 200ng to 5ng input for cDNA synthesis prior to library prep and sequencing on an Illumina MiSeq. Sequencing data was analyzed by MixCR and VDJtools.

3.4.3.2 TCRseq of low-input samples of less than 10,000 cells

Although TCRseq from 5 ng of RNA was successful, it was unknown if TCRseq using RNA from very low numbers of cells (<10,000) would also be successful. To determine whether preparation of RNA from very few cells would be sufficient for RNA-based TCRseq, healthy donor PBMC were stimulated with either CEF peptide pool or anti-CD3 antibody and 4,000 and 100 $CD137^+$ T cells, respectively, were FACS-purified from each sample. RNA was extracted from each of these samples and subjected to TCRseq to best mimic my anticipated small, tumor-reactive T cell populations. TCRseq of 100 $CD137^+$ anti-CD3-stimulated T cells (c100) resulted in the identification of 10 abundant T cell clones. Further, these 10 clones made up 98.4% of the total sequencing reads (Figure 23A), while the remaining low-abundance clonotypes made up only 1.6% of the total reads. TCRseq profiling of the 4,000 cells purified from CEF-peptide-pool-stimulated PBMC (c4000) yielded 125 unique TCR clones, and the top 11 most abundant clones made up 99.6% of the total sequencing reads (Figure 23B). Further, one of the top 10 most abundant TCR clonotypes was shared between each sample (Figure 23, black slice). In theory, anti-CD3 antibody should stimulate all T cells in a polyclonal population equally. Therefore, it is expected that any CEF-reactive T cells in the PBMC would also be activated by anti-CD3-antibody, sorted from the mixture, and identified by TCRseq. In summary, it is feasible to profile TCR sequences from very small T cell samples, suggesting profiling small populations of potentially rare, tumor-reactive TAL by TCRseq is feasible.

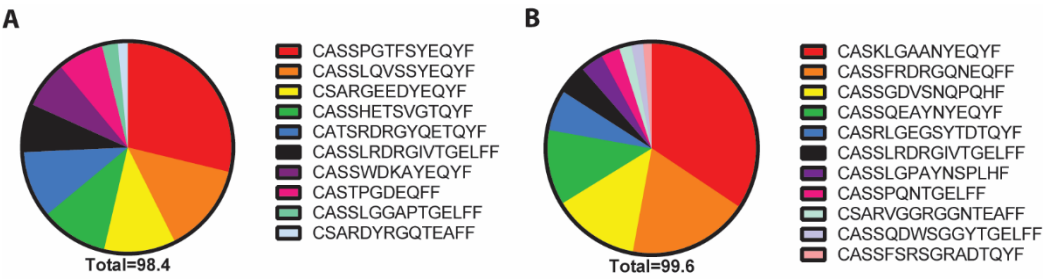

Figure 23. T cell clonotypes of FACS-purified CD137$^+$ T cells from one healthy donor's PBMC following anti-CD3 stimulation (A) or CEF peptide pool stimulation (B). (A) 100 CD137$^+$ T cells or (B) 4000 CD137$^+$ T cells were sorted directly into lysis buffer and RNA was extracted. cDNA was synthesized, next-generation sequencing libraries were prepared, and samples were sequenced on an Illumina MiSeq. The total listed underneath each pie chart is the percentage of total sequencing reads generated that are represented by the top 10 (A) and top 11 (B) most abundant clonotypes. The black slice is the only shared clone between each sample.

3.4.4 TCRseq of FACS-purified CD137$^+$-tumor-reactive TAL.

The aim of this study was to profile the tumor-reactive T cells from primary and recurrent disease to determine how these T cells change over time. To do so, TAL were cultured overnight in the presence or absence of autologous bulk ascites cells, CD45$^+$, or CD45$^-$ ascites cells. As discussed in chapter 2, following co-culture of IROC 060 primary TAL with recurrent ascites, over 6% of CD3$^+$ T cells were CD137$^+$ (Figure 8A) while only 3% each of recurrent CD3$^+$ TAL were CD137$^+$ following culture with recurrent ascites (Figure 8C). For IROC 106, over 6% of CD3$^+$ primary TAL were CD137$^+$ following stimulation with autologous primary ascites while nearly 8% of CD3$^+$ primary TAL were CD137$^+$ in response to recurrent ascites (Figure 10A). For her recurrent TAL, over 6% of CD3$^+$ T cells were CD137$^+$ following stimulation with primary tumor while only 2% CD3$^+$ recurrent TAL were CD137$^+$ in response to recurrent tumor (Figure 10C). Tumor-reactive CD4$^+$ and CD8$^+$ CD137$^+$ T cells were sorted into separate collection tubes and between 123 and 23,400 CD137$^+$ cells were purified from these populations by FACS. For each sorted sample RNA was extracted and submitted to the GSC for TCRseq.

To determine the pattern of tumor-reactive T cell evolution in IROC 060 and IROC 106, I first assessed whether any tumor-reactive T cell clones were unique to primary or recurrent disease. In IROC 060 there were two CD4$^+$ and four CD8$^+$ tumor-reactive clones that were uniquely present among primary TAL and 10 CD4$^+$ and 11 CD8$^+$ clones that were uniquely present among recurrent TAL (Figure 24A). Likewise, in IROC 106, there were 25 CD4$^+$ and 21 CD8$^+$ tumor-reactive T cell clones uniquely

present in primary TAL and 32 $CD4^+$ and 13 $CD8^+$ clones uniquely present among recurrent TAL (Figure 24B). Next, I assessed whether either patient had tumor-reactive T cell clones that were shared between primary and recurrent TAL. IROC 060 had no shared tumor-reactive T cell clones (Figure 24A), whereas IROC 106 had four $CD4^+$ and 5 $CD8^+$ tumor-reactive T cell clones that were shared by both primary and recurrent TAL (Figure 24B). Together, these results suggest IROC 060 and IROC 106 shared a mechanism of T cell evolution where tumor-reactive clones were lost over time, while other tumor-reactive clones emerged in the time between primary and recurrent disease. Moreover, IROC 106 had shared tumor-reactive T cell clones, suggesting there may be recognition of a shared tumor antigen and maintenance of that T cell response over time. For more detailed results and further discussion of the data, see Appendix B.

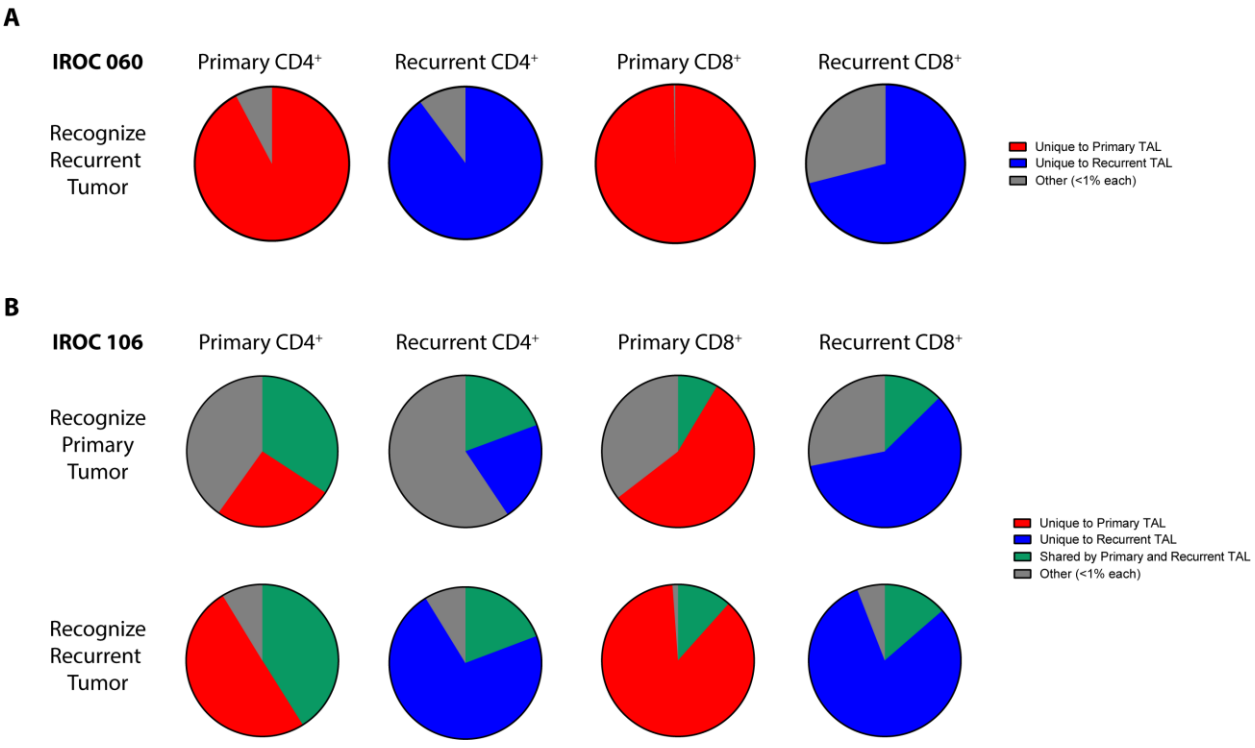

Figure 24. (A) IROC 060 and (B) IROC 106 tumor-reactive T cell evolution patterns. Red shading represents tumor-reactive T cell clones that were unique to primary TAL, blue shading represents tumor-reactive T cell clones that were unique to recurrent TAL, and green shading represents tumor-reactive T cell clones that were shared by primary and recurrent TAL. Grey shading represents the population of low-frequency TCR clones (<1% abundance in the purified, tumor-reactive subsets). (A)

For IROC 060, T cell clones reacted only to recurrent tumor. (B) For IROC 106, the top row of pie charts represents T cell clones that responded to primary tumor, whereas the bottom row represents T cell clones that responded to recurrent tumor.

3.5 Discussion

It is unclear how TIL respond to ITH in HGSC. Therefore, I aimed to profile tumor-reactive T cell clones over time in HGSC patients. Previous studies have shown HGSC tumors can have a large degree of ITH spatially and temporally.[107,108] Further, recent studies in melanoma and HGSC have shown specific populations of neoantigen-reactive T cells are dynamic over time.[48,49] However, the predominant mechanisms by which TIL respond to ITH are unknown. To determine this, I compared the clonal repertoire of FACS-purified CD137$^+$ tumor-reactive T cells from primary and recurrent ascites using TCRseq. Results show very few T cells are sufficient for profiling oligoclonal populations by TCRseq and TCRseq results profiling tumor-reactive populations of T cells from primary and recurrent disease from both IROC 060 and IROC 106 are discussed in depth in Appendix B.

Since ovarian cancer has a much lower mutation burden compared to highly immunoreactive tumor types such as melanoma and non-small cell lung carcinoma, few tumor-reactive T cells were expected in ascites of these patients.[228] To overcome this issue, I aimed to expand purified CD137$^+$ tumor-reactive T cells. Unfortunately, in my hands, these T cells would not expand *in vitro*, likely due to terminal differentiation induced by numerous rounds of expansion[282] prior to FACS-purification. Therefore, measures had to be taken to ensure TCRseq of very few cell numbers would provide accurate data for profiling of tumor-reactive T cells. By use of TCR cloning and Sanger sequencing, I FACS-purified 100 and 1000 CD137$^+$ T cells from a bi-clonal mixture of T cell clones with known antigen-specificities (Figure 20). All but one TCR sequence identified from two samples of only 100 purified T cells was correct. Therefore, as few as 100 cells were sufficient to identify the correct CDR3 sequence using this method (Figures 18B,G), suggesting even rare populations of cells can be sorted and accurately profiled using TCRseq.

Next, I evaluated whether the same approach would yield robust data in a more heterogeneous patient sample setting. TCRseq on as little as 2.5% (5 ng) of the optimal RNA input suggested for TCRseq (200 ng) identified thousands of unique CDR3 sequences from a polyclonal expanded TAL sample. Moreover, the top 10 most abundant clonotypes overlapped almost perfectly with clonotypes identified using 200 ng of the same RNA sample (Figure 20). Further, two separate vials of the same expanded TAL, TAL-1 and TAL-2, appeared nearly identical down to the 10th most abundant clonotype in each titration sample (200 ng, 75 ng, 25 ng, and 5 ng; Figure 20). To further confirm that TCRseq could be performed on low-RNA samples, I tested RNA samples from either 4000 (c4000) or 100 (c100) FACS-purified CD137$^+$

T cells from healthy donor PBMC to more precisely mimic the anticipated small, tumor-reactive T cell populations. Remarkably, despite exceptionally small amounts of RNA extracted from each population (<1 ng RNA, data not shown), multiple TCR sequences were identified in both samples. Further, one of the top 10 most abundant TCR clonotypes was shared between each sample, lending further confidence that TCR clonotype profiling by TCRseq was accurate. Therefore, I feel confident that using this method I will be able to analyze small, potentially heterogeneous, tumor-reactive TAL samples.

Although the technology for single-cell RNA sequencing as well as RNA sequencing from low-abundance samples was developed years ago,[283] challenges, such as RNA transcript loss and contamination, remain. First, loss of RNA transcripts through RNA isolation and library preparation is a significant challenge in single-cell or low-cell RNAseq.[284] This is particularly the case when assessing low-frequency TCR clones from polyclonal populations, as loss of one TCR transcript may significantly impact the relative abundance of that specific T cell clone. This may explain why there was a high-degree of overlap in clonotype abundance only within the top 10 most abundant T cell clones identified in samples of less than 200ng input RNA (Figure 22). Therefore, for sequences that do not fall within the top 10 most abundant clonotypes, frequencies may not be informative. Thus, for low-abundance samples in this study, it may be most accurate to assess only the presence or absence of specific T cell clones when comparing populations of tumor-reactive TAL from primary and recurrent disease.

Second, contamination is a major issue in genomic analyses of single-cell or low-cell input samples.[285] In our study, there were two probable sources of contamination: (a) FACS purification and (b) PCR error. First, even though FACS purification is highly accurate, contamination from debris (e.g. dead cells) can be high.[285] For example, when sorting only 100 cells, even if 95% purity was obtained, 5 of the 100 total cells may be non-specific T cells. In a population of very few cells, transcripts of each clonotype are at a low abundance and therefore, it is possible that contaminants may appear as legitimate clonotypes. Indeed, Illumina-based TCRseq of only 100 T cells resulted in 163 unique TCRs identified. Even though sorting was capped at 100 cells, additional dead cells and debris that may contain RNA could have been co-purified with the $CD137^{+}$ T cells. Second, the high number of PCR cycles required to amplify the TCR sequences prior to sequencing may lead to contamination from PCR error. Incorrect CDR3 sequences identified in samples of FACS-purified cells from the bi-clonal mixture share high sequence homology with the correct CDR3 sequence identified (Figure 20), suggesting these differences are due to PCR error. Therefore, when analyzing small samples, contamination from both FACS-purification and PCR error are factors to be considered.

Given the pilot experiments showed TCRseq is possible on samples with low cell numbers, I FACS-purified tumor-reactive $CD4^+$ and $CD8^+$ T cell samples from primary and recurrent disease from both IROC 060 and IROC 106 and submitted the samples for TCRseq. Using the results, I compared tumor-reactive repertoires between primary and recurrent disease to elucidate potential mechanisms of T cell evolution for contending with ITH in HGSC. Further discussion of the data can be found in Appendix B.

Previous studies investigating anti-tumor T cell responses by TCRseq have focused on T cells with known reactivity to tumor antigens. A recent study by Stevanović *et al*[47] interrogated TIL for reactivity to either Human Papilloma Virus (HPV)-specific proteins, patient-specific neoantigens, and cancer testis (CT) antigens. Similar to my study, they purified $CD137^+$ T cell subsets from polyclonal populations. However, these $CD137^+$ T cells were activated by tumor-specific antigens, rather than bulk tumor. Further, to track these tumor-reactive T cells in patients, they first identified TCR sequences using RT-PCR of single antigen-specific cells, followed by engineering autologous peripheral T cells to express these TCRs to validate specificity against tumor antigens. Finally, they performed TCR deep sequencing on both bulk TIL and peripheral blood following ACT to determine the relative frequencies of the identified tumor antigen-specific T cell clones within the polyclonal populations.[47] Ultimately, the authors determined that complete responses to ACT in cases of HPV^+ cervical cancer were largely due to the presence of neoantigen- or cancer-specific T cell reactivity, rather than reactivity to HPV viral antigens, shedding light on the heterogeneity of anti-tumor T cell responses.

Another recent study investigated the dynamics of the anti-tumor T cell response in melanoma.[48] Like my study, they investigated changes in T cell populations over time in two melanoma patients. However, the authors only looked in depth at neoantigen-reactive T cell subsets, as they found limited reactivity to shared cancer antigens. Despite the finding that strong neoantigen-specific responses contributed the most to the tumor-reactivity of TIL, the results suggested the presence of additional T cells that recognized other tumor-specific antigens.[48] Therefore, the method of analysis used in this study limited the analysis of T cell temporal dynamics to neoantigen-specific T cells and failed to elucidate temporal differences in other tumor-reactive T cell populations.

The pipeline I have developed can be used to improve methods and overcome challenges identified in earlier studies. Results from this study show that TCRseq on polyclonal populations of undefined antigen-specificity can be performed with good accuracy. For example, $CD137^+$-purification of oligoclonal populations of activated T cells from PBMC identified numerous TCR clones (Figure 21). In

the context of tumor-reactive T cells, these TCR sequences could be used to engineer T cells and interrogate tumor-specific antigens, eliminating an entire step of current protocols that require up-front determination of antigen-specificity through stimulation using autologous DC's transfected with RNA expressing specific antigens, such as the study outlined above,[47] or screening of T cell reactivity over multiple peptide libraries.[48,49] Further, the pipeline described allows for discovery of tumor-reactive T cell clones for which the cognate antigen is unknown. Using this method, the study described above[48] could have developed an extensive list of tumor-reactive TCR clones for cross-referencing against TCRs identified from neoantigen-specific T cells, thus determining how many additional tumor-reactive T cell clones were not reactive to neoantigens and providing direction for future study.

As I developed this pipeline, I was faced with a few limitations. First, as mentioned before, there were very low sample numbers. For example, one RNA sample sent for sequencing was isolated from only 123 $CD137^+$ cells. In this context, single cell RT-PCR may have yielded more accurate results, however it is not possible to predict the number of tumor-reactive T cells prior to FACS-purification and to reduce the chance of loss of any $CD137^+$ cells, sorting was done directly into lysis buffer for subsequent RNA extraction. Second, technical replicate sequencing libraries were created from cDNA, rather than sampling two populations of $CD137^+$ T cells from two different TAL lines from the same time point. This is not ideal, however it given the limited sample, it was the best way to ensure data were robust. Last, it is unknown whether the $CD137^+$ purified T cells are highly enriched for tumor-reactivity. Therefore, validation of tumor-reactivity must be done on T cell clones identified by TCRseq.

To overcome some of these limitations, it would have been ideal to expand the purified $CD137^+$ TAL and directly assess them for tumor reactivity. However, as mentioned previously, this was not possible in my hands likely due to a terminally differentiated T cell state induced by the T cell expansion methods used.[282] Nonetheless, CD137+ TAL populations are expected to be highly enriched for ascites-reactivity, as numerous studies have shown successful purification of antigen-specific T cells using $CD137^+$-based selection.[40,41,48,159,160,286] However, these studies either purified $CD137^+$ cells directly from tumor or ascites without the need for up-front T cell expansion or used engineered T cells that expressed TCRs identified from T cell clones of known antigen-specificity. Therefore, alternative methods are required for validating the tumor-specificity of $CD137^+$ purified T cell subsets.

In conclusion, I have developed a pipeline for the rapid profiling of the T cell repertoire of purified ascites- or tumor-reactive T cell populations using $CD137^+$-FACS purification followed by TCRseq. This pipeline ultimately provides a resource of tumor-reactive TCR sequences for interrogating tumor-

reactive T cells directly *ex vivo* without the need for *a priori* identification or characterization of tumor antigens. Further, results from TCRseq identified mechanisms of T cell evolution that allow anti-tumor T cell responses to contend with ITH between primary and recurrent HGSC.

Chapter 4. Concluding Remarks and Future Directions

4.1 Summary and Perspectives

The aim of this study was to determine how anti-tumor T cells respond to ITH in HGSC. First, by identifying differences in tumor-recognition patterns between primary and recurrent disease, I determined that anti-tumor T cell responses are both diverse between patients and dynamic within patients. Second, by comparing the tumor-reactive T cell repertoire between primary and recurrent disease, I could more precisely define the mechanisms by which anti-tumor T cells contend with ITH in HGSC. Results from this study could be used to inform the design of optimized ACT protocols for treating recurrent HGSC.

In Chapter 2, I assessed how anti-tumor T cell responses change over time in three HGSC patients. Given two previous studies showed tumor-reactive T cell clones emerged over time with their cognate antigens,[48,49] I hypothesized patients would share a common mechanism of T cell evolution between primary and recurrent disease. However, results showed this may not be the case. Each of the three patients in the study cohort exhibited diverse patterns of tumor reactivity. IROC 060 tumor changed from poorly immunogenic to highly immunogenic between primary and recurrent disease. IROC 106 tumor remained highly immunogenic from primary to recurrent disease. Finally, tumor from IROC 034 remained poorly immunogenic from primary to recurrent disease time points. Nonetheless, in both patients who had anti-tumor reactivity (IROC 060 and 106), primary TAL recognized recurrent tumor. Indeed, primary TAL had more robust responses to recurrent tumor compared to recurrent TAL. Together, these results suggest ACT using primary TIL to treat recurrent tumors may be a feasible and clinically effective option.

A reduction in the overall frequency of tumor-reactive TAL over time in both IROC 060 and 106 suggests that progressive T cell loss/impairment may be a significant challenge in HGSC. In the context of chronic antigen stimulation, such as in cancer,[148] T cells may enter a state of terminal exhaustion and ultimately become deleted from the patient repertoire.[287,288] In HGSC, PD-L1^{+} is expressed in nearly 60% of cases.[88] This raises the possibility that PD-1^{+} T cells are functionally exhausted and, over time, could become terminally exhausted and deleted from the patient repertoire. Further, in 40% of HGSC cases, PD-L1 was expressed on tumor-infiltrating macrophages. Tumor infiltrating macrophages have been shown to induce apoptosis in activated T cells.[289] Perhaps a common mechanism of immune resistance

in HGSC is terminal exhaustion and deletion of T cells, which would contribute to the overall reduction of tumor-reactive T cells over time.

In Chapter 3, I aimed to examine at the level of individual T cell clones the mechanisms by which tumor-reactive T cells contend with ITH in HGSC. Given two previous studies showed neoantigen-specific T cell clones emerged together with their cognate antigens,[48,49] I hypothesized that new tumor-reactive T cell clones would emerge over time to contend with ITH in HGSC. I showed that accurate profiling of T cell clones by deep sequencing of TCRβ chains is technically feasible even from samples consisting of very few cells. TCRseq results in Appendix B outline the changes in the tumor-reactive T cell populations over time from IROC 060 and IROC 106.

4.2 Future directions

Results from this study have implications for both studying the immune response to tumors and treating tumors using ACT and other T cell-based forms of immunotherapy. Given that each of the three patients had different patterns of tumor recognition, in the near future these findings will be expanded to a larger patient cohort to identify the predominant mechanisms underlying T cell evolution in HGSC. Additionally, to study T cell evolution patterns in a variety of immunological settings within cancers, these methods could be applied to other cancer types described to have either higher or lower mutation burden compared to HGSC, such as melanoma, lung cancers, pancreatic cancers, and glioblastomas.[244] If patterns of T cell evolution were shared among numerous tumor types or unique to tumors with high or low mutation burden, it would allow development of general theories about T cell evolution in the context of the immune response to cancer.

TCR sequences could be used to assess tumor-reactive T cells directly *ex vivo*, without the need for identifying and characterizing tumor antigens. *In situ* PCR is a novel technique that allows for specific amplification and visualization of both DNA and RNA targets on tissue sections.[290,291] This visualization of specific nucleic acid targets can be done concurrently with IHC detection of cellular antigens, which makes it possible to look at co-localization of specific target sequences with various cell types based on cellular markers.[290] Using TCR sequences identified from purified tumor-reactive T cells, *in situ* PCR protocols could be developed that allow for visualization of these T cells directly within the patient's tumor tissue. This could identify the precise locations of tumor-reactive T cells within the tumor microenvironment. Further, it could help to identify cell surface markers that are expressed

predominantly on tumor-reactive T cells. Together, this will allow the study of specific tumor-reactive T cells within the TME and provide more information about the immune response to tumors *in situ*.

Identification of tumor-reactive TCR sequences gives rise to the possibility of engineering a polyclonal population of tumor-reactive T cells for ACT. One of the biggest challenges in ACT is persistence of the T cell product post-infusion.[292] Several studies have shown that TIL with less-differentiated phenotypes persist longer and lead to better clinical responses compared to ACT using more terminally differentiated T cells.[12,216,218,293,293,294] By expanding the tumor-reactive TCR sequences generated using the pipeline developed in this study to include sequencing of both TCRα and TCRβ sequences, it may be possible to engineer less differentiated T cells that may lead to improved clinical responses in HGSC.

Findings from this study support the general notion that immunological checkpoints play a critical role in tumor immune evasion. In particular, tumor cells from ascites expressed high levels of PD-L1, and interestingly, a study in HGSC found PD-L1 expression in tumors was primarily limited to $CD68^{+}$ macrophages, rather than epithelial tumor cells.[88] This suggests ascites tumor cells be may even more immunosuppressive compared to those from solid tumor. Further, TAL expressed PD-1 and its expression was associated with the subpopulation of TAL that mediated anti-tumor responses. Together, this suggests combining ACT with checkpoint blockade therapy may yield improved clinical responses compared to either therapy alone. In a mouse model of melanoma, combination treatment of anti-PD-1 and ACT with tumor-specific T cells improved both recruitment of T cells into the tumor and tumor regression compared to ACT or anti-PD-1 alone.[295] Indeed, there are 5 clinical trials currently listed in the clincialtrials.gov database that combine ACT with checkpoint blockade to treat ovarian, gastrointestinal, and melanoma cancers, highlighting the promise of this novel therapeutic strategy.

Last, this pipeline can rapidly identify T cell clones of interest for immune monitoring following ACT. Post-infusion, tumor-reactive T cells can be tracked in patient's peripheral blood by determining the presence or absence of specific TCR sequences determined by TCRseq. By assessing the expansion or contraction of specific tumor-reactive T cell populations, it will provide insight into the behaviour of tumor-reactive T cell populations post-ACT. Further, by profiling tumor-reactive T cells in patient blood following ACT and correlating the prevalence of these cells with the size and duration of clinical responses, this pipeline could ultimately be used to predict patient outcomes to ACT.

4.3 Conclusion

A significant challenge in the treatment of recurrent tumors is ITH. Tumor clonal evolution can mediate dramatic changes to the subclonal architecture of recurrent tumors. These differences over time may impact the ability of tumor-reactive T cells to recognize recurrent disease. Therefore, it was important to elucidate the mechanisms used by tumor-reactive T cells to contend with ITH over time to develop improved strategies for ACT of recurrent HGSC.

This was the first study to systematically assess both patterns of tumor-recognition and the tumor-reactive T cell repertoire between primary and recurrent disease in HGSC. Results indicate anti-tumor T cell responses from ascites are diverse between patients and dynamic within a patient, suggesting various mechanisms of T cell evolution to respond to ITH in HGSC. Further, I developed a pipeline for the identification of tumor-reactive TCR sequences without the need for *a priori* knowledge of specific antigens. Results profiling the tumor-reactive repertoire over time in HGSC revealed precise mechanisms through which T cells evolve to respond to ITH. Ultimately, this study will be used to inform the best approach to ACT for recurrent HGSC.

References

1. Janeway, C. A., Travers, P., Walport, M. & Shlomchik, M. J. Principles of innate and adaptive immunity. (2001).
2. Janeway, C., Travers, P., Walport, M. & Shlomchick, M. The production of armed effector T cells. in *Immunobiology* (2001).
3. Janeway, C. A., Travers, P., Walport, M. & Shlomchik, M. J. Antigen recognition by T cells. (2001).
4. Janeway, C. A., Travers, P., Walport, M. & Shlomchik, M. J. T cell-mediated cytotoxicity. (2001).
5. Doherty, P. C., Knowles, B. B. & Wettstein, P. J. Immunological surveillance of tumors in the context of major histocompatibility complex restriction of T cell function. *Adv. Cancer Res.* **42,** 1–65 (1984).
6. Aebersold, P. *et al.* Lysis of autologous melanoma cells by tumor-infiltrating lymphocytes: association with clinical response. *J. Natl. Cancer Inst.* **83,** 932–937 (1991).
7. Zhang, L. *et al.* Intratumoral T Cells, Recurrence, and Survival in Epithelial Ovarian Cancer. *N. Engl. J. Med.* **348,** 203–213 (2003).
8. Huh, J. W., Lee, J. H. & Kim, H. R. Prognostic significance of tumor-infiltrating lymphocytes for patients with colorectal cancer. *Arch. Surg. Chic. Ill 1960* **147,** 366–372 (2012).
9. Brambilla, E. *et al.* Prognostic Effect of Tumor Lymphocytic Infiltration in Resectable Non-Small-Cell Lung Cancer. *J. Clin. Oncol. Off. J. Am. Soc. Clin. Oncol.* **34,** 1223–1230 (2016).
10. Stevanović, S. *et al.* Complete Regression of Metastatic Cervical Cancer After Treatment With Human Papillomavirus–Targeted Tumor-Infiltrating T Cells. *J. Clin. Oncol.* **33,** 1543–1550 (2015).
11. Tran, E. *et al.* Cancer immunotherapy based on mutation-specific CD4+ T cells in a patient with epithelial cancer. *Science* **344,** 641–645 (2014).
12. Rosenberg, S. A. & Restifo, N. P. Adoptive cell transfer as personalized immunotherapy for human cancer. *Science* **348,** 62–68 (2015).

13. Sharma, P. & Allison, J. P. The future of immune checkpoint therapy. *Science* **348,** 56–61 (2015).

14. Wucherpfennig, K. W., Gagnon, E., Call, M. J., Huseby, E. S. & Call, M. E. Structural Biology of the T-cell Receptor: Insights into Receptor Assembly, Ligand Recognition, and Initiation of Signaling. *Cold Spring Harb. Perspect. Biol.* **2,** (2010).

15. Brownlie, R. J. & Zamoyska, R. T cell receptor signalling networks: branched, diversified and bounded. *Nat. Rev. Immunol.* **13,** 257–269 (2013).

16. Davis, M. M. & Bjorkman, P. J. T-cell antigen receptor genes and T-cell recognition. *Nature* **334,** 395–402 (1988).

17. Nikolich-Žugich, J., Slifka, M. K. & Messaoudi, I. The many important facets of T-cell repertoire diversity. *Nat. Rev. Immunol.* **4,** 123–132 (2004).

18. Haeryfar, S. M. M. *et al.* Terminal Deoxynucleotidyl Transferase Establishes and Broadens Anti-Viral CD8+ T Cell Immunodominance Hierarchies. *J. Immunol. Baltim. Md 1950* **181,** 649 (2008).

19. Janeway, C., Travers, P., Walport, M. & Shlomchik, M. J. T-cell receptor gene rearrangement. (2001).

20. Radulovic, K. *et al.* The Early Activation Marker CD69 Regulates the Expression of Chemokines and CD4 T Cell Accumulation in Intestine. *PLoS ONE* **8,** (2013).

21. Simms, P. E. & Ellis, T. M. Utility of flow cytometric detection of CD69 expression as a rapid method for determining poly- and oligoclonal lymphocyte activation. *Clin. Diagn. Lab. Immunol.* **3,** 301–304 (1996).

22. Esplugues, E. *et al.* Enhanced antitumor immunity in mice deficient in CD69. *J. Exp. Med.* **197,** 1093–1106 (2003).

23. Radulovic, K. *et al.* CD69 regulates type I IFN-induced tolerogenic signals to mucosal CD4 T cells that attenuate their colitogenic potential. *J. Immunol. Baltim. Md 1950* **188,** 2001–2013 (2012).

24. Sancho, D. *et al.* CD69 downregulates autoimmune reactivity through active transforming growth factor-beta production in collagen-induced arthritis. *J. Clin. Invest.* **112,** 872–882 (2003).

25. Yamazaki, T. *et al.* Expression of programmed death 1 ligands by murine T cells and APC. *J. Immunol. Baltim. Md 1950* **169,** 5538–5545 (2002).

26. Hui, E. *et al.* T cell costimulatory receptor CD28 is a primary target for PD-1–mediated inhibition. *Science* **355,** 1428–1433 (2017).

27. Kamphorst, A. O. *et al.* Rescue of exhausted CD8 T cells by PD-1–targeted therapies is CD28-dependent. *Science* eaaf0683 (2017). doi:10.1126/science.aaf0683

28. Bardhan, K. *et al.* PD-1 inhibits the TCR signaling cascade by sequestering SHP-2 phosphatase, preventing its translocation to lipid rafts and facilitating Csk-mediated inhibitory phosphorylation of Lck. *J. Immunol.* **196,** 128.15-128.15 (2016).

29. Jurado, J. O. *et al.* Programmed Death (PD)-1:PD-Ligand 1/PD-Ligand 2 Pathway Inhibits T Cell Effector Functions during Human Tuberculosis. *J. Immunol.* **181,** 116–125 (2008).

30. Latchman, Y. *et al.* PD-L2 is a second ligand for PD-1 and inhibits T cell activation. *Nat. Immunol.* **2,** 261–268 (2001).

31. Freeman, G. J. *et al.* Engagement of the PD-1 immunoinhibitory receptor by a novel B7 family member leads to negative regulation of lymphocyte activation. *J. Exp. Med.* **192,** 1027–1034 (2000).

32. Watts, T. H. Tnf/Tnfr Family Members in Costimulation of T Cell Responses. *Annu. Rev. Immunol.* **23,** 23–68 (2005).

33. Wen, T., Bukczynski, J. & Watts, T. H. 4-1BB Ligand-Mediated Costimulation of Human T Cells Induces CD4 and CD8 T Cell Expansion, Cytokine Production, and the Development of Cytolytic Effector Function. *J. Immunol.* **168,** 4897–4906 (2002).

34. Gramaglia, I., Weinberg, A. D., Lemon, M. & Croft, M. Ox-40 Ligand: A Potent Costimulatory Molecule for Sustaining Primary CD4 T Cell Responses. *J. Immunol.* **161,** 6510–6517 (1998).

35. Croft, M., So, T., Duan, W. & Soroosh, P. The Significance of OX40 and OX40L to T cell Biology and Immune Disease. *Immunol. Rev.* **229,** 173–191 (2009).

36. Elgueta, R. *et al.* Molecular mechanism and function of CD40/CD40L engagement in the immune system. *Immunol. Rev.* **229,** (2009).

37. Casamayor-Palleja, M., Khan, M. & Ian, M. A subset of CD4+ memory T cells contains preformed CD40 ligand that is rapidly but transiently expressed on their surface after activation through the T cell receptor complex. *J. Exp. Med.* **181,** 1293 (1995).

38. Noelle, R. J. CD40 and Its Ligand in Host Defense. *Immunity* **4,** 415–419 (1996).

39. Dawicki, W. & Watts, T. H. Expression and function of 4-1BB during CD4 versus CD8 T cell responses in vivo. *Eur. J. Immunol.* **34,** 743–751 (2004).

40. Ye, Q. *et al.* CD137 accurately identifies and enriches for naturally-occurring tumor-reactive T cells in tumor. *Clin. Cancer Res. Off. J. Am. Assoc. Cancer Res.* **20,** 44 (2014).

41. Parkhurst, M. R. *et al.* Isolation of T cell receptors specifically reactive with mutated tumor associated antigens from tumor infiltrating lymphocytes based on CD137 expression. *Clin. Cancer Res.* clincanres.2680.2016 (2016). doi:10.1158/1078-0432.CCR-16-2680

42. Prehn, R. T. & Main, J. M. Immunity to methylcholanthrene-induced sarcomas. *J. Natl. Cancer Inst.* **18,** 769–778 (1957).

43. Hunder, N. N. *et al.* Treatment of Metastatic Melanoma with Autologous CD4+ T Cells against NY-ESO-1. *N. Engl. J. Med.* **358,** 2698–2703 (2008).

44. Ramos, C. A. *et al.* Human Papillomavirus Type 16 E6/E7-Specific Cytotoxic T Lymphocytes for Adoptive Immunotherapy of HPV-Associated Malignancies. *J. Immunother. Hagerstown Md 1997* **36,** 66 (2013).

45. Salmaninejad, A. *et al.* Cancer/Testis Antigens: Expression, Regulation, Tumor Invasion, and Use in Immunotherapy of Cancers. *Immunol. Invest.* **45,** 619–640 (2016).

46. Schumacher, T. N. & Hacohen, N. Neoantigens encoded in the cancer genome. *Curr. Opin. Immunol.* **41,** 98–103 (2016).

47. Stevanović, S. *et al.* Landscape of immunogenic tumor antigens in successful immunotherapy of virally induced epithelial cancer. *Science* **356,** 200–205 (2017).

48. Verdegaal, E. M. E. *et al.* Neoantigen landscape dynamics during human melanoma–T cell interactions. *Nature* **536,** 91–95 (2016).

49. Wick, D. A. *et al.* Surveillance of the tumor mutanome by T cells during progression from primary to recurrent ovarian cancer. *Clin. Cancer Res. Off. J. Am. Assoc. Cancer Res.* **20,** 1125–1134 (2014).

50. Donato, F. *et al.* Alcohol and hepatocellular carcinoma: the effect of lifetime intake and hepatitis virus infections in men and women. *Am. J. Epidemiol.* **155,** 323–331 (2002).

51. Mueller, N. *et al.* Hodgkin's disease and Epstein-Barr virus. Altered antibody pattern before diagnosis. *N. Engl. J. Med.* **320,** 689–695 (1989).

52. Goldenberg, D. *et al.* Epstein-Barr virus in head and neck cancer assessed by quantitative polymerase chain reaction. *The Laryngoscope* **114,** 1027–1031 (2004).

53. Douglas, J. L., Gustin, J. K., Moses, A. V., Dezube, B. J. & Pantanowitz, L. Kaposi Sarcoma Pathogenesis: A Triad of Viral Infection, Oncogenesis and Chronic Inflammation. *Transl. Biomed.* **1,**

54. Giraldo, G., Beth, E. & Huang, E. S. Kaposi's sarcoma and its relationship to cytomegalovirus (CMNV). III. CMV DNA and CMV early antigens in Kaposi's sarcoma. *Int. J. Cancer* **26,** 23–29 (1980).

55. Psyrri, A. & DiMaio, D. Human papillomavirus in cervical and head-and-neck cancer. *Nat. Clin. Pract. Oncol.* **5,** 24–31 (2008).

56. Crook, T., Vousden, K. H. & Tidy, J. A. Degradation of p53 can be targeted by HPV E6 sequences distinct from those required for p53 binding and trans-activation. *Cell* **67,** 547–556 (1991).

57. Vousden, K. Interactions of human papillomavirus transforming proteins with the products of tumor suppressor genes. *FASEB J.* **7,** 872–879 (1993).

58. Münger, K. *et al.* Mechanisms of Human Papillomavirus-Induced Oncogenesis. *J. Virol.* **78,** 11451–11460 (2004).

59. Nilges, K. *et al.* Human Papillomavirus Type 16 E7 Peptide-Directed CD8+ T Cells from Patients with Cervical Cancer Are Cross-Reactive with the Coronavirus NS2 Protein. *J. Virol.* **77,** 5464–5474 (2003).

60. Rosenberg, S. A. A New Era for Cancer Immunotherapy Based on the Genes that Encode Cancer Antigens. *Immunity* **10,** 281–287 (1999).

61. Traversari, C. *et al.* Transfection and expression of a gene coding for a human melanoma antigen recognized by autologous cytolytic T lymphocytes. *Immunogenetics* **35,** 145–152 (1992).

62. van der Bruggen, P. *et al.* A gene encoding an antigen recognized by cytolytic T lymphocytes on a human melanoma. *Science* **254,** 1643–1647 (1991).

63. Boël, P. *et al.* BAGE: a new gene encoding an antigen recognized on human melanomas by cytolytic T lymphocytes. *Immunity* **2,** 167–175 (1995).

64. Van den Eynde, B. *et al.* A new family of genes coding for an antigen recognized by autologous cytolytic T lymphocytes on a human melanoma. *J. Exp. Med.* **182,** 689 (1995).

65. Szender, J. B. *et al.* NY-ESO-1 expression predicts an aggressive phenotype of ovarian cancer. *Gynecol. Oncol.* **145,** 420–425 (2017).

66. Odunsi, K. *et al.* Epigenetic potentiation of NY-ESO-1 vaccine therapy in human ovarian cancer. *Cancer Immunol. Res.* **2,** 37 (2014).

67. Ayyoub, M., Pignon, P., Classe, J.-M., Odunsi, K. & Valmori, D. CD4+ T effectors specific for the tumor antigen NY-ESO-1 are highly enriched at ovarian cancer sites and coexist with, but are distinct from, tumor-associated Treg. *Cancer Immunol. Res.* **1,** 303–308 (2013).

68. Matsuzaki, J. *et al.* Tumor-infiltrating NY-ESO-1-specific CD8+ T cells are negatively regulated by LAG-3 and PD-1 in human ovarian cancer. *Proc. Natl. Acad. Sci. U. S. A.* **107,** 7875–7880 (2010).

69. Gilboa, E. The Makings of a Tumor Rejection Antigen. *Immunity* **11,** 263–270 (1999).

70. Nielsen, J. S. *et al.* Toward Personalized Lymphoma Immunotherapy: Identification of Common Driver Mutations Recognized by Patient CD8+ T Cells. *Clin. Cancer Res.* **22,** 2226–2236 (2016).

71. Kvistborg, P. *et al.* TIL therapy broadens the tumor-reactive CD8+ T cell compartment in melanoma patients. *Oncoimmunology* **1,** 409–418 (2012).

72. McGranahan, N. *et al.* Clonal neoantigens elicit T cell immunoreactivity and sensitivity to immune checkpoint blockade. *Science* aaf1490 (2016). doi:10.1126/science.aaf1490

73. Rizvi, N. A. *et al.* Mutational landscape determines sensitivity to PD-1 blockade in non–small cell lung cancer. *Science* **348,** 124–128 (2015).

74. Snyder, A. *et al.* Genetic basis for clinical response to CTLA-4 blockade in melanoma. *N. Engl. J. Med.* **371,** 2189–2199 (2014).

75. Bowtell, D. D. *et al.* Rethinking ovarian cancer II: reducing mortality from high-grade serous ovarian cancer. *Nat. Rev. Cancer* **15,** 668–679 (2015).

76. Høgdall, E. Cancer antigen 125 and prognosis: *Curr. Opin. Obstet. Gynecol.* **20,** 4–8 (2008).

77. Yin, B. W. & Lloyd, K. O. Molecular cloning of the CA125 ovarian cancer antigen: identification as a new mucin, MUC16. *J. Biol. Chem.* **276,** 27371–27375 (2001).

78. Carson, D. D. *et al.* Mucin expression and function in the female reproductive tract. *Hum. Reprod. Update* **4,** 459–464 (1998).

79. Luvero, D., Milani, A. & Ledermann, J. A. Treatment options in recurrent ovarian cancer: latest evidence and clinical potential. *Ther. Adv. Med. Oncol.* **6,** 229 (2014).

80. Milne, K. *et al.* Absolute lymphocyte count is associated with survival in ovarian cancer independent of tumor-infiltrating lymphocytes. *J. Transl. Med.* **10,** 33 (2012).

81. Stumpf, M. *et al.* Intraepithelial CD8-positive T lymphocytes predict survival for patients with serous stage III ovarian carcinomas: relevance of clonal selection of T lymphocytes. *Br. J. Cancer* **101,** 1513–1521 (2009).

82. deLeeuw, R. J. *et al.* CD25 identifies a subset of $CD4^{+}FoxP3^{-}$ TIL that are exhausted yet prognostically favorable in human ovarian cancer. *Cancer Immunol. Res.* **3,** 245–253 (2015).

83. Curiel, T. J. *et al.* Specific recruitment of regulatory T cells in ovarian carcinoma fosters immune privilege and predicts reduced survival. *Nat. Med.* **10,** 942–949 (2004).

84. Sato, E. *et al.* Intraepithelial CD8+ tumor-infiltrating lymphocytes and a high CD8+/regulatory T cell ratio are associated with favorable prognosis in ovarian cancer. *Proc. Natl. Acad. Sci. U. S. A.* **102,** 18538 (2005).

85. Milne, K. *et al.* Tumor-Infiltrating T Cells Correlate with NY-ESO-1-Specific Autoantibodies in Ovarian Cancer. *PLOS ONE* **3,** e3409 (2008).

86. Wouters, M. C. A. *et al.* Treatment Regimen, Surgical Outcome, and T-cell Differentiation Influence Prognostic Benefit of Tumor-Infiltrating Lymphocytes in High-Grade Serous Ovarian Cancer. *Clin. Cancer Res. Off. J. Am. Assoc. Cancer Res.* **22,** 714–724 (2016).

87. Webb, J. R., Milne, K., Watson, P., Deleeuw, R. J. & Nelson, B. H. Tumor-infiltrating lymphocytes expressing the tissue resident memory marker CD103 are associated with increased survival in high-grade serous ovarian cancer. *Clin. Cancer Res. Off. J. Am. Assoc. Cancer Res.* **20,** 434–444 (2014).

88. Webb, J. R., Milne, K., Kroeger, D. R. & Nelson, B. H. PD-L1 expression is associated with tumor-infiltrating T cells and favorable prognosis in high-grade serous ovarian cancer. *Gynecol. Oncol.* **141,** 293–302 (2016).

89. Kroeger, D. R., Milne, K. & Nelson, B. H. Tumor-Infiltrating Plasma Cells Are Associated with Tertiary Lymphoid Structures, Cytolytic T-Cell Responses, and Superior Prognosis in Ovarian Cancer. *Clin. Cancer Res.* **22,** 3005–3015 (2016).

90. Nielsen, J. S. *et al.* CD20+ tumor-infiltrating lymphocytes have an atypical CD27- memory phenotype and together with CD8+ T cells promote favorable prognosis in ovarian cancer. *Clin. Cancer Res. Off. J. Am. Assoc. Cancer Res.* **18,** 3281–3292 (2012).

91. Turcotte, M. *et al.* CD73 is associated with poor prognosis in high-grade serous ovarian cancer. *Cancer Res.* **75,** 4494–4503 (2015).

92. Jacoby, M. A., Duncavage, E. J. & Walter, M. J. Implications of Tumor Clonal Heterogeneity in the Era of Next-Generation Sequencing. *Trends Cancer* **0,**

93. Nowell, P. C. The clonal evolution of tumor cell populations. *Science* **194,** 23–28 (1976).

94. Hanahan, D. & Weinberg, R. A. Hallmarks of Cancer: The Next Generation. *Cell* **144,** 646–674 (2011).

95. McGranahan, N. & Swanton, C. Biological and Therapeutic Impact of Intratumor Heterogeneity in Cancer Evolution. *Cancer Cell* **27,** 15–26 (2015).

96. Ovens, K. & Naugler, C. Preliminary evidence of different selection pressures on cancer cells as compared to normal tissues. *Theor. Biol. Med. Model.* **9,** 44 (2012).

97. Klein, C. A. Parallel progression of primary tumours and metastases. *Nat. Rev. Cancer* **9,** 302–312 (2009).

98. Ahmed, N. *et al.* Unique proteome signature of post-chemotherapy ovarian cancer ascites-derived tumor cells. *Sci. Rep.* **6,** 30061 (2016).

99. Gameiro, S. R., Caballero, J. A. & Hodge, J. W. Defining the Molecular Signature of Chemotherapy-Mediated Lung Tumor Phenotype Modulation and Increased Susceptibility to T-Cell Killing. *Cancer Biother. Radiopharm.* **27,** 23 (2012).

100. Gelbard, A. *et al.* Combination Chemotherapy and Radiation of Human Squamous Cell Carcinoma of the Head and Neck Augments CTL-Mediated Lysis. *Clin. Cancer Res.* **12,** 1897–1905 (2006).

101. Ohtsukasa, S., Okabe, S., Yamashita, H., Iwai, T. & Sugihara, K. Increased expression of CEA and MHC class I in colorectal cancer cell lines exposed to chemotherapy drugs. *J. Cancer Res. Clin. Oncol.* **129,** 719–726 (2003).

102. Wan, S. *et al.* Chemotherapeutics and Radiation Stimulate MHC Class I Expression through Elevated Interferon-beta Signaling in Breast Cancer Cells. *PLoS ONE* **7,** (2012).

103. Dunn, G. P., Old, L. J. & Schreiber, R. D. The three Es of cancer immunoediting. *Annu. Rev. Immunol.* **22,** 329–360 (2004).

104. Schreiber, R. D., Old, L. J. & Smyth, M. J. Cancer immunoediting: integrating immunity's roles in cancer suppression and promotion. *Science* **331,** 1565–1570 (2011).

105. Mittal, D., Gubin, M. M., Schreiber, R. D. & Smyth, M. J. New insights into cancer immunoediting and its three component phases--elimination, equilibrium and escape. *Curr. Opin. Immunol.* **27,** 16–25 (2014).

106. Calderwood, S. K. Tumor heterogeneity, clonal evolution, and therapy resistance: an opportunity for multitargeting therapy. *Discov. Med.* **15,** 188–194 (2013).

107. Castellarin, M. *et al.* Clonal evolution of high-grade serous ovarian carcinoma from primary to recurrent disease. *J. Pathol.* **229,** 515–524 (2013).

108. Bashashati, A. *et al.* Distinct evolutionary trajectories of primary high-grade serous ovarian cancers revealed through spatial mutational profiling: Evolutionary trajectories of ovarian cancers. *J. Pathol.* **231,** 21–34 (2013).

109. Strauss, R. *et al.* Analysis of Epithelial and Mesenchymal Markers in Ovarian Cancer Reveals Phenotypic Heterogeneity and Plasticity. *PLOS ONE* **6,** e16186 (2011).

110. Alsuliman, A. *et al.* Bidirectional crosstalk between PD-L1 expression and epithelial to mesenchymal transition: Significance in claudin-low breast cancer cells. *Mol. Cancer* **14,** 149 (2015).

111. Lou, Y. *et al.* Epithelial–Mesenchymal Transition Is Associated with a Distinct Tumor Microenvironment Including Elevation of Inflammatory Signals and Multiple Immune Checkpoints in Lung Adenocarcinoma. *Clin. Cancer Res.* **22,** 3630–3642 (2016).

112. Cooke, S. L. & Brenton, J. D. Evolution of platinum resistance in high-grade serous ovarian cancer. *Lancet Oncol.* **12,** 1169–1174 (2011).

113. Dunn, G. P., Bruce, A. T., Ikeda, H., Old, L. J. & Schreiber, R. D. Cancer immunoediting: from immunosurveillance to tumor escape. *Nat. Immunol.* **3,** 991–998 (2002).

114. Greaves, M. & Maley, C. C. CLONAL EVOLUTION IN CANCER. *Nature* **481,** 306

115. Schatton, T. *et al.* Modulation of T-cell activation by malignant melanoma initiating cells. *Cancer Res.* **70,** 697–708 (2010).

116. Lake, R. A. & Robinson, B. W. S. Immunotherapy and chemotherapy--a practical partnership. *Nat. Rev. Cancer* **5,** 397–405 (2005).

117. Ding, L. *et al.* Clonal evolution in relapsed acute myeloid leukaemia revealed by whole-genome sequencing. *Nature* **481,** 506–510 (2012).

118. Johnson, B. E. *et al.* Mutational analysis reveals the origin and therapy-driven evolution of recurrent glioma. *Science* **343,** 189–193 (2014).

119. Murugaesu, N. *et al.* Tracking the Genomic Evolution of Esophageal Adenocarcinoma through Neoadjuvant Chemotherapy. *Cancer Discov.* **5,** 821–831 (2015).

120. Gerlinger, M. *et al.* Ultra-deep T cell receptor sequencing reveals the complexity and intratumour heterogeneity of T cell clones in renal cell carcinomas. *J. Pathol.* **231,** 424–432 (2013).

121. Emerson, R. O. *et al.* High-throughput sequencing of T-cell receptors reveals a homogeneous repertoire of tumour-infiltrating lymphocytes in ovarian cancer. *J. Pathol.* **231,** 433–440 (2013).

122. Hagemann, A. R. *et al.* Tissue-based immune monitoring II: multiple tumor sites reveal immunologic homogeneity in serous ovarian carcinoma. *Cancer Biol. Ther.* **12,** 367–377 (2011).

123. Nowak, A. K. *et al.* Induction of Tumor Cell Apoptosis In Vivo Increases Tumor Antigen Cross-Presentation, Cross-Priming Rather than Cross-Tolerizing Host Tumor-Specific CD8 T Cells. *J. Immunol.* **170,** 4905–4913 (2003).

124. Chang, C.-L. *et al.* Dose-Dense Chemotherapy Improves Mechanisms of Antitumor Immune Response. *Cancer Res.* **73,** 119–127 (2013).

125. Lo, C. S. *et al.* Neoadjuvant Chemotherapy of Ovarian Cancer Results in Three Patterns of Tumor-Infiltrating Lymphocyte Response with Distinct Implications for Immunotherapy. *Clin. Cancer Res.* (2016). doi:10.1158/1078-0432.CCR-16-1433

126. Kalina, J. L. *et al.* Immune Modulation by Androgen Deprivation and Radiation Therapy: Implications for Prostate Cancer Immunotherapy. *Cancers* **9,** (2017).

127. Robin, H. I., AuBuchon, J., Varanasi, V. R. & Weinstein, A. B. The abscopal effect: demonstration in lymphomatous involvement of kidneys. *Med. Pediatr. Oncol.* **9,** 473–476 (1981).

128. Okuma, K., Yamashita, H., Niibe, Y., Hayakawa, K. & Nakagawa, K. Abscopal effect of radiation on lung metastases of hepatocellular carcinoma: a case report. *J. Med. Case Reports* **5,** 111 (2011).

129. Stamell, E. F., Wolchok, J. D., Gnjatic, S., Lee, N. Y. & Brownell, I. The abscopal effect associated with a systemic anti-melanoma immune response. *Int. J. Radiat. Oncol. Biol. Phys.* **85,** 293–295 (2013).

130. Wersäll, P. J. *et al.* Regression of non-irradiated metastases after extracranial stereotactic radiotherapy in metastatic renal cell carcinoma. *Acta Oncol. Stockh. Swed.* **45,** 493–497 (2006).

131. Ehlers, G. & Fridman, M. Abscopal effect of radiation in papillary adenocarcinoma. *Br. J. Radiol.* **46,** 220–222 (1973).

132. Demaria, S. *et al.* Ionizing radiation inhibition of distant untreated tumors (abscopal effect) is immune mediated. *Int. J. Radiat. Oncol. Biol. Phys.* **58,** 862–870 (2004).

133. Yoshimoto, Y. *et al.* Radiotherapy-induced anti-tumor immunity contributes to the therapeutic efficacy of irradiation and can be augmented by CTLA-4 blockade in a mouse model. *PloS One* **9,** e92572 (2014).

134. Demaria, S. *et al.* Immune-mediated inhibition of metastases after treatment with local radiation and CTLA-4 blockade in a mouse model of breast cancer. *Clin. Cancer Res. Off. J. Am. Assoc. Cancer Res.* **11,** 728–734 (2005).

135. Hillman, G. G. *et al.* Radiotherapy and MVA-MUC1-IL-2 vaccine act synergistically for inducing specific immunity to MUC-1 tumor antigen. *J. Immunother. Cancer* **5,** 4 (2017).

136. Nagasaka, M. *et al.* PD1/PD-L1 inhibition as a potential radiosensitizer in head and neck squamous cell carcinoma: a case report. *J. Immunother. Cancer* **4,** 83 (2016).

137. Stutman, O. Immunodepression and malignancy. *Adv. Cancer Res.* **22,** 261–422 (1975).

138. Kaplan, H. S. Role of Immunologic Disturbance in Human Oncogenesis: Some Facts and Fancies. *Br. J. Cancer* **25,** 620 (1971).

139. Kaplan, D. H. *et al.* Demonstration of an interferon gamma-dependent tumor surveillance system in immunocompetent mice. *Proc. Natl. Acad. Sci. U. S. A.* **95,** 7556–7561 (1998).

140. van den Broek, M. E. *et al.* Decreased tumor surveillance in perforin-deficient mice. *J. Exp. Med.* **184,** 1781–1790 (1996).

141. Shankaran, V. *et al.* IFNgamma and lymphocytes prevent primary tumour development and shape tumour immunogenicity. *Nature* **410,** 1107–1111 (2001).

142. Boehmer, L. von *et al.* NY-ESO-1–specific immunological pressure and escape in a patient with metastatic melanoma. *Cancer Immun.* **13,** (2013).

143. Kasajima, A. *et al.* Down-regulation of the antigen processing machinery is linked to a loss of inflammatory response in colorectal cancer. *Hum. Pathol.* **41,** 1758–1769 (2010).

144. Garcia-Lora, A., Algarra, I. & Garrido, F. MHC class I antigens, immune surveillance, and tumor immune escape. *J. Cell. Physiol.* **195,** 346–355 (2003).

145. Greenwald, R. J., Freeman, G. J. & Sharpe, A. H. The B7 Family Revisited. *Annu. Rev. Immunol.* **23,** 515–548 (2005).

146. Zou, W. & Chen, L. Inhibitory B7-family molecules in the tumour microenvironment. *Nat. Rev. Immunol.* **8,** 467–477 (2008).

147. Azuma, M. *et al.* B70 antigen is a second ligand for CTLA-4 and CD28. *Nature* **366,** 76–79 (1993).

148. Pardoll, D. M. The blockade of immune checkpoints in cancer immunotherapy. *Nat. Rev. Cancer* **12,** 252–264 (2012).

149. Lines, J. L. *et al.* VISTA Is an Immune Checkpoint Molecule for Human T Cells. *Cancer Res.* **74,** 1924–1932 (2014).

150. Johnston, R. J. *et al.* The immunoreceptor TIGIT regulates antitumor and antiviral CD8(+) T cell effector function. *Cancer Cell* **26,** 923–937 (2014).

151. Lindsten, T. *et al.* Characterization of CTLA-4 structure and expression on human T cells. *J. Immunol.* **151,** 3489–3499 (1993).

152. Wing, K. *et al.* CTLA-4 Control over Foxp3^{+} Regulatory T Cell Function. *Science* **322,** 271–275 (2008).

153. Tivol, E. A. *et al.* Loss of CTLA-4 leads to massive lymphoproliferation and fatal multiorgan tissue destruction, revealing a critical negative regulatory role of CTLA-4. *Immunity* **3,** 541–547 (1995).

154. Waterhouse, P. *et al.* Lymphoproliferative disorders with early lethality in mice deficient in Ctla-4. *Science* **270,** 985–988 (1995).

155. Nishimura, H., Nose, M., Hiai, H., Minato, N. & Honjo, T. Development of lupus-like autoimmune diseases by disruption of the PD-1 gene encoding an ITIM motif-carrying immunoreceptor. *Immunity* **11,** 141–151 (1999).

156. Eppihimer, M. J. *et al.* Expression and Regulation of the PD-L1 Immunoinhibitory Molecule on Microvascular Endothelial Cells. *Microcirc. N. Y. N 1994* **9,** 133 (2002).

157. Dong, H. *et al.* Tumor-associated B7-H1 promotes T-cell apoptosis: A potential mechanism of immune evasion. *Nat. Med.* **8,** 793–800 (2002).

158. Patel, S. P. & Kurzrock, R. PD-L1 Expression as a Predictive Biomarker in Cancer Immunotherapy. *Mol. Cancer Ther.* **14,** 847–856 (2015).

159. Gros, A. *et al.* Prospective identification of neoantigen-specific lymphocytes in the peripheral blood of melanoma patients. *Nat. Med.* **22,** 433–438 (2016).

160. Gros, A. *et al.* PD-1 identifies the patient-specific $CD8^+$ tumor-reactive repertoire infiltrating human tumors. *J. Clin. Invest.* **124,** 2246–2259 (2014).

161. Robert, C. *et al.* Nivolumab in previously untreated melanoma without BRAF mutation. *N. Engl. J. Med.* **372,** 320–330 (2015).

162. Weiss, L., Huemer, F., Mlineritsch, B. & Greil, R. Immune checkpoint blockade in ovarian cancer. *Memo* **9,** 82 (2016).

163. Carbone, D. P. *et al.* First-Line Nivolumab in Stage IV or Recurrent Non-Small-Cell Lung Cancer. *N. Engl. J. Med.* **376,** 2415–2426 (2017).

164. Center for Drug Evaluation and. Approved Drugs - Hematology/Oncology (Cancer) Approvals & Safety Notifications. *U.S. Food & Drug Administration* Available at: https://www.fda.gov/drugs/informationondrugs/approveddrugs/ucm279174.htm. (Accessed: 5th July 2017)

165. Zaretsky, J. M. *et al.* Mutations Associated with Acquired Resistance to PD-1 Blockade in Melanoma. *N. Engl. J. Med.* **375,** 819–829 (2016).

166. Gao, J. *et al.* Loss of IFN-γ Pathway Genes in Tumor Cells as a Mechanism of Resistance to Anti-CTLA-4 Therapy. *Cell* **167,** 397–404.e9 (2016).

167. Koyama, S. *et al.* Adaptive resistance to therapeutic PD-1 blockade is associated with upregulation of alternative immune checkpoints. *Nat. Commun.* **7,** (2016).

168. Shin, D. S. *et al.* Primary Resistance to PD-1 Blockade Mediated by JAK1/2 Mutations. *Cancer Discov.* **7,** 188–201 (2017).

169. Roh, W. *et al.* Integrated molecular analysis of tumor biopsies on sequential CTLA-4 and PD-1 blockade reveals markers of response and resistance. *Sci. Transl. Med.* **9,** eaah3560 (2017).

170. Huang, Y.-H. *et al.* CEACAM1 regulates TIM-3-mediated tolerance and exhaustion. *Nature* **517,** 386–390 (2015).

171. Rangachari, M. *et al.* Bat3 promotes T cell responses and autoimmunity by repressing Tim-3-mediated cell death and exhaustion. *Nat. Med.* **18,** 1394–1400 (2012).

172. Bamias, A. *et al.* Correlation of NK T-like CD3+CD56+ cells and CD4+CD25+(hi) regulatory T cells with VEGF and TNFα in ascites from advanced ovarian cancer: Association with platinum resistance and prognosis in patients receiving first-line, platinum-based chemotherapy. *Gynecol. Oncol.* **108,** 421–427 (2008).

173. Kryczek, I. *et al.* B7-H4 expression identifies a novel suppressive macrophage population in human ovarian carcinoma. *J. Exp. Med.* **203,** 871–881 (2006).

174. Demoulin, S., Herfs, M., Delvenne, P. & Hubert, P. Tumor microenvironment converts plasmacytoid dendritic cells into immunosuppressive/tolerogenic cells: insight into the molecular mechanisms. *J. Leukoc. Biol.* **93,** 343–352 (2013).

175. Mantovani, A., Sozzani, S., Locati, M., Allavena, P. & Sica, A. Macrophage polarization: tumor-associated macrophages as a paradigm for polarized M2 mononuclear phagocytes. *Trends Immunol.* **23,** 549–555 (2002).

176. Spranger, S. *et al.* Up-Regulation of PD-L1, IDO, and Tregs in the Melanoma Tumor Microenvironment Is Driven by CD8+ T Cells. *Sci. Transl. Med.* **5,** 200ra116 (2013).

177. Chaudhary, B. & Elkord, E. Regulatory T Cells in the Tumor Microenvironment and Cancer Progression: Role and Therapeutic Targeting. *Vaccines* **4,** 28 (2016).

178. Klimp, A. H. *et al.* Expression of cyclooxygenase-2 and inducible nitric oxide synthase in human ovarian tumors and tumor-associated macrophages. *Cancer Res.* **61,** 7305–7309 (2001).

179. Singel, K. L. *et al.* Ovarian cancer ascites-activated neutrophils suppress T cell proliferation in a contact-dependent mechanism. *J. Immunol.* **196,** 211.16-211.16 (2016).

180. Takaishi, K. *et al.* Involvement of M2-polarized macrophages in the ascites from advanced epithelial ovarian carcinoma in tumor progression via Stat3 activation. *Cancer Sci.* **101,** 2128–2136 (2010).

181. Lesokhin, A. M. *et al.* Monocytic $CCR2^+$ Myeloid-Derived Suppressor Cells Promote Immune Escape by Limiting Activated CD8 T-cell Infiltration into the Tumor Microenvironment. *Cancer Res.* **72,** 876–886 (2012).

182. Ostrand-Rosenberg, S. & Sinha, P. Myeloid-Derived Suppressor Cells: Linking Inflammation and Cancer. *J. Immunol.* **182,** 4499–4506 (2009).

183. Sisirak, V. *et al.* Impaired IFN-α production by plasmacytoid dendritic cells favors regulatory T-cell expansion that may contribute to breast cancer progression. *Cancer Res.* **72,** 5188–5197 (2012).

184. Wei, S. *et al.* Plasmacytoid dendritic cells induce CD8+ regulatory T cells in human ovarian carcinoma. *Cancer Res.* **65,** 5020–5026 (2005).

185. Munn, D. H. *et al.* Expression of indoleamine 2,3-dioxygenase by plasmacytoid dendritic cells in tumor-draining lymph nodes. *J. Clin. Invest.* **114,** 280 (2004).

186. Arlauckas, S. P. *et al.* In vivo imaging reveals a tumor-associated macrophage-mediated resistance pathway in anti-PD-1 therapy. *Sci. Transl. Med.* **9,** (2017).

187. Gorchs, L. *et al.* Cancer-Associated Fibroblasts from Lung Tumors Maintain Their Immunosuppressive Abilities after High-Dose Irradiation. *Front. Oncol.* **5,** (2015).

188. Feig, C. *et al.* Targeting CXCL12 from FAP-expressing carcinoma-associated fibroblasts synergizes with anti–PD-L1 immunotherapy in pancreatic cancer. *Proc. Natl. Acad. Sci.* **110,** 20212–20217 (2013).

189. Uccelli, A., Moretta, L. & Pistoia, V. Mesenchymal stem cells in health and disease. *Nat. Rev. Immunol.* **8,** 726–736 (2008).

190. Aggarwal, S. & Pittenger, M. F. Human mesenchymal stem cells modulate allogeneic immune cell responses. *Blood* **105,** 1815–1822 (2005).

191. Orimo, A. *et al.* Stromal fibroblasts present in invasive human breast carcinomas promote tumor growth and angiogenesis through elevated SDF-1/CXCL12 secretion. *Cell* **121,** 335–348 (2005).

192. Ghannam, S., Bouffi, C., Djouad, F., Jorgensen, C. & Noël, D. Immunosuppression by mesenchymal stem cells: mechanisms and clinical applications. *Stem Cell Res. Ther.* **1,** 2 (2010).

193. Su, J. *et al.* Phylogenetic distinction of iNOS and IDO function in mesenchymal stem cell-mediated immunosuppression in mammalian species. *Cell Death Differ.* **21,** 388–396 (2014).

194. Yoshimura, A. & Muto, G. TGF-β function in immune suppression. *Curr. Top. Microbiol. Immunol.* **350,** 127–147 (2011).

195. Mellor, A. Indoleamine 2,3 dioxygenase and regulation of T cell immunity. *Biochem. Biophys. Res. Commun.* **338,** 20–24 (2005).

196. Mbongue, J. C. *et al.* The Role of Indoleamine 2, 3-Dioxygenase in Immune Suppression and Autoimmunity. *Vaccines* **3,** 703–729 (2015).

197. Friberg, M. *et al.* Indoleamine 2,3-dioxygenase contributes to tumor cell evasion of T cell-mediated rejection. *Int. J. Cancer* **101,** 151–155 (2002).

198. Bird, L. Regulatory T cells: Nurtured by TGFβ. *Nat. Rev. Immunol.* **10,** 466–466 (2010).

199. Gigante, M., Gesualdo, L. & Ranieri, E. TGF-beta: a master switch in tumor immunity. *Curr. Pharm. Des.* **18,** 4126–4134 (2012).

200. Pickup, M., Novitskiy, S. & Moses, H. L. The roles of TGFβ in the tumour microenvironment. *Nat. Rev. Cancer* **13,** 788–799 (2013).

201. Pg, R. Surgery for recurrent ovarian cancer. *Semin. Oncol.* **27,** 17–23 (2000).

202. Ahmed, N. & Stenvers, K. L. Getting to Know Ovarian Cancer Ascites: Opportunities for Targeted Therapy-Based Translational Research. *Front. Oncol.* **3,** (2013).

203. Latifi, A. *et al.* Isolation and Characterization of Tumor Cells from the Ascites of Ovarian Cancer Patients: Molecular Phenotype of Chemoresistant Ovarian Tumors. *PLoS ONE* **7,** (2012).

204. Krimmel, J. D. *et al.* Ultra-deep sequencing detects ovarian cancer cells in peritoneal fluid and reveals somatic TP53 mutations in noncancerous tissues. *Proc. Natl. Acad. Sci. U. S. A.* **113,** 6005–6010 (2016).

205. Rosenberg, S. A. *et al.* Use of Tumor-Infiltrating Lymphocytes and Interleukin-2 in the Immunotherapy of Patients with Metastatic Melanoma. *N. Engl. J. Med.* **319,** 1676–1680 (1988).

206. Dudley, M. E. *et al.* Cancer Regression and Autoimmunity in Patients After Clonal Repopulation with Antitumor Lymphocytes. *Science* **298,** 850–854 (2002).

207. Karlsson, M. *et al.* Pilot Study of Sentinel-Node-Based Adoptive Immunotherapy in Advanced Colorectal Cancer. *Ann. Surg. Oncol.* **17,** 1747–1757 (2010).

208. Figlin, R. A. *et al.* Treatment of metastatic renal cell carcinoma with nephrectomy, interleukin-2 and cytokine-primed or CD8(+) selected tumor infiltrating lymphocytes from primary tumor. *J. Urol.* **158,** 740–745 (1997).

209. Aoki, Y. *et al.* Use of adoptive transfer of tumor-infiltrating lymphocytes alone or in combination with cisplatin-containing chemotherapy in patients with epithelial ovarian cancer. *Cancer Res.* **51,** 1934–1939 (1991).

210. Freedman, R. S. *et al.* Intraperitoneal adoptive immunotherapy of ovarian carcinoma with tumor-infiltrating lymphocytes and low-dose recombinant interleukin-2: a pilot trial. *J. Immunother. Emphas. Tumor Immunol. Off. J. Soc. Biol. Ther.* **16,** 198–210 (1994).

211. Ikarashi, H. *et al.* Immunomodulation in patients with epithelial ovarian cancer after adoptive transfer of tumor-infiltrating lymphocytes. *Cancer Res.* **54,** 190–196 (1994).

212. Fujita, K. *et al.* Prolonged disease-free period in patients with advanced epithelial ovarian cancer after adoptive transfer of tumor-infiltrating lymphocytes. *Clin. Cancer Res. Off. J. Am. Assoc. Cancer Res.* **1,** 501–507 (1995).

213. Dudley, M. E., Wunderlich, J. R., Shelton, T. E., Even, J. & Rosenberg, S. A. Generation of tumor-infiltrating lymphocyte cultures for use in adoptive transfer therapy for melanoma patients. *J. Immunother. Hagerstown Md 1997* **26,** 332–342 (2003).

214. Klebanoff, C. A. *et al.* Memory T cell–driven differentiation of naive cells impairs adoptive immunotherapy. *J. Clin. Invest.* **126,** 318–334 (2015).

215. Li, Y., Bleakley, M. & Yee, C. IL-21 Influences the Frequency, Phenotype, and Affinity of the Antigen-Specific CD8 T Cell Response. *J. Immunol.* **175,** 2261–2269 (2005).

216. Tran, K. Q. *et al.* Minimally cultured tumor-infiltrating lymphocytes display optimal characteristics for adoptive cell therapy. *J. Immunother. Hagerstown Md 1997* **31,** 742–751 (2008).

217. Rosenberg, S. A. *et al.* Durable complete responses in heavily pretreated patients with metastatic melanoma using T-cell transfer immunotherapy. *Clin. Cancer Res. Off. J. Am. Assoc. Cancer Res.* **17,** 4550–4557 (2011).

218. Dudley, M. E. *et al.* CD8+ enriched 'young' tumor infiltrating lymphocytes can mediate regression of metastatic melanoma. *Clin. Cancer Res. Off. J. Am. Assoc. Cancer Res.* **16,** 6122–6131 (2010).

219. Chodon, T. *et al.* Adoptive transfer of MART-1 T-cell receptor transgenic lymphocytes and dendritic cell vaccination in patients with metastatic melanoma. *Clin. Cancer Res. Off. J. Am. Assoc. Cancer Res.* **20,** 2457–2465 (2014).

220. Rapoport, A. P. *et al.* NY-ESO-1-specific TCR-engineered T cells mediate sustained antigen-specific antitumor effects in myeloma. *Nat. Med.* **21,** 914–921 (2015).

221. Morgan, R. A. *et al.* Cancer Regression in Patients After Transfer of Genetically Engineered Lymphocytes. *Science* **314,** 126–129 (2006).

222. Maude, S. L. *et al.* Chimeric antigen receptor T cells for sustained remissions in leukemia. *N. Engl. J. Med.* **371,** 1507–1517 (2014).

223. Lee, D. W. *et al.* T cells expressing CD19 chimeric antigen receptors for acute lymphoblastic leukaemia in children and young adults: a phase 1 dose-escalation trial. *Lancet Lond. Engl.* **385,** 517–528 (2015).

224. Huston, J. S. *et al.* Protein engineering of antibody binding sites: recovery of specific activity in an anti-digoxin single-chain Fv analogue produced in Escherichia coli. *Proc. Natl. Acad. Sci.* **85,** 5879–5883 (1988).

225. Tedder, T. F. & Isaacs, C. M. Isolation of cDNAs encoding the CD19 antigen of human and mouse B lymphocytes. A new member of the immunoglobulin superfamily. *J. Immunol. Baltim. Md 1950* **143,** 712–717 (1989).

226. Lamers, C. H. *et al.* Treatment of Metastatic Renal Cell Carcinoma With CAIX CAR-engineered T cells: Clinical Evaluation and Management of On-target Toxicity. *Mol. Ther.* **21,** 904–912 (2013).

227. Adusumilli, P. S. *et al.* Regional delivery of mesothelin-targeted CAR T cell therapy generates potent and long-lasting CD4-dependent tumor immunity. *Sci. Transl. Med.* **6,** 261ra151-261ra151 (2014).

228. Martin, S. D. *et al.* Low Mutation Burden in Ovarian Cancer May Limit the Utility of Neoantigen-Targeted Vaccines. *PLOS ONE* **11,** e0155189 (2016).

229. Morgan, R. A. *et al.* Case report of a serious adverse event following the administration of T cells transduced with a chimeric antigen receptor recognizing ERBB2. *Mol. Ther. J. Am. Soc. Gene Ther.* **18,** 843–851 (2010).

230. Lowe, D. More Juno CAR-T Deaths. *In the Pipeline* (2016). Available at: http://blogs.sciencemag.org/pipeline/archives/2016/11/23/more-juno-car-t-deaths. (Accessed: 8th July 2017)

231. Morgan, R. A. *et al.* Cancer regression and neurological toxicity following anti-MAGE-A3 TCR gene therapy. *J. Immunother. Hagerstown Md 1997* **36,** 133–151 (2013).

232. Varga, A. *et al.* Antitumor activity and safety of pembrolizumab in patients (pts) with PD-L1 positive advanced ovarian cancer: Interim results from a phase Ib study. *J. Clin. Oncol.* **33,** 5510–5510 (2015).

233. Disis, M. L. *et al.* Avelumab (MSB0010718C), an anti-PD-L1 antibody, in patients with previously treated, recurrent or refractory ovarian cancer: A phase Ib, open-label expansion trial. *J. Clin. Oncol.* **33,** 5509–5509 (2015).

234. Dudley, M. E. & Rosenberg, S. A. Adoptive-cell-transfer therapy for the treatment of patients with cancer. *Nat. Rev. Cancer* **3,** 666–675 (2003).

235. Janetzki, S. & Rabin, R. Enzyme-Linked ImmunoSpot (ELISpot) for Single-Cell Analysis. in *Single Cell Protein Analysis* (eds. Singh, A. K. & Chandrasekaran, A.) **1346,** 27–46 (Springer New York, 2015).

236. Vinay, D. S. & Kwon, B. S. Role of 4-1BB in immune responses. *Semin. Immunol.* **10,** 481–489 (1998).

237. Janeway, C. A., Travers, P., Walport, M. & Shlomchik, M. J. The major histocompatibility complex and its functions. (2001).

238. Reeves, E. & James, E. Antigen processing and immune regulation in the response to tumours. *Immunology* **150,** 16–24 (2017).

239. Garrido, F., Ruiz-Cabello, F. & Aptsiauri, N. Rejection versus escape: the tumor MHC dilemma. *Cancer Immunol. Immunother. CII* **66,** 259–271 (2017).

240. Keskinen, P., Ronni, T., Matikainen, S., Lehtonen, A. & Julkunen, I. Regulation of HLA class I and II expression by interferons and influenza A virus in human peripheral blood mononuclear cells. *Immunology* **91,** 421 (1997).

241. Garcia-Diaz, A. *et al.* Interferon Receptor Signaling Pathways Regulating PD-L1 and PD-L2 Expression. *Cell Rep.* **19,** 1189–1201 (2017).

242. Webb, J. R., Milne, K. & Nelson, B. H. PD-1 and CD103 Are Widely Coexpressed on Prognostically Favorable Intraepithelial CD8 T Cells in Human Ovarian Cancer. *Cancer Immunol. Res.* **3,** 926–935 (2015).

243. Hwang, W.-T., Adams, S. F., Tahirovic, E., Hagemann, I. S. & Coukos, G. Prognostic significance of tumor-infiltrating T cells in ovarian cancer: A meta-analysis. *Gynecol. Oncol.* **124,** 192–198 (2012).

244. Alexandrov, L. B. *et al.* Signatures of mutational processes in human cancer. *Nature* **500,** 415–421 (2013).

245. Lawrence, M. S. *et al.* Mutational heterogeneity in cancer and the search for new cancer-associated genes. *Nature* **499,** 214–218 (2013).

246. Giuntoli, R. L. *et al.* Ovarian cancer-associated ascites demonstrates altered immune environment: implications for antitumor immunity. *Anticancer Res.* **29,** 2875–2884 (2009).

247. Tran, E. *et al.* Polyfunctional T-Cell Responses Are Disrupted by the Ovarian Cancer Ascites Environment and Only Partially Restored by Clinically Relevant Cytokines. *PLOS ONE* **5,** e15625 (2010).

248. Bains, S. J. *et al.* Characterization of Immunosuppressive Properties of Malignant Ascites in Ovarian Carcinoma. *Gynecol. Obstet.* **6,** 1–6 (2016).

249. Simpson-Abelson, M. R. *et al.* Human ovarian tumor ascites fluids rapidly and reversibly inhibit T cell receptor-induced NF-κB and NFAT signaling in tumor-associated T cells. *Cancer Immun.* **13,** (2013).

250. Yaguchi, T. *et al.* Immune Suppression and Resistance Mediated by Constitutive Activation of Wnt/β-Catenin Signaling in Human Melanoma Cells. *J. Immunol.* **189,** 2110–2117 (2012).

251. Boone, J. D. *et al.* Targeting the Wnt/β-catenin pathway in primary ovarian cancer with the porcupine inhibitor WNT974. *Lab. Investig. J. Tech. Methods Pathol.* **96,** 249–259 (2016).

252. Mueller, D. L., Jenkins, M. K. & Schwartz, R. H. Clonal expansion versus functional clonal inactivation: a costimulatory signalling pathway determines the outcome of T cell antigen receptor occupancy. *Annu. Rev. Immunol.* **7,** 445–480 (1989).

253. Croft, M. *et al.* TNF superfamily in inflammatory disease: translating basic insights. *Trends Immunol.* **33,** 144–152 (2012).

254. Chang, C.-S., Chang, J. H., Hsu, N. C., Lin, H.-Y. & Chung, C.-Y. Expression of CD80 and CD86 costimulatory molecules are potential markers for better survival in nasopharyngeal carcinoma. *BMC Cancer* **7,** 88 (2007).

255. Dimberg, J., Hugander, A. & Wågsäter, D. Expression of CD137 and CD137 ligand in colorectal cancer patients. *Oncol. Rep.* **15,** 1197–1200 (2006).

256. Salih, H. R. *et al.* Constitutive expression of functional 4-1BB (CD137) ligand on carcinoma cells. *J. Immunol. Baltim. Md 1950* **165,** 2903–2910 (2000).

257. Pollok, K. E. *et al.* 4-1BB T-cell antigen binds to mature B cells and macrophages, and costimulates anti-mu-primed splenic B cells. *Eur. J. Immunol.* **24,** 367–374 (1994).

258. Alderson, M. R. *et al.* Molecular and biological characterization of human 4-1BB and its ligand. *Eur. J. Immunol.* **24,** 2219–2227 (1994).

259. Larsen, C. P., Ritchie, S. C., Pearson, T. C., Linsely, P. S. & Lowry, R. P. Functional expression of the costimulatory molecule, B7/BB1, on murine dendritic cell populations. *J. Exp. Med.* **176,** 1215 (1992).

260. Webb, J. R., Milne, K. & Nelson, B. H. Location, location, location: CD103 demarcates intraepithelial, prognostically favorable CD8(+) tumor-infiltrating lymphocytes in ovarian cancer. *Oncoimmunology* **3,** e27668 (2014).

261. Franciszkiewicz, K. *et al.* Intratumoral Induction of CD103 Triggers Tumor-Specific CTL Function and CCR5-Dependent T-Cell Retention. *Cancer Res.* **69,** 6249–6255 (2009).

262. Kelderman, S. *et al.* Antigen-specific TIL therapy for melanoma: A flexible platform for personalized cancer immunotherapy. *Eur. J. Immunol.* **46,** 1351–1360 (2016).

263. Hendriks, J. *et al.* CD27 is required for generation and long-term maintenance of T cell immunity. *Nat. Immunol.* **1,** 433–440 (2000).

264. Salmon, H. *et al.* Matrix architecture defines the preferential localization and migration of T cells into the stroma of human lung tumors. *J. Clin. Invest.* **122,** 899–910 (2012).

265. Joyce, J. A. & Fearon, D. T. T cell exclusion, immune privilege, and the tumor microenvironment. *Science* **348,** 74–80 (2015).

266. Chen, D. S. & Mellman, I. Elements of cancer immunity and the cancer-immune set point. *Nature* **541,** 321–330 (2017).

267. Barreira da Silva, R. *et al.* Dipeptidylpeptidase 4 inhibition enhances lymphocyte trafficking, improving both naturally occurring tumor immunity and immunotherapy. *Nat. Immunol.* **16,** 850–858 (2015).

268. Poznansky, M. C. *et al.* Active movement of T cells away from a chemokine. *Nat. Med.* **6,** 543–548 (2000).

269. Harter, P. *et al.* Surgery in Recurrent Ovarian Cancer: The Arbeitsgemeinschaft Gynaekologische Onkologie (AGO) DESKTOP OVAR Trial. *Ann. Surg. Oncol.* **13,** 1702–1710 (2006).

270. Wilke, C. M., Kryczek, I. & Zou, W. Antigen-Presenting Cell (APC) Subsets in Ovarian Cancer. *Int. Rev. Immunol.* **30,** 120–126 (2011).

271. Preynat-Seauve, O. *et al.* Tumor-infiltrating dendritic cells are potent antigen-presenting cells able to activate T cells and mediate tumor rejection. *J. Immunol. Baltim. Md 1950* **176,** 61–67 (2006).

272. Manusama, E. R. *et al.* Synergistic antitumour effect of recombinant human tumour necrosis factor alpha with melphalan in isolated limb perfusion in the rat. *Br. J. Surg.* **83,** 551–555 (1996).

273. Xu, X., Fu, X.-Y., Plate, J. & Chong, A. S.-F. IFN-γ Induces Cell Growth Inhibition by Fas-mediated Apoptosis: Requirement of STAT1 Protein for Up-Regulation of Fas and FasL Expression | Cancer Research. Available at: http://cancerres.aacrjournals.org.ezproxy.library.uvic.ca/content/58/13/2832.short. (Accessed: 30th June 2017)

274. Freeman, J. D., Warren, R. L., Webb, J. R., Nelson, B. H. & Holt, R. A. Profiling the T-cell receptor beta-chain repertoire by massively parallel sequencing. *Genome Res.* **19,** 1817–1824 (2009).

275. Warren, R. L. *et al.* Exhaustive T-cell repertoire sequencing of human peripheral blood samples reveals signatures of antigen selection and a directly measured repertoire size of at least 1 million clonotypes. *Genome Res.* **21,** 790–797 (2011).

276. Ozawa, T., Tajiri, K., Kishi, H. & Muraguchi, A. Comprehensive analysis of the functional TCR repertoire at the single-cell level. *Biochem. Biophys. Res. Commun.* **367,** 820–825 (2008).

277. Peters, D. G. *et al.* Comprehensive transcript analysis in small quantities of mRNA by SAGE-Lite. *Nucleic Acids Res.* **27,** e39–e44 (1999).

278. Brochet, X., Lefranc, M.-P. & Giudicelli, V. IMGT/V-QUEST: the highly customized and integrated system for IG and TR standardized V-J and V-D-J sequence analysis. *Nucleic Acids Res.* **36,** W503-508 (2008).

279. Bolotin, D. A. *et al.* MiXCR: software for comprehensive adaptive immunity profiling. *Nat. Methods* **12,** 380–381 (2015).

280. Shugay, M. *et al.* VDJtools: Unifying Post-analysis of T Cell Receptor Repertoires. *PLOS Comput. Biol.* **11,** e1004503 (2015).

281. R Core Team. *R: A language and environment for statistical computing.* (R Foundation for Statistical Computing).

282. Fearon, D. T. The expansion and maintenance of antigen-selected CD8(+) T cell clones. *Adv. Immunol.* **96,** 103–139 (2007).

283. Gundry, M., Li, W., Maqbool, S. B. & Vijg, J. Direct, genome-wide assessment of DNA mutations in single cells. *Nucleic Acids Res.* **40,** 2032 (2012).

284. Saliba, A.-E., Westermann, A. J., Gorski, S. A. & Vogel, J. Single-cell RNA-seq: advances and future challenges. *Nucleic Acids Res.* **42,** 8845–8860 (2014).

285. Zhang, K. *et al.* Sequencing genomes from single cells by polymerase cloning. *Nat. Biotechnol.* **24,** 680–686 (2006).

286. Anna, P. *et al.* High frequency CD8+PD-1+ TCR clonotypes isolated from fresh melanomas display anti-tumor activity. *J. Immunother. Cancer* **3,** P42 (2015).

287. Wherry, E. J., Blattman, J. N., Murali-Krishna, K., Most, R. van der & Ahmed, R. Viral Persistence Alters CD8 T-Cell Immunodominance and Tissue Distribution and Results in Distinct Stages of Functional Impairment. *J. Virol.* **77,** 4911 (2003).

288. Moskophidis, D., Lechner, F., Pircher, H. & Zinkernagel, R. M. Virus persistence in acutely infected immunocompetent mice by exhaustion of antiviral cytotoxic effector T cells. *Nature* **362,** 758–761 (1993).

289. Saio, M., Radoja, S., Marino, M. & Frey, A. B. Tumor-infiltrating macrophages induce apoptosis in activated CD8(+) T cells by a mechanism requiring cell contact and mediated by both the cell-associated form of TNF and nitric oxide. *J. Immunol. Baltim. Md 1950* **167,** 5583–5593 (2001).

290. Bagasra, O. Protocols for the in situ PCR-amplification and detection of mRNA and DNA sequences. *Nat. Protoc.* **2,** 2782–2795 (2007).

291. Athman, A. *et al.* Protocol: a fast and simple in situ PCR method for localising gene expression in plant tissue. *Plant Methods* **10,** 29 (2014).

292. Redeker, A. & Arens, R. Improving Adoptive T Cell Therapy: The Particular Role of T Cell Costimulation, Cytokines, and Post-Transfer Vaccination. *Front. Immunol.* **7,** (2016).

293. Hinrichs, C. S. *et al.* Adoptively transferred effector cells derived from naive rather than central memory CD8+ T cells mediate superior antitumor immunity. *Proc. Natl. Acad. Sci. U. S. A.* **106,** 17469–17474 (2009).

294. Dudley, M. E. *et al.* Randomized selection design trial evaluating CD8+-enriched versus unselected tumor-infiltrating lymphocytes for adoptive cell therapy for patients with melanoma. *J. Clin. Oncol. Off. J. Am. Soc. Clin. Oncol.* **31,** 2152–2159 (2013).

295. Peng, W. *et al.* PD-1 blockade enhances T-cell migration to tumors by elevating IFN-γ inducible chemokines. *Cancer Res.* **72,** 5209–5218 (2012).

Appendix A: Gating Strategies

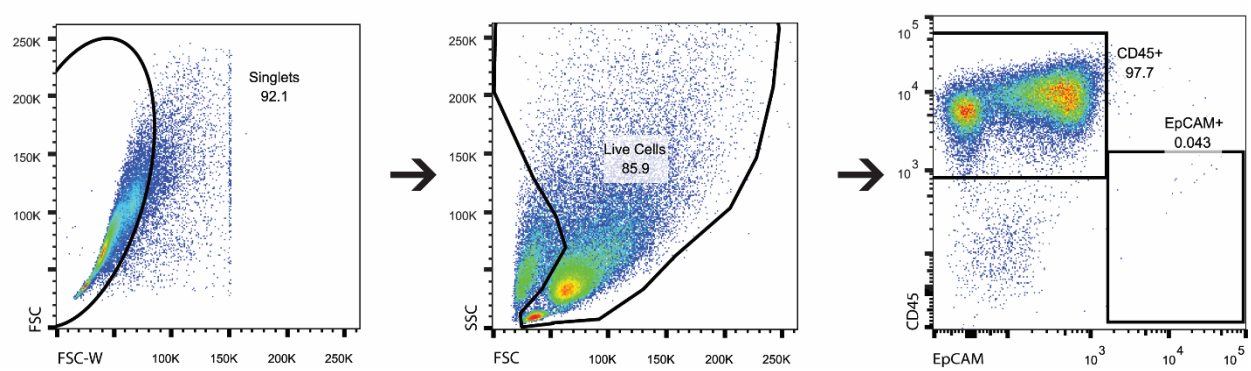

Figure A1. Gating strategy for analyzing MHC class I and II on ascites *ex vivo* as well as ascites cells post-IFNγ-treatment of primary ascites tumor cells.

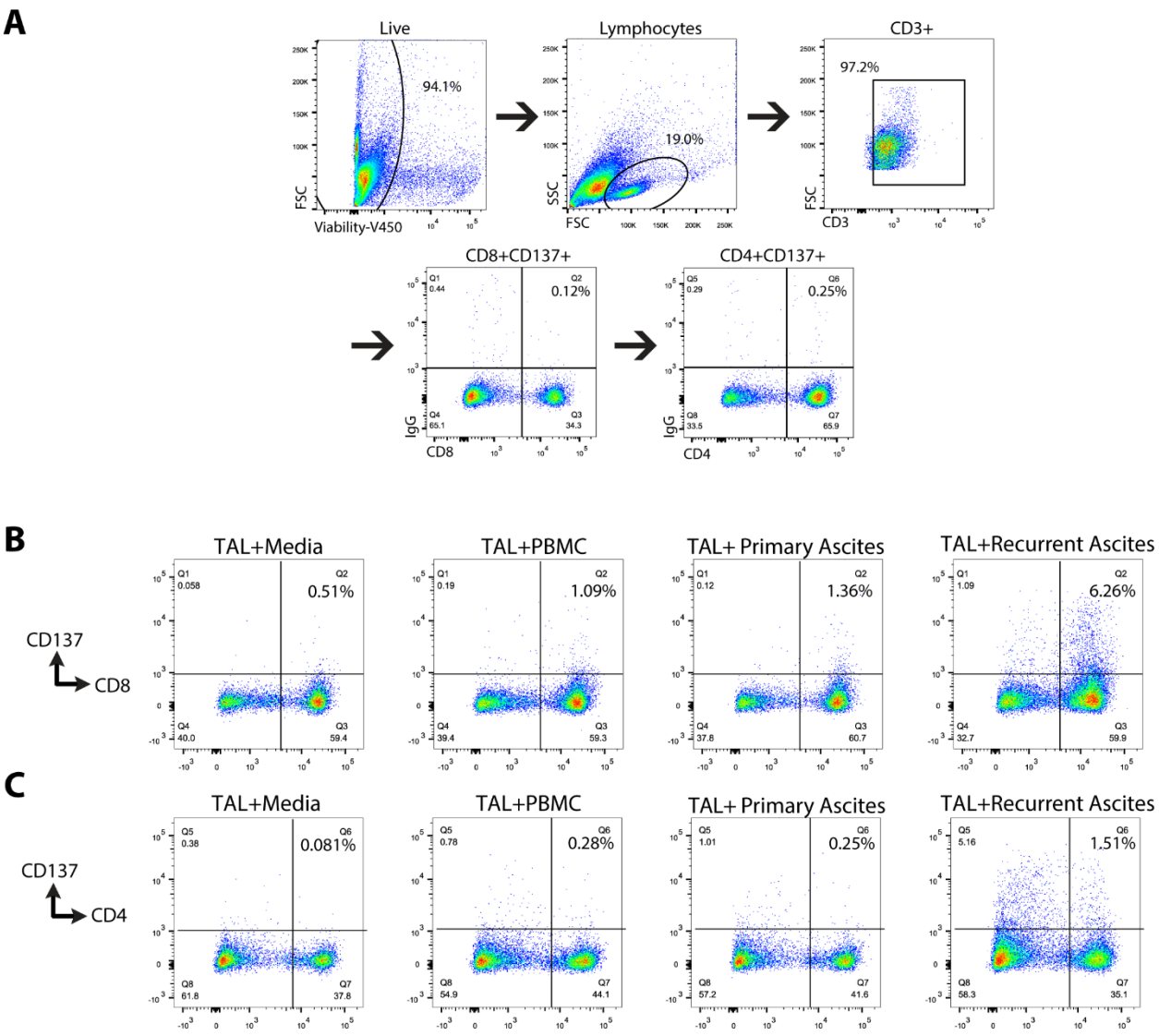

Figure A2. IROC 060 Tumor vs TAL gating strategy for analyzing CD137 on TAL (A) and representative dot plots showing CD137 on $CD8^+$ TAL (B) and $CD4^+$ TAL (C).

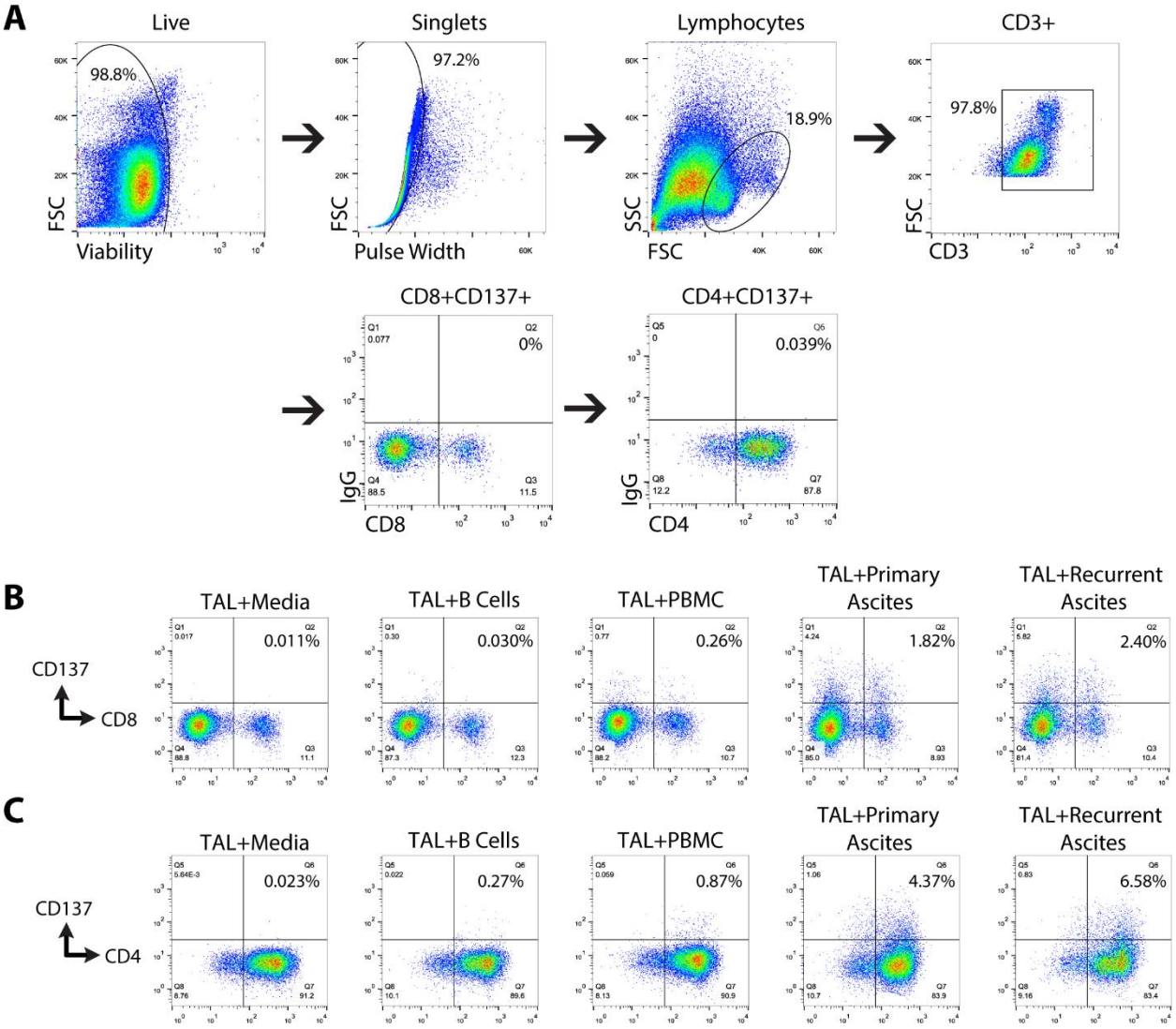

Figure A3. IROC 106 Tumor vs TAL gating strategy for analyzing CD137 on TAL (A) and representative dot plots showing CD137 on $CD8^+$ TAL (B) and $CD4^+$ TAL (C).

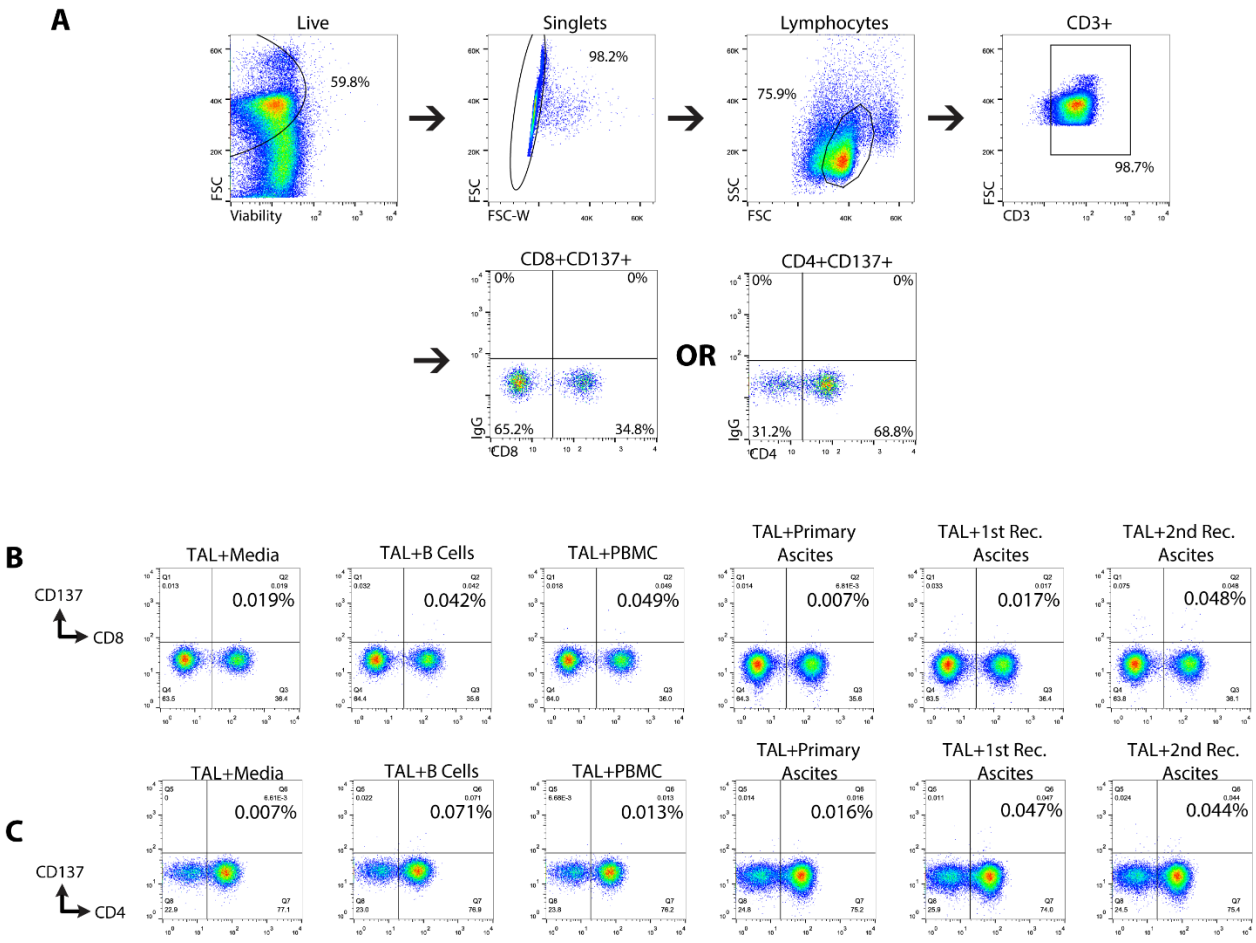

Figure A4. IROC 034 Tumor vs TAL gating strategy for analyzing CD137 on TAL (A) and representative dot plots showing CD137 on $CD8^+$ TAL (B) and $CD4^+$ TAL (C).

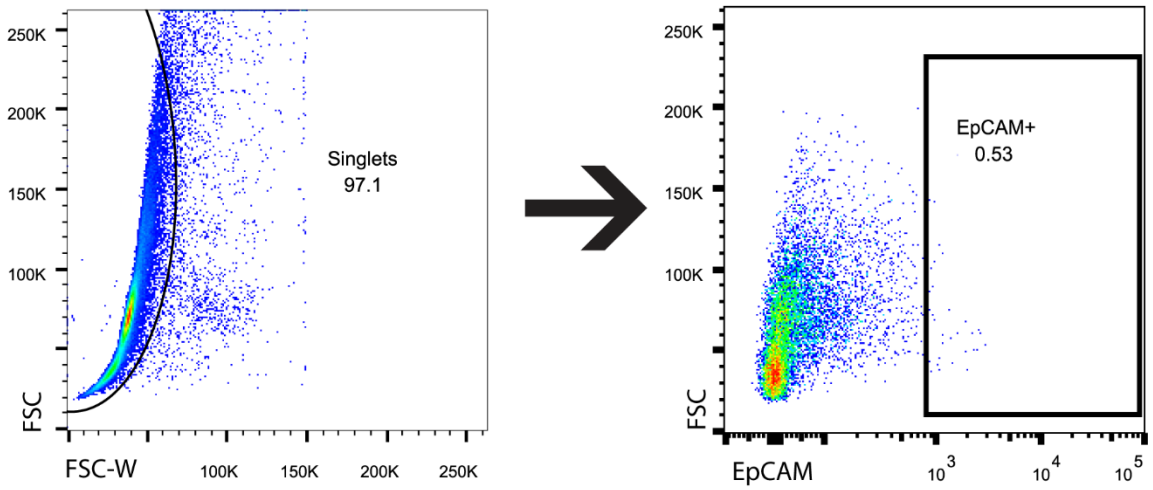

Figure A5. Ascites EpCAM+ Ex Vivo Gating Strategy. Events were first gated on singlets by FSC-width and FSC. The unstained control (second plot) was used to draw the gate for $EpCAM^+$ cells.

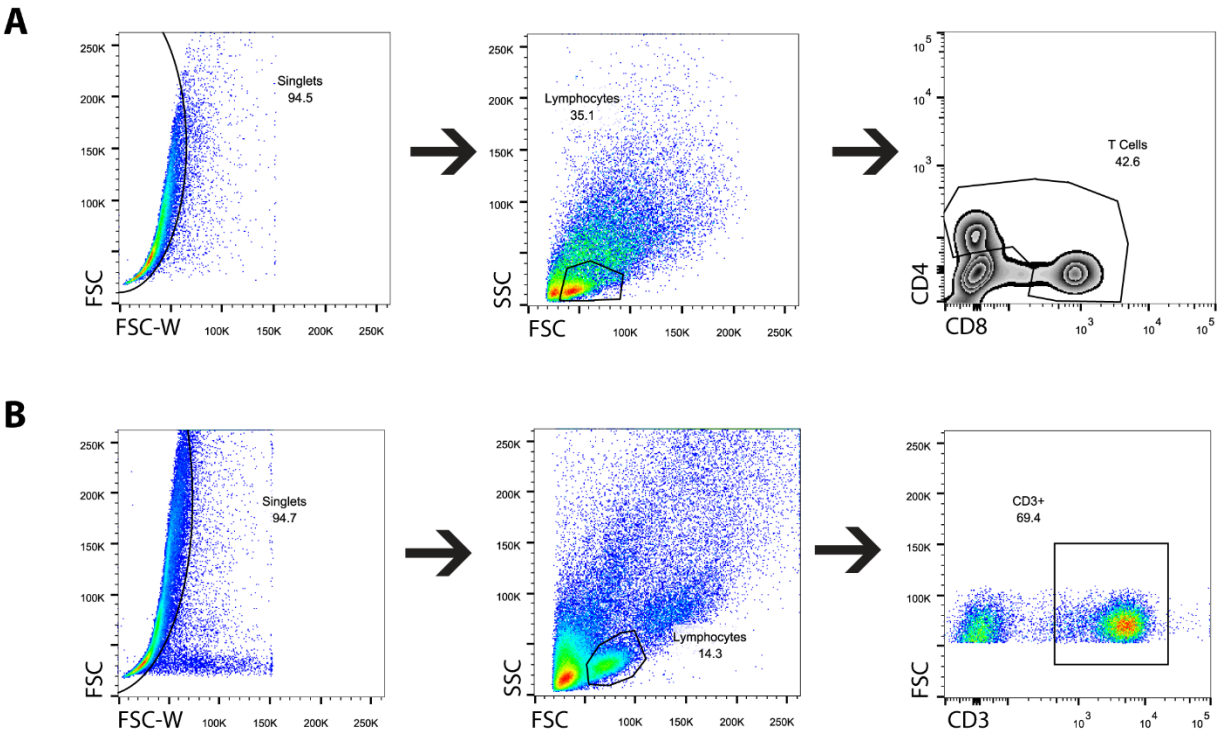

Figure A6. Gating Strategy for analyzing *ex vivo* TAL phenotypes from (A) IROC 060, (B) IROC 106 and 034

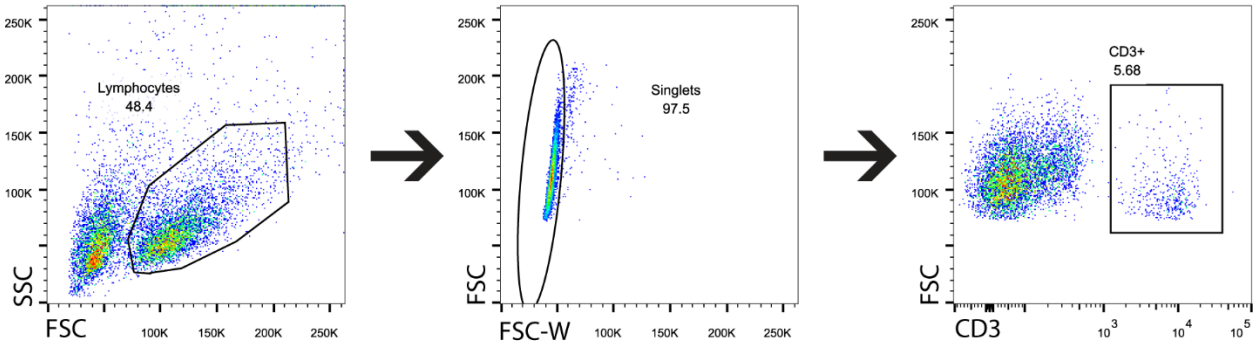

Figure A7. Gating strategy for analyzing phenotypes of TAL following high-dose IL-2 expansions of bulk ascites.

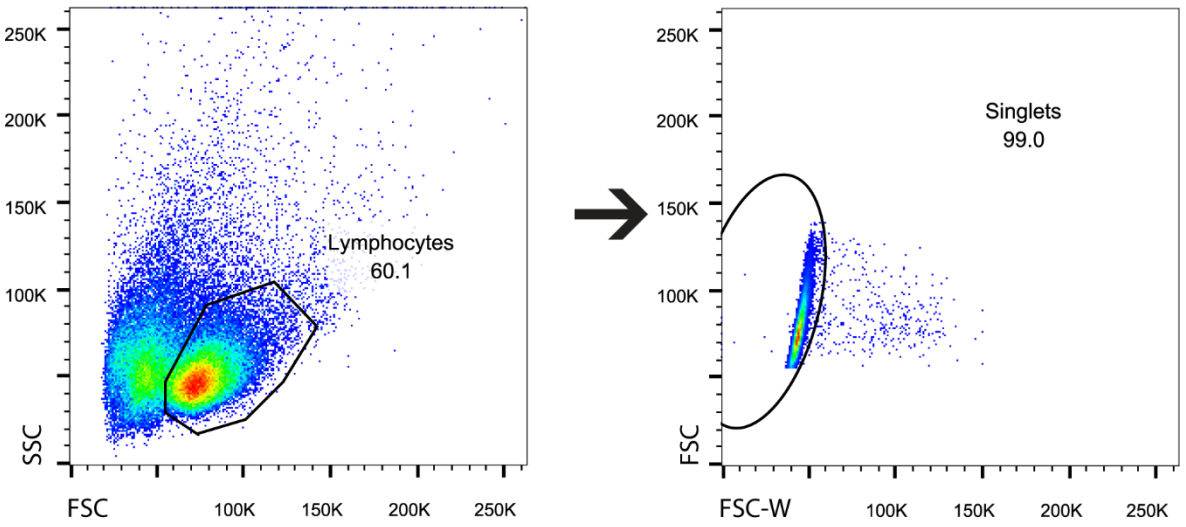

Figure A8. Gating strategy for analyzing phenotypes of TAL following a conventional REP of IL-2-expanded TAL.

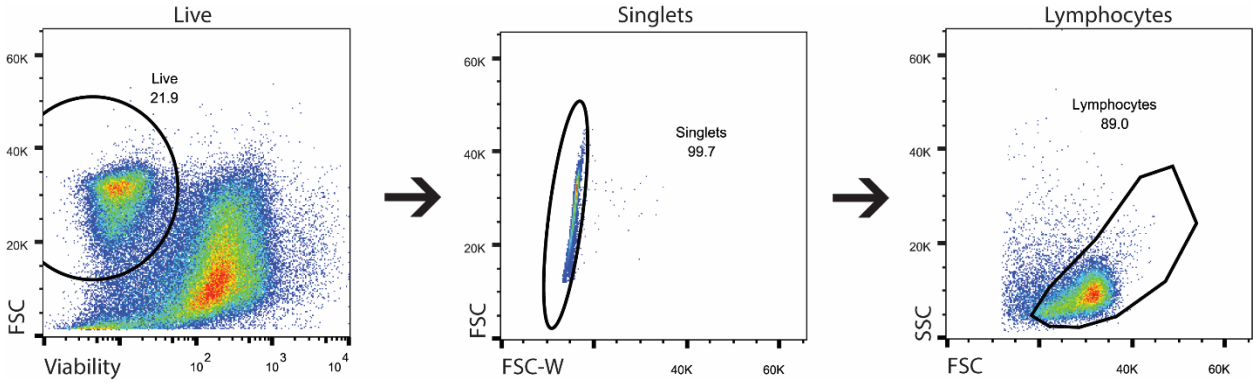

Figure A9. Gating strategy for analyzing activation of bi-clonal mixtures of clone D6 and clone F2 prior to FACS-purification.

Appendix B – TCRseq of Tumor-Reactive T Cell Clones from Primary and Recurrent Disease

B1. Introduction

High-grade serous carcinoma (HGSC) tumors can have high intratumoral heterogeneity (ITH).[1,2] To successfully contend with recurrent, heterogeneous tumor, anti-tumor T cells may utilize certain approaches to deal with the diversity of tumor subclones. One possible approach could be to recognize several tumor-specific antigens, which may result in the emergence of new tumor-reactive T cell clones over time. For example, in renal cell carcinoma, deep sequencing of tumor sites showed a heterogeneous population of T cells that were diverse between each tumor site, suggesting a diversity of tumor-reactive T cell clones contributing to tumor control.[3] In contrast, the tumor-reactive T cells may recognize antigens that are maintained by the tumor over time. In line with this, HGSC tumor sites revealed a more homogeneous T cell infiltrate, suggesting recognition of a homogeneous set of tumor antigens.[4] However, these studies did not assess tumor-reactivity of TIL nor did they provide insight on how TIL populations change over time within a patient's tumor.

Two recent studies provided some insight on how tumor-reactive TAL contend with ITH in recurrent tumors. Both studies, one in melanoma and the other in HGSC, found new tumor-reactive T cell clones emerged while other tumor-reactive T cell clones were subsequently lost between primary and recurrent disease.[5,6] However, these studies investigated T cells that were reactive to specific neoantigens or cancer testis antigens, rather than the polyclonal repertoire of tumor-reactive T cells. In my study, I assessed the reactivity of polyclonal populations of TAL expanded from ascites for reactivity to tumor, rather than tumor-specific antigens. In chapter 2, it was determined that both patients' tumor-reactive recurrent TAL had a lower frequency of tumor-reactive TAL compared to primary TAL and became equal mixtures of both $CD4^+$ and $CD8^+$ T cells. To elucidate whether a common mechanism resulted in both patients' TAL to both have a reduced frequency of tumor-reactive T cells and to become comprised of equal numbers of $CD4^+$ and $CD8^+$ T cells, I subjected tumor-reactive T cell populations to deep sequencing of the TCR-β chain (TCRseq). Based on the two previous studies, I hypothesized that new tumor-reactive T cell clones would emerge over time to contend with ITH. Therefore, I expected to see new TCR clonotypes identified in populations of tumor-reactive recurrent TAL that were distinct from tumor-reactive primary TAL.

B2. Results

The aim of this study was to discover predominant mechanisms used by T cells to control recurrent tumors. To do so, TAL were cultured overnight in the presence or absence of autologous bulk ascites cells, $CD45^+$ ascites cells, or $CD45^-$ ascites cells and evaluated for reactivity by interferon-γ ELISPOT and flow cytometry for CD137. $CD137^+$ tumor-reactive T cells were FACS-purified for TCRseq. Each patients' tumor-reactive T cell repertoires were profiled and tracked from primary to recurrent disease. As discussed in chapter 2, IROC 060 TAL only reacted to recurrent ascites cells (Figure 8). IROC 060 tumor-reactive primary TAL were predominantly $CD8^+$ (Figure 8A), while responsive recurrent TAL were an equal mixture of both $CD4^+$ and $CD8^+$ T cells (Figure 8C). Additionally, 8% of primary TAL were tumor-reactive compared to just over 2% of recurrent TAL (Figures 8A, C). In contrast to IROC 060, IROC 106 TAL were reactive to both primary and recurrent ascites cells (Figure 10). Responsive primary TAL were predominantly $CD4^+$ (Figure 10A), while responsive recurrent TAL were an equal mixture of both $CD4^+$ and $CD8^+$ T cells (Figure 10C). Up to 10% of primary TAL and up to 6% of recurrent TAL recognized ascites (Figures 10A, C), indicating primary TAL had a higher frequency of tumor-reactive T cells compared to recurrent TAL. $CD4^+CD137^+$ and $CD8^+CD137^+$ T cells were sorted into separate collection tubes and RNA was extracted. Between 129 and 23,400 tumor-reactive $CD137^+$ cells were obtained for each purified, tumor-reactive sample. RNA samples were submitted for TCRseq at the Michael Smith Genome Sciences Centre (GSC).

B2.1 IROC 060 Tumor-Reactive T Cell Evolution from Primary to Recurrent Disease

To determine the pattern of tumor-reactive T cell evolution in IROC 060, I first assessed whether any tumor-reactive T cell clones were shared between primary and recurrent TAL. No tumor-reactive T cell clones were shared between primary and recurrent TAL. Six unique T cell clones were highly abundant in the purified, tumor-reactive primary TAL subset. Two $CD4^+$ clones comprised 41% and 51% of the total tumor-reactive $CD4^+$ primary T cells (Figure B1A). Four $CD8^+$ clones were identified at between 4% and 50% of the total tumor-reactive $CD8^+$ primary clones (Figure B1C). In contrast, tumor-reactive recurrent TAL were more polyclonal than tumor-reactive primary TAL, with 10 $CD4^+$ and 11 $CD8^+$ tumor-reactive T cell clones that ranged in frequency from 1-25% of the purified, tumor-reactive subset (Figures B1B,D). Most tumor-reactive T cell clones were identified at very low frequencies directly *ex vivo* or post-IL-2-expansion (Figure B1). Additionally, some tumor-reactive clones were not identified either directly *ex vivo* or post-IL-2-expansion (Figure B1). Together, the results suggest the evolution of

tumor-reactive T cell clones in IROC 060 was highly dynamic, with multiple clones being lost over time while many others emerged between primary and recurrent disease.

B2.2 IROC 106 Tumor-Reactive T Cell Evolution from Primary to Recurrent Disease

To determine whether IROC 106 shared common mechanisms of tumor-reactive T cell evolution with IROC 060, I first assessed whether tumor-reactive T cells were lost over time. Indeed, there were numerous tumor-reactive clones that were uniquely present among primary TAL (Figures B2A,C-D, B3A,C-D). Of these, 6 $CD4^+$ and 7 $CD8^+$ primary T cell clones responded to both primary and recurrent tumor (Figures B2A, B3A), and 19 $CD4^+$ and 14 $CD8^+$ clones that responded to either primary or recurrent tumor but not both (Figures B2C-D, B3C-D). The unique primary $CD4^+$ clones were all found at >6% abundance (Figures B2A,C-D), while the unique $CD8^+$ clones were found at up to 24% abundance (Figure B3A). Further, there were several tumor-reactive T cell clones that were uniquely present among recurrent TAL (Figures B2B,E-F, B3B,E-F). Of these, 5 $CD4^+$ and 6 $CD8^+$ T cell clones recognized both primary and recurrent tumor (Figures B2B, B3B), and 27 $CD4^+$ and 7 $CD8^+$ clones responded to either primary or recurrent tumor but not both (Figures B2E-F, B3E-F). Further, these unique $CD4^+$ clones were again found at >6% abundance (Figure B2B,E-F), while unique $CD8^+$ T cell clones were found at up to 45% abundance (Figure B3B).

To determine if IROC 106 exhibited any additional mechanisms of T cell evolution, I looked for tumor-reactive T cell clones that were shared between primary and recurrent TAL. Indeed, there were numerous shared tumor-reactive T cell clones identified in IROC 106 TAL. One highly abundant $CD4^+$ T cell clone was identified at over 38% of the primary tumor-reactive subset of primary TAL (Figure B2G). By the time of recurrent disease, this $CD4^+$ clone had decreased in frequency to around 16-17% (Figure B2G). There were an additional 2 $CD4^+$ (Figure B2G) and 4 $CD8^+$ T cell clones (Figure B3G) that were shared by both primary and recurrent TAL and recognized both primary and recurrent tumor. In addition, there was one $CD4^+$ T cell clone that was shared by both primary and recurrent TAL yet only recognized recurrent tumor (Figure B2H) and one $CD8^+$ clone shared by both primary and recurrent TAL that only recognized primary tumor (Figure B3H). All tumor-reactive T cell clones were identified at frequencies between 0 and 9% of TAL directly *ex vivo* and post-IL-2-expansion (Figures B2, B3), except for two shared $CD4^+$ clones, which were identified at up to 10% abundance directly *ex vivo* (Figure B2G). Indeed, most tumor-reactive clones that were under 5% of the tumor-reactive T cell subsets were found at between 0% and 1% abundance directly *ex vivo* and post-IL-2-expansion (Figures B2, B3).

Due to the low abundance of RNA in IROC 060 tumor-reactive T cell samples, TCRseq results showed some level of contamination from high-abundance TCR clonotypes from IROC 106. Likewise, some high-abundance IROC 060 clones were identified in IROC 106 samples. Further, low levels of contamination were evident between $CD4^+$ and $CD8^+$ clonotypes. For example, high-abundance $CD8^+$ clones were occasionally found at low abundance (<1%) in the $CD4^+$ samples. Because the contaminating clone was found at such high abundance in its native sample and such low abundance in its non-native sample, it was straightforward to distinguish the clone from the native clones within each sample and exclude it from the analysis. However, for clones identified at low-abundance in both patients' samples or both $CD4^+$ and $CD8^+$ samples, it was impossible to determine the true origin of these clonotypes. Therefore, shared clonotypes found at low abundance were excluded from the analysis. Further, to improve the validity of TCRseq on such low-abundance samples, replicate libraries were created from the cDNA synthesized from RNA extracted from the tumor-reactive T cell samples from each patient. Unfortunately, in one library 5 of the top 20 clones identified for IROC 060 were highly abundant in IROC 106 T cell samples. Further, the top 3 clones identified for IROC 060 were highly abundant in IROC 106 samples, suggesting there was widespread contamination in one replicate library, making interpretation of this library unreliable. Therefore, the TCRseq data was analysed in singlicate using the less contaminated library.

B3. Discussion

I successfully profiled the repertoire of tumor-reactive $CD8^+$ and $CD4^+$ T cell clones from primary to recurrent disease in two HGSC patients. Results from both patients indicate there are common mechanisms of T-cell mediated control of ITH in HGSC. IROC 060 had no shared tumor-reactive clones between primary and recurrent TAL, suggesting some tumor-reactive T cells are lost over time while others emerge by recurrent disease. Likewise, IROC 106 also had tumor-reactive T cell clones that were unique to either primary or recurrent TAL. However, IROC 106 also had tumor-reactive T cell clones that were shared between primary and recurrent TAL, suggesting TAL used additional mechanisms to control ITH in HGSC. These findings provide insight into the dynamics of tumor-reactive T cells over time in HGSC.

Previous studies in HGSC and in melanoma showed tumor-reactive T cells share common evolutionary mechanisms to contend with ITH where tumor-reactive T cell clones emerged over time to contend with new tumor antigens.[5,6] Further, the study in HGSC showed tumor-antigen-specific T cells were lost at later time points.[6] In agreement with these previous studies, IROC 060 and IROC 106 had several T cell clones that were unique to their primary TAL. This suggests in both patients, there were numerous tumor-reactive T cell clones that were lost between primary and recurrent disease. Additionally, there were numerous tumor-reactive T cell clones that were unique to recurrent TAL, suggesting emergence of new tumor-reactive T cell clones by recurrent disease. Although it is possible that numerous T cell clones may recognize the same antigen,[7] it is likely that tumor-reactive TAL recognize numerous antigens. This suggests that new, tumor-reactive T cell clones that recognize new tumor antigens emerge over time to control ITH.

Although some IROC 106 tumor-reactive T cells evolved through mechanisms identified in IROC 060 and patients in previous studies,[5,6] there was evidence of additional mechanisms of T cell evolution. Indeed, there were numerous tumor-reactive T cells shared by both primary and recurrent TAL (Figures B2G-H, B3G-H). In fact, the most abundant $CD4^+$ tumor-reactive clone was shared by both primary and recurrent TAL and was found at up to 38% in tumor-reactive primary TAL (Figure B2G). These results indicate T cells can utilize several mechanisms to contend with ITH over time in HGSC. These findings are similar to those from Verdegaal *et al*, who found that despite T cell and tumor antigen loss, T cells from all disease time points were able to recognize tumor from all disease time points. This suggested tumor-reactive T cells may recognize a shared antigen or shared groups of antigens, although the authors did not follow-up on this finding in their study.[5] Together, results from both HGSC patients in the current study suggest tumor-reactive TAL can utilize several mechanisms to contend with ITH over time in HGSC.

In IROC 060, tumor-reactive primary TAL were predominantly $CD8^+$ while her tumor-reactive recurrent TAL were comprised of equal amounts of $CD4^+$ and $CD8^+$ T cells (Figures 8A,C). Indeed, tumor-reactive primary TAL had two times more $CD8^+$ T cell clones compared to $CD4^+$ clones, while recurrent TAL had nearly equal numbers of tumor-reactive $CD4^+$ and $CD8^+$ T cell clones (10 and 11 clones, respectively). However, despite the lack of common tumor-reactive T cell clones, both primary and recurrent TAL only recognized recurrent ascites (Figure 8). Nonetheless, because both primary and recurrent TAL recognize recurrent tumor, results suggest tumor antigens were maintained over time and tumor-reactive T cell clones form primary disease are lost from the patient repertoire over time.

For IROC 106, tumor-reactive primary TAL were predominantly $CD4^+$ while her tumor-reactive recurrent TAL were equally both $CD4^+$ and $CD8^+$ (Figures 10A,C). In line with this, tumor-reactive primary TAL were dominated by one $CD4^+$ clone that was found at between 30 and 40% of the purified, tumor-reactive populations (Figure B2G). In contrast, this $CD4^+$ clone was found at lower abundance in recurrent TAL (between 15% and 17% of tumor-reactive T cell clones; Figure B2G). At the same time, a new $CD8^+$ T cell clone emerged was found at a frequency between 41% and 45% of the purified, tumor-reactive $CD8^+$ T cell clones (Figure B3C). Together this suggests that the reduced frequency of tumor-reactive $CD4^+$ T cells at recurrent disease could be due to loss of a shared, high-abundance $CD4^+$ T cell clone and the simultaneous emergence of a high-abundance $CD8^+$ T cell clone at recurrent disease.

Both IROC 060 and IROC 106 had a lower frequency of tumor-reactive T cells in their recurrent TAL compared to primary TAL. By TCRseq, IROC 106 primary TAL had 109 different TCR clonotypes that were found above 1% abundance in the purified, tumor-reactive subset. In contrast, recurrent TAL had only 54 different TCR clonotypes found at greater than 1% abundance in the purified, tumor-reactive subset. However, IROC 060 had only 6 tumor-reactive T cell clones that were above 1% abundance in the purified, tumor-reactive population and 21 clones identified in recurrent TAL. Therefore, this reduction in frequency of tumor-reactive T cells over time is unlikely due to a reduction in the diversity of tumor-reactive T cell clones at recurrent disease. Although PD-1 wasn't expressed at higher levels on recurrent TAL compared to primary TAL, it is possible that other immunosuppressive molecules, such as TIGIT[8], VISTA[9], TIM-3[10], or LAG-3[10] are expressed at higher levels on recurrent TAL, which would contribute to the observed reduction in tumor-reactivity, although these markers were not analyzed in this study.

The TCRseq of samples with low RNA abundance was technically challenging. Low-level contamination from each patient was seen, despite efforts to minimize contamination through separate sample preparation for each patient and the use of dedicated spaces for RNA sequencing at the GSC.

Nonetheless, at some point during RNA extraction, cDNA synthesis, or library preparation, low levels of T cell clones from IROC 106 contaminated IROC 060 samples. Additionally, low levels of high abundance $CD8^+$ T cell clones contaminated $CD4^+$ T cell samples and vice versa. These contaminating sequences were relatively straightforward to exclude, because they were found at very high abundance in the native sample and at very low abundance in the non-native (contaminated) sample. Nonetheless, for TCR clonotypes found at low abundance in both patients, it was not possible to determine which clone was native to which patient or whether the TCR was from a $CD4^+$ or $CD8^+$ T cell. Therefore, these shared, low-abundance TCR clonotypes were excluded from analysis.

To increase confidence in the identified frequencies of tumor-reactive T cells, each sample's cDNA was split into two and replicate libraries were prepared for sequencing. Unfortunately, one library had widespread contamination where 5 of the top 20 clones identified for IROC 060 were highly abundant in IROC 106 T cell samples. Further, the top 3 clones identified for IROC 060 were highly abundant in IROC 106 samples. Because of this, it made the replicate library uninterpretable and consequently, all TCRseq data was analyzed in singlicate. Because of the small sample sizes, particularly from IROC 060, replicate libraries would have indicated whether the variety of TCR sequences identified was simply due to sampling error. However, at least for IROC 106, the TCR-Vβ of the most abundant $CD4^+$ and $CD8^+$ T cell clones matched perfectly with Vβ-spectratyping data from IROC 106 primary TAL directly *ex vivo* and primary TAL post-IL-2 expansion (data not shown). Future TCRseq analysis will be performed using additional T cells when specimen is available. Alternatively, when specimen is limiting, efforts will be made to investigate methods that generate less terminally differentiated T cells that may allow for tumor-reactive T cell expansion post-sorting. Nonetheless, my results show that profiling of these TCR clonotypes was accurate, despite such a small number of tumor-reactive T cells.

Several clones identified in tumor-reactive T cell populations were not identified in either *ex vivo* or IL-2 expanded TAL populations. For example, one IROC 060 tumor-reactive clone was identified at 18% abundance in tumor-reactive recurrent TAL, despite not being found directly ex vivo or in IL-2 expanded T cell populations (Figures B1B). One interpretation is some tumor-reactive clones identified by TCRseq were simply contaminants found at high abundance, particularly because of the overall low-abundance of RNA from the T cells of interest given such few cells. However, a recent study highlighted the challenges of identifying clinically relevant T cells prior to expansion *in vitro*.[11] The authors found most T cells that were identified at high abundance in a T cell infusion product and shown to have tumor-reactivity were found at very low levels directly *ex vivo*.[11] Further, *ex vivo* frequencies of these T cell clones often fell below the limit of detection of TCRseq, 0.001%.[11–14] Indeed, the inability to detect

tumor-reactive T cell clones directly *ex vivo* in my study may be due to *ex vivo* and post-IL-2 expansion T cell frequencies below 0.001%. Further, the MiXCR analysis package used to analyze the TCR deep sequencing results excludes sequencing reads only mapped once. Therefore, it is possible that low-abundance T cell clones were present and only had one sequencing read, and were subsequently excluded from the *in silico* TCRseq analysis.

In conclusion, I identified several mechanisms that allow T cell-mediated control of recurrent HGSC tumors. Both IROC 060 and IROC 106 showed evidence that tumor-reactive T cell clones are lost over time, as indicated by the presence of tumor-reactive T cell clones that were unique to primary TAL. However, both patients also showed evidence of tumor-reactive T cell clones that emerged over time, as both patients had tumor-reactive T cell clones that were unique to recurrent TAL. While this was the only mechanism identified in IROC 060, IROC 106 TAL exhibited additional mechanisms of T cell evolution, including tumor-reactive T cell clones shared by both primary and recurrent disease as well as T cell clones that uniquely recognize either primary or recurrent disease. Together, results from this study suggest anti-tumor T cells may utilize several mechanisms of evolution to control ITH in HGSC.

B4. Conclusions

In this study, I elucidated mechanisms used by tumor-reactive T cells to contend with ITH in HGSC. In line with previous research, both IROC 060 and IROC 106 TAL had new tumor-reactive clones that emerged over time, which may recognize new tumor antigens present at recurrent disease. The results of TCRseq, together with the observation that the frequency of tumor-reactive T cells decreases over time, suggests T cell loss is a significant challenge in HGSC. Nonetheless, in each patient, both primary and recurrent TAL recognized recurrent tumor. Subsequent TCRseq identified new tumor-reactive T cell clones that emerged over time in both patients, supporting my hypothesis. However, in IROC 106, there was also evidence of both T cell and antigen maintenance from primary and recurrent disease. Specifically, certain tumor-reactive clones were identified at high abundance in both primary and recurrent TAL and these T cell clones reacted to both primary and recurrent tumor. IROC 106 was the only patient whose primary tumor lacked T cell infiltrate (Figures 15A-B). Perhaps, due to the lack of T cell infiltration compared to that of IROC 060 (Figures 14A-B), IROC 106 tumor was subjected to less immune-mediated pressure, therefore there was no immunological pressure to mediate immunoediting[15], therefore maintaining tumor-specific antigens over time. In contrast, results for IROC 060 suggest antigens may have been lost over time, perhaps due to the presence of immune infiltrate and high expression of MHC class I and class II (Figure 14).

This study was ultimately designed to inform clinical trial protocols for ACT of recurrent HGSC tumors. Based on the results from these two patients, both primary and recurrent TAL are equally capable of recognizing recurrent tumor. However, primary TAL had a higher frequency of tumor-reactive T cells compared to recurrent TAL. Results from both patients suggest this was not due to an overall loss of tumor-reactive T cell clones over time. While this was indeed the case for IROC 106, with half the number of abundant tumor-reactive T cell clones identified at recurrent disease compared to at primary disease, IROC 060 had a greater number of tumor-reactive T cell clones at recurrent disease. Although the data suggests recurrent TAL do not express PD-1 at higher levels than primary TAL, there are numerous other T cell exhaustion pathways and mechanisms that are utilized by tumors to suppress the anti-tumor immune response.[8–10] Therefore, the overall reduction in tumor-reactivity at recurrent disease could be due to the expression of other immunosuppressive markers not profiled in this study. This supports study of checkpoint blockade therapies in HGSC patients and suggests combining ACT with checkpoint blockade may yield better clinical responses than ACT alone. Nonetheless, the results of this study suggest it may be best to use primary T cells to yield the best possible clinical responses for the treatment of recurrent HGSC.

This was the first systematic assessment of the dynamics of tumor-recognition and the tumor-reactive T cell repertoire between primary and recurrent disease in HGSC. Results suggest anti-tumor T cell responses from ascites are both diverse between patients and dynamic within a patient, indicating diverse mechanisms of T cell evolution are utilized to contend with ITH in HGSC. Nonetheless, in both patients there was evidence that tumor-reactive T cell clones were lost over time while other clones emerged to contend with possibly new tumor-specific antigens at recurrence. This suggests a shared mechanism of T cell control of ITH is through the emergence of new, tumor-reactive T cells over time. However, IROC 106 had evidence of antigens, shared by both primary and recurrent tumor, that were recognized by highly abundant T cell clones identified in both primary and recurrent TAL. Together, these results show there are numerous mechanisms utilized by tumor-reactive T cells to contend with tumors over time in HGSC patients. Further, results show that primary T cells may be the best population to create a therapeutic T cell product for mediating strong clinical responses following ACT of recurrent HGSC.

B5. Figures

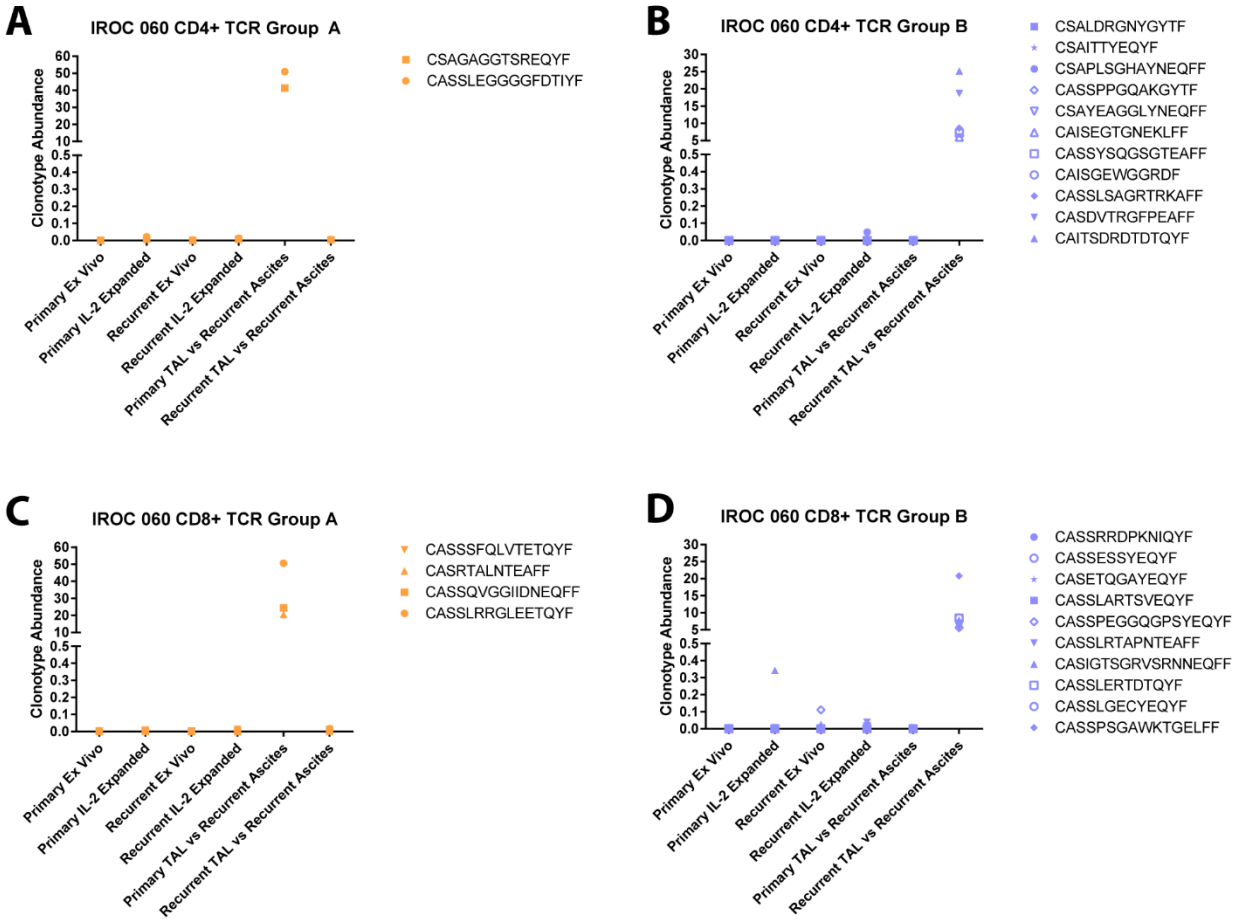

Figure B1. Patterns of tumor-reactive T cell clones from primary to recurrent disease in IROC 060. The T cell clones included in each graph constituted ≥ 1% of the total number of reads in at least one purified tumor-reactive TAL sample and exhibited the same pattern of T cell recognition. On each graph, each TCR clonotype has a unique CDR3 sequence that is noted in the graph legend. Clonotype abundance was determined by dividing the total number of sequencing reads corresponding to one specific clone by the total number of sequencing reads in the whole sample. The abundance of each TCR clonotype within each population: primary or recurrent TAL directly *ex vivo*, primary or recurrent IL-2

expanded TAL, and CD137^{+} primary or recurrent TAL that reacted to recurrent ascites, is plotted. (A,C) The yellow points represent groups of (C) CD4^{+} and (B) CD8^{+} TCRs that were unique to primary TAL (TCR group A). (B,D) The lilac points represent groups of (B) CD4^{+} and (D) CD8^{+} TCRs that were unique to recurrent TAL (TCR group B).

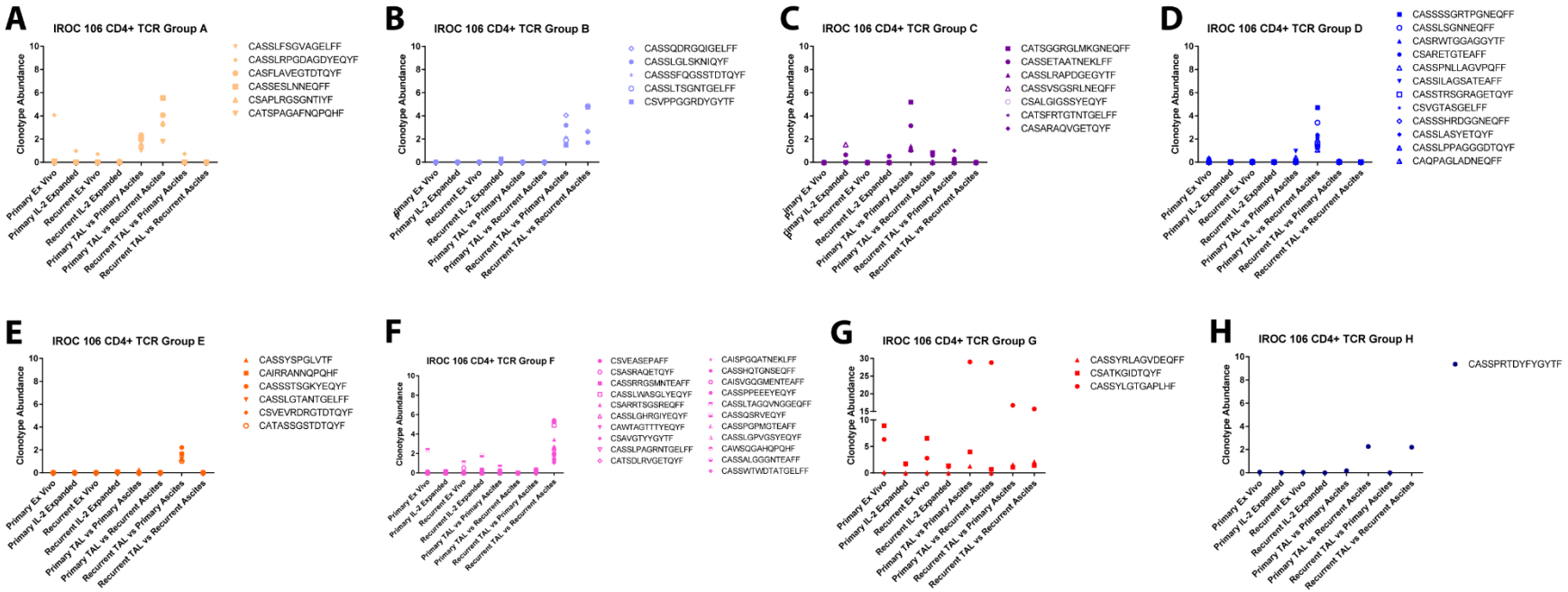

Figure B2. IROC 106 CD4+ tumor-reactive T cell clone patterns from primary to recurrent disease. The T cell clones included in each graph constituted ≥ 1% of the total number of reads in at least one purified tumor-reactive TAL sample and exhibited the same pattern of T cell recognition. On each graph, each TCR clonotype has a unique CDR3 sequence that is noted in the graph legend. Clonotype abundance was determined by dividing the total number of sequencing reads corresponding to one specific clone by the total number of sequencing reads in the whole sample. The abundance of each TCR clonotype within each population: primary or recurrent TAL directly *ex vivo*, primary or recurrent IL-2 expanded TAL, and CD137^{+} primary or recurrent TAL that reacted to recurrent ascites, is plotted. (A) The yellow points represent CD4^{+} TAL that were unique to primary TAL and responded to both primary and recurrent tumor (TCR group A). (B) The lilac points represent CD4^{+} TAL that were unique to recurrent TAL and responded to both primary and recurrent tumor (TCR group B). (C) The purple points represent CD4^{+} TAL that were unique to primary TAL and responded to only primary tumor (TCR group C). (D) The blue points represent CD4^{+} TAL that were unique to primary TAL and responded to only recurrent tumor (TCR group D). (E) The orange points represent CD4^{+} TAL that were unique to recurrent tumor and responded to only primary tumor (TCR group E). (F) The pink points represent CD4^{+} TAL that were unique to recurrent TAL and

responded to only recurrent tumor (TCR group F). (G) The red points represent $CD4^+$ TAL that were shared by both primary and recurrent TAL and responded to both primary and recurrent tumor (TCR group G). (H) The navy points represent a $CD4^+$ T cell clone that was shared by both primary and recurrent TAL but only recognized recurrent tumor (TCR group H).

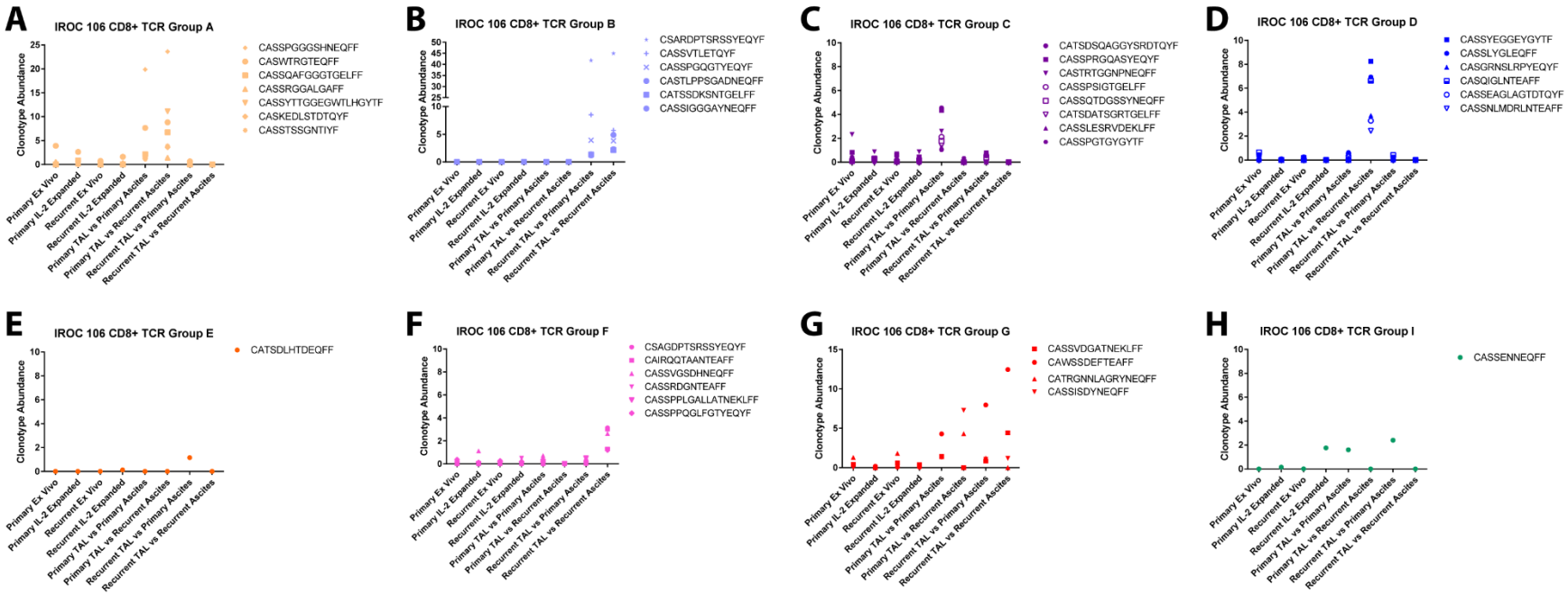

Figure B3. IROC 106 CD8+ tumor-reactive T cell clone patterns from primary to recurrent disease. The T cell clones included in each graph constituted ≥ 1% of the total number of reads in at least one purified tumor-reactive TAL sample and exhibited the same pattern of T cell recognition. On each graph, each TCR clonotype has a unique CDR3 sequence that is noted in the graph legend. Clonotype abundance was determined by dividing the total number of sequencing reads corresponding to one specific clone by the total number of sequencing reads in the whole sample. The abundance of each TCR clonotype within each population: primary or recurrent TAL directly *ex vivo*, primary or recurrent IL-2 expanded TAL, and CD137$^+$ primary or recurrent TAL that reacted to recurrent ascites, is plotted. (A) The yellow points represent CD8$^+$ TAL that were unique to primary TAL and responded to both primary and recurrent tumor (TCR group A). (B) The lilac points represent CD8$^+$ TAL that were unique to recurrent TAL and responded to both primary and recurrent tumor (TCR group B). (C) The purple points represent CD8$^+$ TAL that were unique to primary TAL and responded to only primary tumor (TCR group C). (D) The blue points represent CD8$^+$ TAL that were unique to primary TAL and responded to only recurrent tumor (TCR group D). (E) The orange points represent CD8$^+$ TAL that were unique to recurrent tumor and responded to only primary tumor (TCR group E). (F) The pink points represent CD8$^+$ TAL that were unique to recurrent TAL and

responded to only recurrent tumor (TCR group F). (G) The red points represent $CD8^+$ TAL that were shared by both primary and recurrent TAL and responded to both primary and recurrent tumor (TCR group G). (H) The green points represent a $CD8^+$ T cell clone that was shared by both primary and recurrent TAL but only recognized primary tumor (TCR group I).

B6. References

1. Bashashati, A. *et al.* Distinct evolutionary trajectories of primary high-grade serous ovarian cancers revealed through spatial mutational profiling: Evolutionary trajectories of ovarian cancers. *J. Pathol.* **231,** 21–34 (2013).
2. Castellarin, M. *et al.* Clonal evolution of high-grade serous ovarian carcinoma from primary to recurrent disease. *J. Pathol.* **229,** 515–524 (2013).
3. Gerlinger, M. *et al.* Ultra-deep T cell receptor sequencing reveals the complexity and intratumour heterogeneity of T cell clones in renal cell carcinomas. *J. Pathol.* **231,** 424–432 (2013).
4. Emerson, R. O. *et al.* High-throughput sequencing of T-cell receptors reveals a homogeneous repertoire of tumour-infiltrating lymphocytes in ovarian cancer. *J. Pathol.* **231,** 433–440 (2013).
5. Verdegaal, E. M. E. *et al.* Neoantigen landscape dynamics during human melanoma–T cell interactions. *Nature* **536,** 91–95 (2016).
6. Wick, D. A. *et al.* Surveillance of the tumor mutanome by T cells during progression from primary to recurrent ovarian cancer. *Clin. Cancer Res. Off. J. Am. Assoc. Cancer Res.* **20,** 1125–1134 (2014).
7. Wooldridge, L. *et al.* A Single Autoimmune T Cell Receptor Recognizes More Than a Million Different Peptides. *J. Biol. Chem.* **287,** 1168–1177 (2012).
8. Johnston, R. J. *et al.* The immunoreceptor TIGIT regulates antitumor and antiviral CD8(+) T cell effector function. *Cancer Cell* **26,** 923–937 (2014).
9. Lines, J. L. *et al.* VISTA Is an Immune Checkpoint Molecule for Human T Cells. *Cancer Res.* **74,** 1924–1932 (2014).
10. Anderson, A. C., Joller, N. & Kuchroo, V. K. Lag-3, Tim-3, and TIGIT: Co-inhibitory Receptors with Specialized Functions in Immune Regulation. *Immunity* **44,** 989–1004 (2016).
11. Chapuis, A. G. *et al.* Tracking the fate and origin of clinically relevant adoptively transferred $CD8^+$ T cells in vivo. *Sci. Immunol.* **2,** eaal2568 (2017).

12. Robins, H. S. *et al.* Overlap and effective size of the human CD8+ T-cell receptor repertoire. *Sci. Transl. Med.* **2,** 47ra64 (2010).
13. Robins, H. *et al.* Ultra-sensitive detection of rare T cell clones. *J. Immunol. Methods* **375,** 14–19 (2012).
14. Robins, H. S. *et al.* Comprehensive assessment of T-cell receptor beta-chain diversity in alphabeta T cells. *Blood* **114,** 4099–4107 (2009).
15. Mittal, D., Gubin, M. M., Schreiber, R. D. & Smyth, M. J. New insights into cancer immunoediting and its three component phases--elimination, equilibrium and escape. *Curr. Opin. Immunol.* **27,** 16–25 (2014).